Classification:	**Restricted**	**BM Code: EP.17.03.07**
Issue Purpose	**Approved for Use**	**April, 2006**

Sakhalin Energy Investment Company LTD.

Acoustic Studies on the North East Sakhalin Shelf, Volume 3: Analysis, Conclusions and Recommendations

Document Number: 0000-S-90-04-T-8079-07-E
Revision 01

Document History

Filename 0000-S-90-04-T-8079-07-E

Date	Issue	Custodian	Process Owner	Authoriser	Consulted	Distributed
21-04-06	01	Lisanne Aerts	Andrew J.Pearce	Andrew J.Pearce		
		AP	AP	AP		

Revision Details

Rev	Location of Change	Brief Description of Change
01		Approved for Use.

V.I. Il`icev Pacific Oceanological Institute
Far East Branch, Academy of Sciences of Russia
Vladivostok, Russian Federation

Acoustic Studies on the North East Sakhalin Shelf
Volume 3: Analysis, Conclusions and Recommendations

7 July to 7 October, 2005

Sakhalin, Russian Federation

M.V. Kruglov
A.N. Rutenko
F.F. Khrapchenkov

Prepared for

Exxon Neftegas Limited
&
Sakhalin Energy Investment Company,

Yuzhno-Sakhalinsk, Sakhalin,
Russian Federation

March, 2006

V.I. Il`icev Pacific Oceanological Institute
Far East Branch, Academy of Sciences of Russia
Vladivostok, Russian Federation

'Approved'
POI FEB RAS Director
Academic V.A. Akulichev

March 2006

Acoustic Studies on the North East Sakhalin Shelf
Volume 3: Analysis, Conclusions and Recommendations

7 July to 7 October, 2005

Sakhalin, Russian Federation

M.V. Kruglov
A.N. Rutenko
F.F. Khrapchenkov

Prepared for

Exxon Neftegas Limited
&
Sakhalin Energy Investment Company,

Yuzhno-Sakhalinsk, Sakhalin,
Russian Federation

March, 2006

Table of Contents

LIST OF TABLES

LIST OF FIGURES

Executive Summary

In 2005 the Pacific Oceanological Institute (POI) deployed sixteen Autonomous Underwater Acoustic Recorders (AUARs) to conduct acoustic measurements on the NE Sakhalin shelf as part of the gray whale research program. The goal of the program was to measure key acoustic and hydrologic data, allowing an estimate of the sound propagation to the Korean-Okhotsk gray whale (*Eschrichtius robustus*)[1] feeding areas to be made.

The 2005 acoustic program measured anthropogenic and ambient noise levels, conducted bathymetric and hydrologic surveys and made Transmission Loss (TL) measurements along profiles from the proposed facilities locations to the edges of the Piltun and offshore feeding areas. These TL measurements will be used to calibrate acoustic models that, in conjunction with the recorded spectra of noise sources will be used to predict the sound levels received in the gray whale feeding areas. The model predictions of the acoustic footprint will be used to plan construction operations and will aid in determining the appropriate mitigation measures to be applied. These measurements showed that for profiles extending from deep water to shallow water the bathymetry and velocity field significantly affects the received acoustic field. For long shallow profiles, such as those parallel to the coast, reflections from the bottom and sea surface have a greater impact than the shallowing bathymetry on acoustic propagation. Significant spatial hydrological variations can be seen on profiles extending into deeper water.

Ambient noise measurements made in 2005 correlated well with relationships between acoustic level and sea-state described in the literature.

A comprehensive bathymetric and hydrologic program was conducted in 2005, consisting of 7788 km of bathymetry data and 354 vertical hydrologic profiles. This data was used to build a bathymetric map of the area and to study the spatial and temporal variation of hydro-physical parameters under the influence of winds, tides and storms. The relationship between benthos development and the hydrology of the area was also analyzed.

[1] The Korean Okhotsk (western) gray whale population is listed as endangered in the Russian Red Book and critically endangered by the International Union for the Conservation of Nature (IUCN).

1 Introduction

The shallow water (6 - 15 m) part of the NE Sakhalin shelf starting south of the mouth of Piltun Bay and extending northwards up the Sakhalin coast is the most important known summer feeding area for the Korean-Okhotsk (western) gray whales. Mother-calf pairs have been seen in water depths of less than 10 m in the Piltun feeding area. Acoustic studies have been conducted in the area since 1999 since some of the planned oil and gas developments are near the Piltun feeding area. In 2001 another gray whale feeding area was discovered offshore in deeper water (30-50 m) approximately 20 km to the South East of the mouth of Chayvo Bay.

The acoustic program conducted on the NE shelf of Sakhalin Island in 2005 had two distinct components which were conducted simultaneously for much of the field season. These components were:

- An acoustic monitoring program designed to monitor sound propagating from the operations associated with the tow and installation of the Orlan platform and PA-B CGBS, the construction of the pipeline from the Orlan platform to the Chayvo OPF and the Molikpaq engineering work. These studies were conducted between the PA-B, Molikpaq and Orlan locations and the inshore feeding area as well as the Chayvo area and the offshore feeding area.
- An acoustic program that broadened the long-term monitoring program initiated in 2003. This acoustic program was designed to study temporal and spatial variations in the amplitude and frequency characteristics of ambient and anthropogenic sound at the edge of the Piltun and offshore gray whale feeding areas. In addition to the program monitoring the background acoustic environment, both ENL and SEIC conducted detailed Transmission Loss (TL) studies between current and proposed facilities and key locations at the edge of the gray whale feeding areas. In conjunction with these measurements a comprehensive grid of bathymetric and hydrologic data was acquired across the study area. This data was also used to investigate the spatial and temporal variations in the hydrology due to weather events (e.g. typhoons). In 2005, two joint studies were initiated in conjunction with the behavioral and benthic teams. One study analyzed the 10-minute energy levels near the behavioral monitoring stations; the second investigated the relationship between the distribution of benthos and the bathymetry and hydrology of the study area.

The results of the 2005 acoustic program are presented in three separate reports. The first report describes the objectives of the 2005 program, the operational (including real time acoustic data acquisition) strategy and methodology as well as the data acquired during the 2005 field season [Rutenko, 2006]. This report includes two DVDs containing the sonograms in 24-hour segments for all the acoustic data recorded in 2005 as well as the

bathymetric and hydrologic data acquired during the 2004 and 2005 field seasons. The second report describes the equipment used during the 2005 field season, its testing and calibration as well as the data processing and analysis methodology [Borisov et. al., 2006].

This report (volume 3) is dedicated to analysis of the data, conclusions and recommendations for future work. This analysis includes the following components:

Acoustic Monitoring

1. An analysis of the acoustic monitoring data recorded at six stations during construction operations and correlation of the acoustic data with construction operations.

Western gray whale research program – Acoustic studies

2. A quantitative spectral analysis of the variation in the ambient acoustic noise level with weather conditions (including cyclones).
3. The results of the comprehensive spectral TL (over the frequency range from 15 Hz to 15 kHz) experiments between the major facilities and key locations at the edge of the gray whale feeding areas.
4. A temporal, spectral and spectral-temporal analysis of the acoustic data recorded at different locations on the Sakhalin shelf[2].
5. The results of experiments to measure the acoustic output from the primary outboard motor on the Photo-ID zodiac and from the *Academik Oparin*.
6. A temporal analysis of acoustic energy levels (10-minute windows) at the 10 m contour directly offshore from the behavioral monitoring positions.
7. Analysis of the hydrologic data (including velocity, temperature, and salinity) recorded in 2004 and 2005.
8. An experimental study of the relationship between the distribution of benthos and the hydrology and bathymetry of the study area. This analysis includes hydrologic data acquired at 96 benthic sampling locations[3] [Fadeev, 2005].

1.1 Acoustic recording and processing equipment

The acoustic measurements were conducted using 14 digital Autonomous Underwater Acoustic Recorders (AUARs) developed at POI FEB RAS[4] (POI). Four of these AUARs

[2] The use of AUARs for the 2005 program allowed an unprecedented characterization of the ambient noise at the Sakhalin monitoring stations. However, since the vessels used to house the scientists (*Academik Lavrent'ev and Academik Oparin*) was often a significant distance from the AUAR the identification and specific location of any transient anthropogenic noise source is generally unknown.
[3] This study was conducted in conjunction with the Benthos program led by Dr. V.I. Fadeev (IBM).
[4] POI FEB RAS - The Pacific Oceanological Institute, Far East Branch of the Russian Academy of Sciences.

were Transmit-AUARs (T-AUARs)[5] (Figure 1.1). An additional two mini-AUARs were constructed for the 2005 field season; these were smaller with a reduced (72 hours) record time and were used for TL and source level measurements. The AUARs were designed to accurately record frequencies between 1 Hz -15 kHz and enable accurate, autonomous, synchronous acoustic measurements over a broad range of frequencies (including infrasounds[6]). Individually deployed acoustic sonobuoys also developed at POI (2 digital and 4 analog) were used to measure acoustic signals and to transmit them to a receiving station. Analog sonobuoys recorded frequencies from 10 Hz to 10 kHz and digital sonobuoys from 1 Hz to 2.6 kHz. When used together an analog and digital sonobuoy pair can record acoustic data from 1 Hz to 10 kHz. A detailed description of this equipment is given in volume 2 of this report [Borisov et. al, 2006].

1.1.1 Acoustic Underwater Acoustic Recorder (AUAR)

The AUARs[7] are made of welded titanium alloy and are rated to depths of up to 100 m. Two external sensors (hydrophones, accelerometers or hydrologic measuring equipment) can be input to the AUAR electronics. Inside the AUAR there are batteries secured in a titanium frame and a tray containing the AUAR electronics and power handling circuitry. The number of batteries depends on the AUAR design. The 2003/2005 AUARs have two sealed batteries which can provide continuous operation of the AUAR for over 18 days, and the 2004 AUARs have three sealed batteries providing continuous operation of the AUAR for over 16 days.[8] Cylindrical hydrophones (model # GI-50 (ГИ-50)) and spherical hydrophones of type G61H (Г61Н) both with integrated pre-amplifiers designed specifically for the hydrophones were used with the AUARs.

[5] The T-AUARs were equipped with a radio channel and were capable of simultaneously recording data on the AUAR hard drive and transmitting data (bandwidth 10 Hz to 5 kHz) to a receiving radio station. The transmission can be continuous or on a pre-programmed schedule.
[6] Infrasounds are sounds with a frequency of less than 20 Hz.
[7] 2003/2005 AUAR dimensions are length 0.8 m, diameter 0.38 m, weight in air ~105 kg. 2004 AUAR dimensions are length 1.2 m, diameter 0.32 m, weight in air ~105 kg.
[8] The two sealed batteries (2003/2005) have a capacity of 115 Ampere-hours each. The three sealed batteries (2004) have a capacity of 65 Ampere-hours each.

Figure 1.1 – T-AUAR being prepared for deployment (note the radio transmission unit connected to the AUAR container).

The AUARs digital recorder is based on the Prometheus single board computer, which has an integrated 16 bit analog to digital converter (ADC). In order to optimize the dynamic

range of the 16-bit ADC the signal amplitudes should be approximately equal across the entire frequency range. However, ambient noise generally has an amplitude maximum at low frequencies and drops off with higher frequencies. The ADC does not therefore have the instantaneous dynamic range required to record frequencies from 1 Hz to 15 kHz. The analog channel of AUARs that use G-33 hydrophones (with high sensitivity at low frequencies) have a low-frequency gain correction at frequencies below 100 Hz using a second-order RC circuit. For AUARs that use the GI-50 hydrophones, which were updated in 2005, low-frequency amplitude correction is effected in the hydrophone preamplifier. These amplitude corrections ensure a consistent signal level across the entire frequency band for the analog channel of the AUARs with these hydrophones. An inverse correction is applied after spectral estimation.

The primary AUAR data storage is a compact laptop 80 GB hard drive. To prevent electromagnetic and acoustic noise generated by the rotating hard drive from contaminating the data a 1 GB flash memory drive is used as a buffer. While data is being recorded on the flash drive the hard drive is in standby mode with its motor off. When the flash memory drive is full, the recording cycle is halted while the flash memory drive writes to the hard drive; the data therefore contains controlled gaps. The size of these gaps was approximately 22 minutes every 4:18 hours. Before each AUAR is deployed its computer is programmed for the desired recording schedule. The acoustic data on the AUAR hard drive was copied to DVDs and a removable hard drive before the files on the AUAR drive were deleted prior to redeployment.

A floating buoy connected to a 24 kg anchor by a 50-70 m rope marks the location of the AUAR on deployment. This anchor is linked to the AUAR by a 100 m long rope weighted down with lead weights. Practical experience has shown that at shallow deployment depths (10-30 m), movement of the surface buoy due to wave action can be mechanically conducted down the rope to the hydrophone, where this mechanical movement can be recorded as acoustic noise. The AUAR is deployed so as to reduce this noise by isolating the hydrophone from the surface buoy with an anchor, thus reducing the mechanical coupling between the surface buoy and the hydrophone. The hydrophone is also deployed 15 m from the AUAR to prevent distortion of the acoustic field by scattering or masking by the AUAR container at high frequencies. The hydrophone is deployed inside a pyramid

shaped wire frame and attached by rubber bands to the frame, isolating it to the best extent possible from the sea floor.

1.1.2 Digital and analog sonobuoys

In 2005 a number of design improvements were made to the sonobuoys. The hydrophone pre-amplifier was redesigned, improving the signal level at the hydrophone, allowing the bottom units to be discarded and a unified design to be used for both the analog and digital sonobuoys. Analog and digital sonobuoys both have advantages and disadvantages. For the analog sonobuoys the advantages are greater bandwidth and longer range (>10 km for a bandwidth of 10 Hz to 10 kHz and >20 km for 10 Hz to 5 kHz). However the dynamic range of an analog sonobuoy is much lower than that of a digital sonobuoy and is highly dependent on the quality of the radio channel. The digital sonobuoy (due to the 16-bit ADC) has a significantly greater dynamic range than the analog sonobuoy, is not susceptible to radio noise and has stable performance characteristics. The digital sonobuoy can also measure frequencies as low as 1 Hz accurately. The disadvantages of a digital sonobuoy are narrower bandwidth and shorter range (≤ 8 km for a bandwidth of 1 Hz to 2.6 kHz).

Figure 1.2 shows a digital sonobuoy. The flotation collar holds a steel (analog) or titanium (digital) canister containing the sonobuoy electronics. The sonobuoy is powered by an external battery pack that can be changed at sea. The sonobuoy antenna is kept upright by a keel to which the batteries are attached. The surface unit is connected by a cable to a G33 (Г33) spherical hydrophone with an integrated pre-amplifier designed specifically for the hydrophone. The hydrophone is suspended in a pyramid shaped metal frame and attached by rubber bands as with the AUAR hydrophone. The hydrophone pre-amplifier amplifies the signal prior to transmission along the 100 m cable to the surface sonobuoy module. The signal is then further filtered and amplified prior to radio transmission (analog sonobuoys) or low pass filtered to 2.6 kHz and digitized prior to encoding and radio transmission (digital sonobuoys).

The radio signals from the analog sonobuoys and the T-AUARs were received at a recording station at Piltun lighthouse[9]. The range of the analog radio channel depended on

[9] During the Lunskoye monitoring program (not discussed in this report), the radio signals from the analog and digital sonobuoys and the T-AUARs were received on the vessel *Academik Lavrent'ev*.

the type of radio receiver used. Narrowband (10-5000 Hz) signals could be received at distances of more than 20 km by the station at Piltun lighthouse. During the 2005 field season (7 July to 7 October), AUARs and sonobuoys were deployed from the research vessels *Academik Lavrent'ev and Academik Oparin* (these vessels also accommodated the biology teams (Benthic, Marine Mammal Observers (MMO) and Photo-ID).

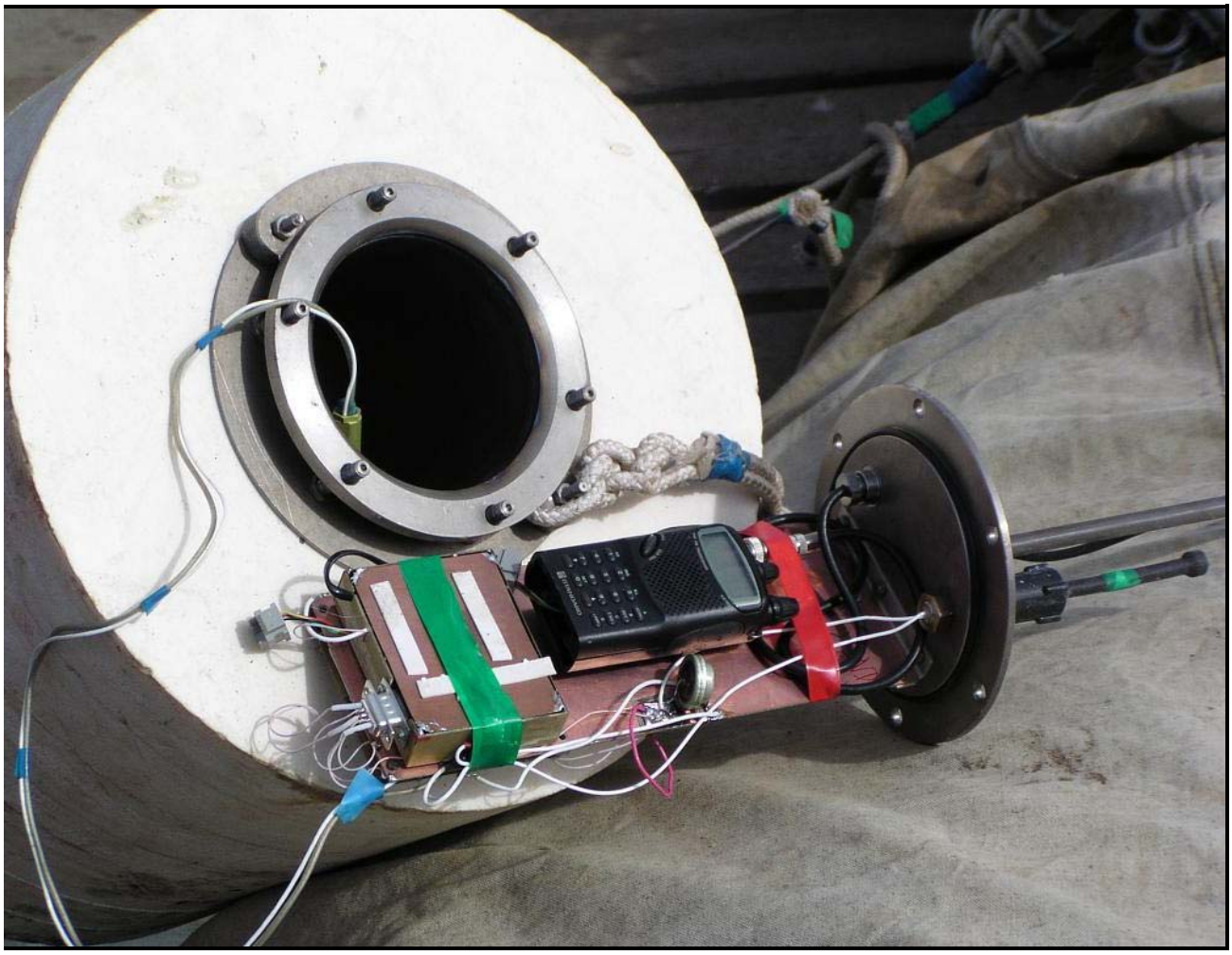

Figure 1.2 - Digital sonobuoy container and electronics.

To compute TL from acoustic measurements made by different AUARs, the data has to be calibrated to an absolute pressure standard. The hydrophones were manufactured with nominal sensitivities and the gains were set in the field. Field cross-calibrations confirmed the absolute calibration of the data. Further details of the AUARs used, their location, deployment depth and recording settings can be found in Appendix A. A detailed description of the characteristics and calibration of the acoustic recording equipment is

provided in volume 2 of this report [Borisov et. al., 2006].

1.2 Low Frequency and High Frequency transducers and hydrological sonde

A low frequency (LF) resonant electromagnetic transducer and high frequency (HF) piezoelectric broadband transducer deployed from the *Academik Oparin* were used for sound propagation and TL studies at frequencies from 15 Hz -15 kHz. The acoustic level of signals generated by the transducers was monitored using a calibrated hydrophone and recorded on the *Academik Oparin* [10]. The LF transducer has a cylindrical container filled with gas[11], and a pair of identical closely spaced radiating pistons oscillating in opposite directions creating a volume displacement[12]. An electromagnetic controller controls the motion of the pistons; hydrostatic compensation is achieved using an air pump. The LF resonance transducer was deployed at a depth of 8 m from the anchored *Academik Oparin*. The 27 Hz acoustic signal has an intensity of ~180 dB re 1 μPa^2/Hz at 2 m from the transducer. The HF broadband piezoelectric (ceramic) transducer is cylindrical[13] and consists of 7 piezoelectric rings connected in parallel coated with a composite material and sealed at the ends with a metal shield.

Calibration with empirical TL data is used to enhance numerical modeling along the TL profiles. To calibrate the model along an acoustic profile, the bathymetry and hydrological characteristics (velocity, temperature and salinity) of the water layer along the profile must be known. Thus, to complement the TL measurements, the bathymetric profile was obtained using the ship's echo sounder and hydrological data was acquired using a hydrological sonde. The sonde is powered by a set of D-cell batteries, providing approximately 180 hours of continuous operation. 7788 km of bathymetric data and 354 vertical hydrologic profiles were acquired in 2005.

[10] While the transducers were operating the acoustic signal levels were measured using a calibrated hydrophone located 1 - 2 m away from the transducer.
[11] Dimensions are diameter 58 cm, height 15 cm, weight 48 kg in air, ~6 kg in water.
[12] Tests in the Sea of Japan using calibrated accelerometers, and conducted at a depth of 2 m, indicated that when the maximum number of springs (30) are used, the resonance frequency of the transducer is 20.2 Hz with marginal frequencies of 15.2 and 30.6 Hz (-3 dB).
[13] Dimensions are diameter 28 cm, height 136 cm, weight ~ 60 kg in air, ~ 15 kg in water.

During the 2005 field season AUARs were deployed and synchronous acoustic measurements recorded at stations ranging from north of the Odoptu license area to the southern edge of the offshore feeding area (Figure 1.3 and Table 1.1), this area extends a distance of 180 km from its northern to southern border.

1.3 Terminology and algorithms used in the report

Ambient and anthropogenic acoustic data recorded by the AUARs was written to disc in microPascals (μPa)[14]. Sound pressure power density spectra *G(f)* (μPa^2/ Hz)[15] were generated, corrected for the hydrophone sensitivity and analog channel gain over the entire frequency range (1 Hz to 15 kHz). These spectra are computed using an FFT, and may be averaged over 10-300 one-second windows to improve the statistical stability of the ambient noise data[16]. The sonograms *G(f,t)* are plots of power spectral density vs. frequency and time, the scales generally run from ~37 to ~120 dB re 1 μPa^2/Hz. The sonograms include plots of the variation in sound pressure level $D\Delta f(t)$ (μPa^2) with time over the annotated bandwidth[17]. A detailed description of the methodology used for normalizing and calculating both the amplitude and spectral data is given in Borisov et.al. [2006], Appendix D.

1.4 Units

During the course of this report a number of different unit notations have been used. This is due to differences in standard notation between different disciplines and nationalities. The following are equivalent units using the different standard nomenclatures:
1 mkPa = 1 μPa and 1 mkV = 1 μV.

For spectral density plots: Although the units for power spectral density are μPa^2/(s Hz), μPa^2/s/Hz or μPa^2, it is common usage to define the units for power spectral density as μPa^2/Hz or $\mu Pa/\sqrt{Hz}$.

[14] The data was scaled (after incorporating hydrophone sensitivity and system gain at 1 kHz) to convert the data to standard units of pressure (measured through an omni-directional hydrophone) in real time.
[15] Energy and power spectra are scaled to 1 Hz whatever the analysis length.
[16] Average of 10 or 300 1-second spectral realizations; the analysis window length is shown on the plot. Spectral averaging will lead to a lower variance spectral estimate, increased spectral fidelity and a reduced trust interval.
[17] Sound pressure level is the integral of the acoustic energy over the specified frequency band.

Table 1.1 - Numbers, names, locations and depths of the proposed stations.

#	Station		Latitude	Longitude	Depth
Monitor Stations:					
1	Lunskoye	Лунское	51° 51' 45" N	143° 37' 27.3" E	50 m
2	OFA (Offshore Feeding area)	ГЗК (Глубоководная зона кормления)	52° 10' 18" N	143° 36' 1.8" E	~40 m
3	Orlan	Орлан	52° 21.6' N	143° 35.0' E	32 m
4	Arkutun-Dagi	Аркутун-Даги	52° 19' 9.6" N	143° 44' 4.6" E	~40 m
5	Piltun-S	Пильтун-Ю	52° 40' 51" N	143° 22' 34" E	10 m
6	Piltun	Пильтун	52° 49.3' N	143° 24.9' E	20 m
7	PA-B-10	ПА-Б-10	52° 53' 2.1" N	143° 20' 10.6" E	10 m
8	PA-B-20	ПА-Б-20	52° 54' 00" N	143° 23' 20.5" E	20 m
9	Odoptu-PA-B	Одопту-ПА-Б	53° 00' 00" N	143° 21' 18" E	20 m
10	Odoptu-S-10	Одопту-Ю-10	53° 03.7' N	143° 18.3' E	10 m
11	Odoptu-S-20	Одопту-Ю-20	53° 03' 42" N	143° 19' 58" E	20 m
12	Odoptu-N-10	Одопту-С-10	53° 09.1' N	143° 17.4' E	10.5 m
13	Odoptu-N-20	Одопту-С-20	53° 09' 6" N	143° 18' 42' E	20 m
14	**Control**	**Контрольная**	**53° 25.95' N**	**143° 11.1' E**	**20 m**
Acoustic Stations:					
A1	#1 (Chayvo-1)	#1 (Чайво-1)	52° 27.8' N	143° 19.0' E	11 m
A2	#2 (Chayvo-2)	#2 (Чайво-2)	52° 25.9' N	143° 20.6' E	11 m
A3	#3 (Chayvo-3)	#3 (Чайво-3)	52° 26.8' N	143° 24.6' E	17 m
A4	#4 (Piltun-1)	#4 (Пильтун-1)	52° 43' 14.4" N	143° 22' 26.7" E	10 m
A5	#5 (Piltun-2)	#5 (Пильтун-2)	52° 43' 48" N	143° 25' 49" E	20 m
A6	#6 (Piltun-3)	#6 (Пильтун-3)	52° 49.3' N	143° 24.9' E	20 m
A7	#7 (PA-B-1)	#7 (ПА-Б-1)	52° 55' 54" N	143° 19' 39" E	10 m
A8	#8 (PA-B-2)	#8 (ПА-Б-2)	52° 55' 54" N	143° 21' 42.4" E	20 m
A9	#9 (BEH-Odoptu)	#9 (Одопту (Пов))	53° 12' 33.1" N	143° 15' 51" E	10 m
A10	#10 (BEH-north)	#10 (Пов-север)	53° 17' 52.4" N	143° 13' 25.4" E	10 m
A11	#11 (Chayvo-4)	#11 (Чайво-4)	52° 34' N	143° 23' E	~18 m

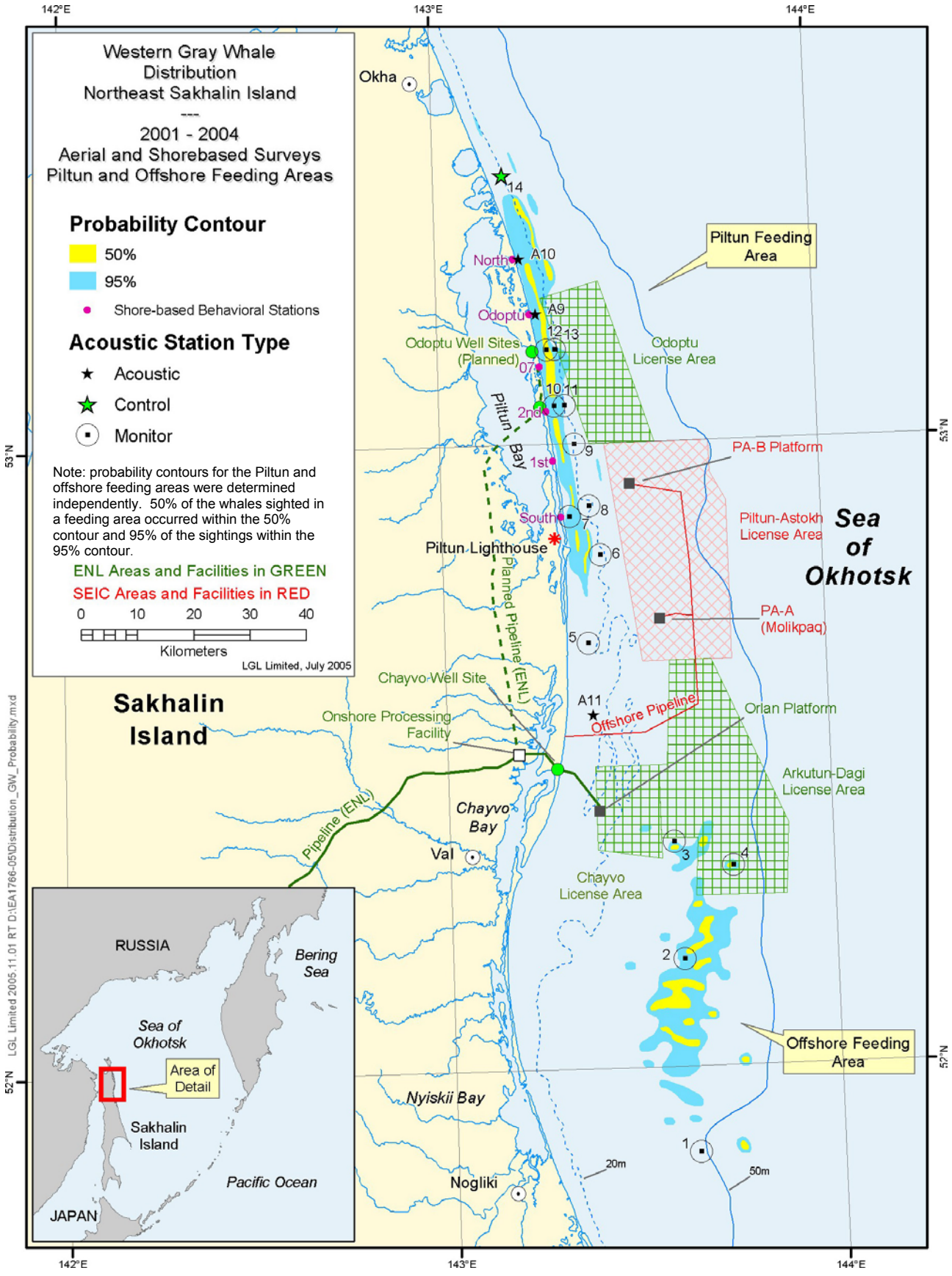

Figure 1.3 - Map of the NE Sakhalin Shelf showing the locations of the PA-B and Orlan platforms as well as the AUAR deployment locations. Also cumulative probability contours showing the density distributions of western gray whales from the 2001 to 2004 aerial surveys, 2001 to 2004 scan stations and the 2004 vehicle-based surveys.

2 Impact of weather conditions on the ambient acoustic field of the NE Sakhalin shelf

This section analyzes the ambient noise measurements recorded in 2005 and discusses the variation in ambient noise with meteorological conditions and sea state. In 2005, as in the previous two years, acoustic data was recorded using AUARs, and ambient noise data was acquired at monitoring stations across the area.

Previous reports have discussed the variation in ambient noise due to wind, surface waves and rain. For example, the broadband noise level near Chayvo rose by 12 dB when the sea state increased from 1 to 4 [Borisov et.al., 2003]. A rainstorm with strong wind squalls pushed the ambient noise level an additional 16-18 dB higher. For frequencies above 2.5 kHz the spectral level of ambient noise recorded during a storm had a peak value of ~64 dB re 1 μPa^2/Hz (56 dB re 1 μPa^2/Hz for a storm without rain). Spectral analysis of the data acquired in 2003 showed that the noise field in the frequency band from 200-800 Hz generated by an approaching storm had the clear interference structure resulting from waveguide propagation on the shelf [Borisov et.al., 2004]. The data showed that noise produced by wind and surface waves is much lower for shallow water (10 m) than for areas outside the 20 m contour. The highest ambient noise level was recorded in the frequency band from 200-1000 Hz. The ambient noise in this frequency band had a peak value of 71 dB re 1 μPa^2/Hz during a storm and 46 dB re 1 μPa^2/Hz in calm weather (no rain).

Figure 2.1 displays spectra *G(f)* of ambient noise data recorded at acoustic station A.5, located at the SE border of the Piltun feeding area (20 m depth) before (31 August 2004) and during (1 September 2004) a strong tropical cyclone. The spectral density plot *G(f)* for 6:53 (Figure 2.1: 31.08 - 6:53) corresponds to good weather conditions, however the vessel *Trias* was close to acoustic station A.5. The broadband sound level above 7 kHz has dropped below the internal noise level of the AUAR (~35 dB re 1 μPa^2/Hz). As the typhoon approached most vessels sailed to the NE to find shelter from the storm. The spectral density plots *G(f)* for the interval between calm weather and a storm (Figure 2.1: 31.08-17:48 and 1.9-03:34 and 13:10) illustrate the increase in the acoustic levels due to wind and surface waves. These plots show that the broadband spectral levels increased by more than 20 dB (for the frequency band from 100 Hz-15 kHz) during a heavy storm (Figure 2.1: 03.34 and 13:10 relative to 06:53). At 13:10 the spectral density values for frequencies

between 500-2000 Hz even exceed the levels predicted for Sea State 6 (SS-6: wind -17.5-20.6 m/s, waves - 4-6 m) [Knudsen et. al., 1948; Richardson et. al., 1995].

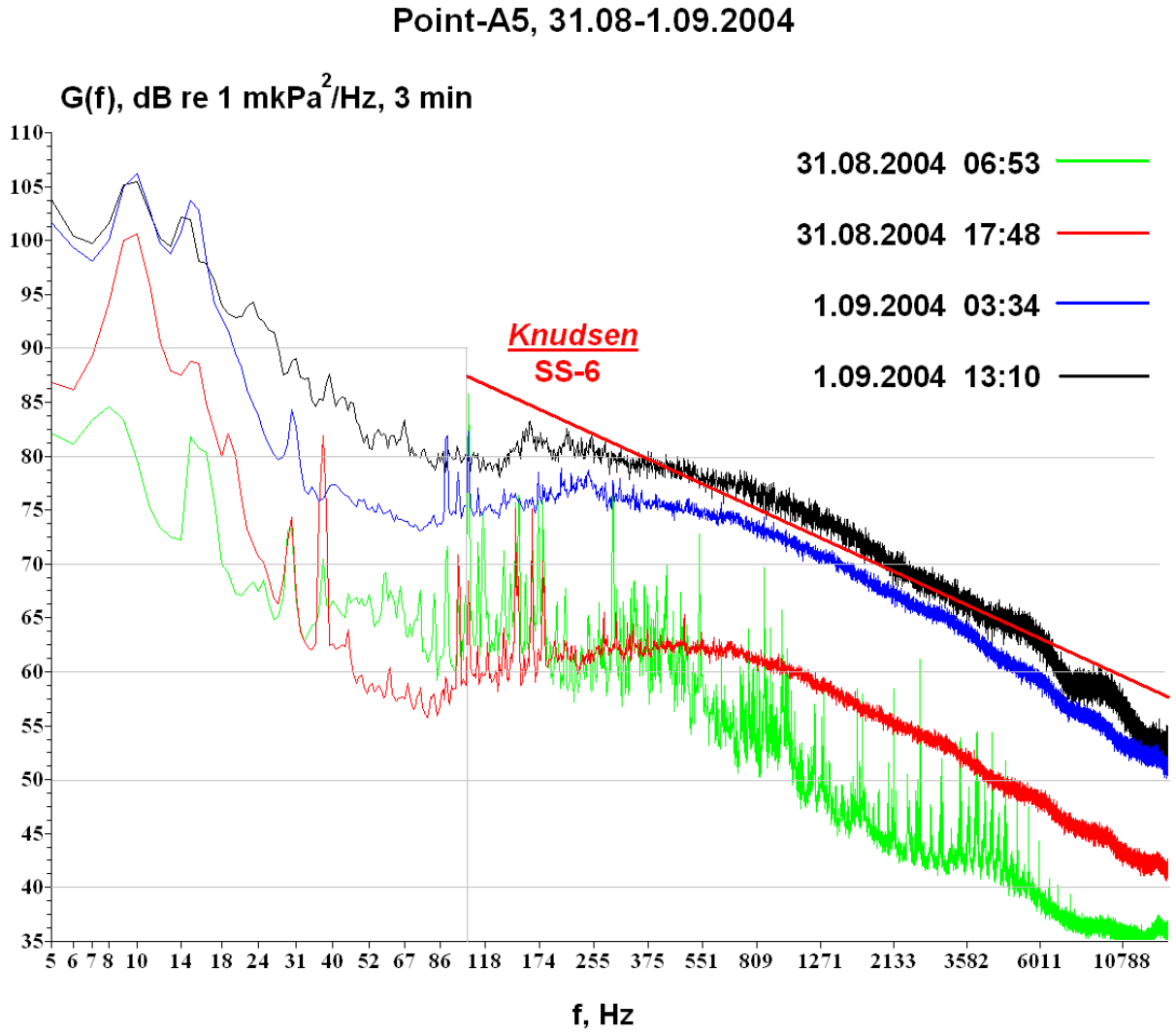

Figure 2.1 - Spectra *G(f)* of ambient noise recorded at acoustic station A.5 before and during a typhoon.

Figure 2.2 displays sonograms of noise synchronously recorded at three monitor stations which are up to 150 km apart. The figure shows that twice a day tidal currents cause intense flow noise at frequencies below 15 Hz[18]. Rotational water movement in surface waves during the typhoon could lead to even higher flow noise and may even move a hydrophone deployed at 10-20 m.

[18] Flow noise is not a real ambient noise measurement, but an artifact caused by vibration of, and turbulent flow around, the hydrophone.

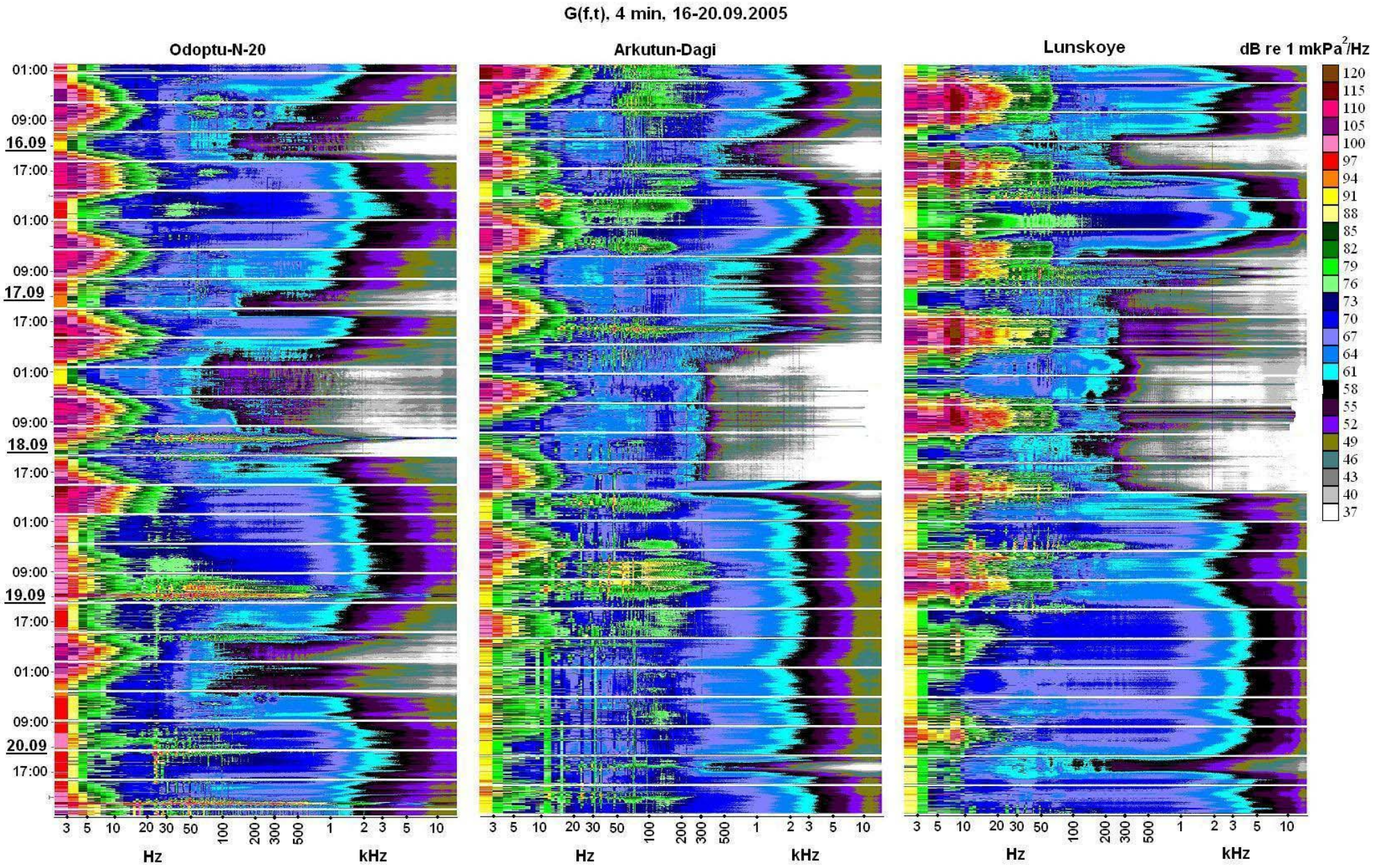

Figure 2.2 - Sonograms *G(f,t)* for data recorded at monitor stations Odoptu-N-20, Arkutun-Dagi and Lunskoye from 16 to 20 September, 2005.

This mechanical motion caused clipping in some of the data. Data recorded during low current periods should be used when analyzing acoustic data below 20 Hz (infrasonic).

The sonograms *G(f,t)* displayed on Figure 2.2 illustrate the frequency and spatial characteristics of ambient noise generated by weather. Figure 2.2 illustrates that the ambient noise level is mainly defined by local meteorological conditions and the level can vary significantly over a distance of less than 150 km. For example during the night of 19-20 September (Figure 2.2:19.9-21:00 to 20.9-05:00), the ambient noise level at the Odoptu-N-20 station was relatively low for frequencies above 100 Hz, but at the Arkutun-Dagi and Lunskoye stations it was considerably higher[19]. The structure and level of the acoustic field is similar at the Arkutun-Dagi and Lunskoye stations, but different at the Odoptu-N-20 station.

[19] The distance from Lunskoye to Arkutun-Dagi is approximately 50 km and from Lunskoye to Odoptu-N-20 approximately 150 km.

3 Analysis of Transmission Loss TL(f,r) experiments conducted on the Sakhalin shelf

The first part of this section discusses the key factors influencing the variation of TL with frequency and range (*TL(f,r)*) along a shallow waveguide with uneven bathymetry. This includes the waveguide parameters as well as the influence of sea surface waves on TL. The later sections show the experimental analysis of sound propagation and TL along a number of profiles from proposed facilities to the western gray whale feeding areas.

3.1 Discussion of the factors controlling TL(f,r) in shallow water

The main characteristics of sound propagation on the NE Sakhalin shelf were discussed in a previous report [Kruglov et. al., 2004]. This showed that the main factors controlling sound propagation in a waveguide were the bathymetric and acoustic properties of the waveguide. Tidal internal waves were shown to cause up to 16 dB variation in the acoustic intensity of 320 Hz signals propagating along profiles oriented approximately parallel the shore. Scattering by sea surface waves was also shown to have a significant impact on sound propagation when the acoustic wavelength (λ) was less than the sea surface wave height (h) (e.g. at frequencies above 2 kHz)[20].

Acoustic propagation and TL data from the oil and gas production facilities to the western gray whale feeding areas are important when estimating the change in the anthropogenic noise levels in the feeding areas due to construction and development activities. Industrial sources predominantly generate acoustic wavelengths shorter than ~50 m (>30 Hz). For these wavelengths the profiled waveguides are shallow (10-50 m) and irregular and the main factors contributing to the variation in frequency dependent TL with range *TL(f,r)* are the bathymetric profile and the elastic parameters of the sub-bottom. Spatial variations in the hydrology do not have a significant impact on propagation in this frequency range.

Figure 3.1 gives acoustic spectra synchronously recorded at Lunskoye during the LUN-A Concrete Gravity Based Structure (CGBS) scour protection in July 2005[21]. The data was recorded using two digital (2.4 km and 10 km from the CGBS) and one analog (8 km from CGBS) sonobuoys. The power spectral density plots *G(f)* shown on Figure 3.1 illustrate

[20] For example, at a frequency of 3 kHz λ =50 cm, therefore surface waves with height of greater than 0.5 m can effectively dissipate its acoustic energy and increase the TL at that frequency. The effect was approximately proportional to sound frequency and profile length.

both the acoustic source spectrum generated by the scour protection vessel and the frequency dependent TL along a 10 km profile with depth varying from 45 m to 25 m. This spectrum shows that there is a narrowband component (23-36 Hz), a broadband component between 80-400 Hz and tonal components from 800-2000 Hz. Above 2 kHz the anthropogenic acoustic level drops below 80 dB at a distance of ~8 km.

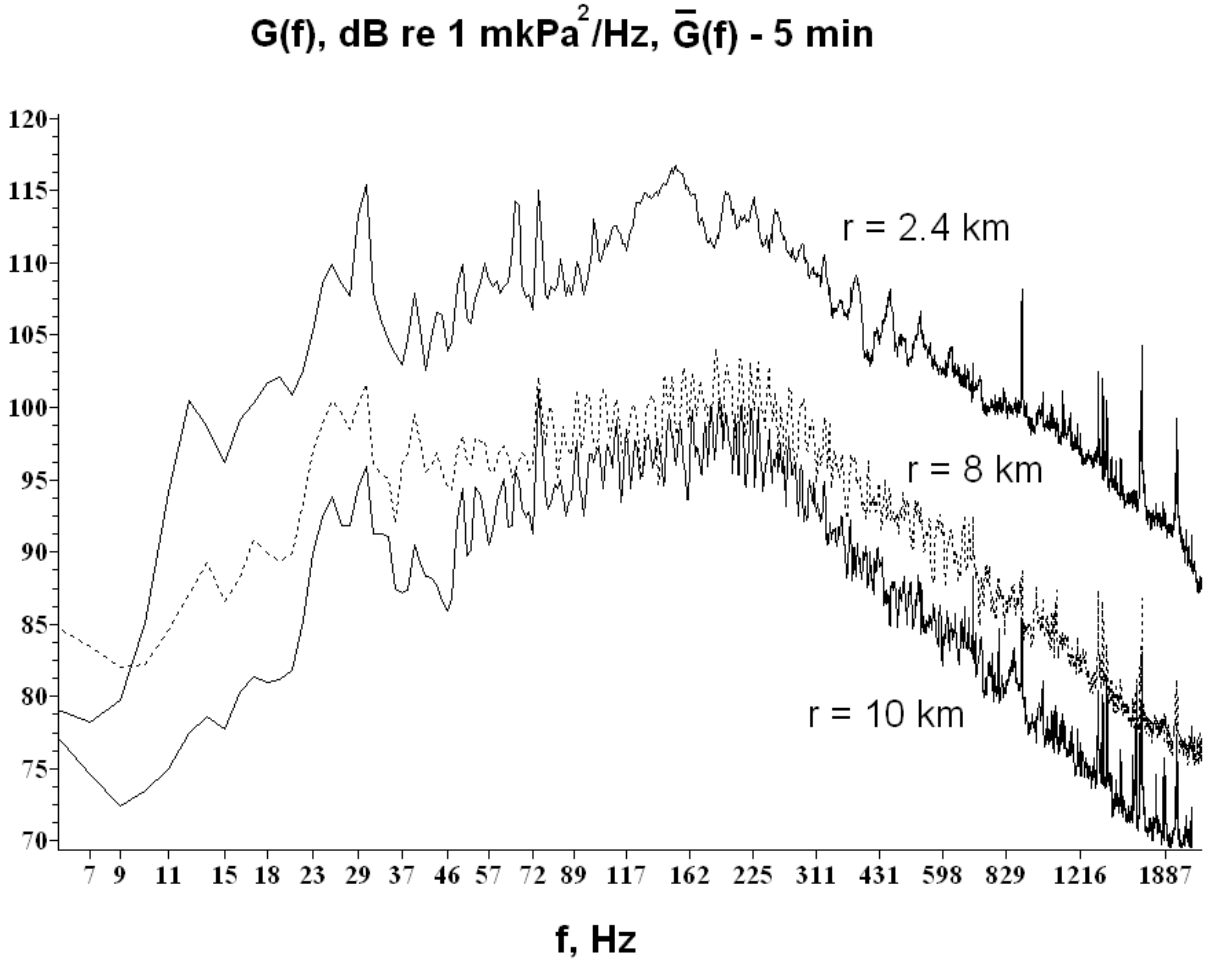

Figure 3.1 – Power spectral density plot G(f) showing the source spectrum of the vessel *Rocky Giant* while performing scour protection at the LUN-A CGBS location. Data was synchronously recorded by 3 sonobuoys at a distance *r* from the CGBS.

Reflections from an irregular bathymetric profile lead to an even distribution of acoustic energy in the water layer. The spatial distribution of the sound velocity field C(z,r) and variations caused by tidal currents and internal waves affect acoustic propagation because the velocity field affects the spatial-interference structure of the acoustic field in the

[21] This report does not cover the installation of the Lunskoye CGBS. However, acoustic data from the CGBS

waveguide. The frequency and range dependent transmission loss TL(f,r) can be estimated from experimental measurements if calibrated signals are transmitted and recorded using AUARs [Borisov et.al., 2005]. Spatial interference caused by intermodal interference and multi-pathing was eliminated by transmitting from the *Academik Oparin* as it drifted. The results of these experiments can be refined with modeling. Thus for a TL profile the frequency and range dependent variation in acoustic level with velocity C(z,r) can be estimated for an anthropogenic sound source.

One of the key objectives of the experimental TLP measurements is to calibrate theoretical acoustic models; the acoustic and hydrologic measurements were therefore acquired to ensure the hydrology did not vary significantly during the experiment. A bathymetric profile, a vertical hydrologic profile at the receiver location, and at each source location as well as at intermediate points if required were acquired for each TL profile. This hydrologic sampling allowed the velocity distribution *C(z,r)* to be obtained along each TL profile.

3.2 Analysis of propagation and TL from the PA-B platform location

Figure 3.2 is a map of the study area showing the profiles along which the TL experiments were conducted. The relationship between the names and numbers for the monitoring and acoustic stations is given in Table 1.1. The main objective of the analysis was to experimentally estimate the TL along a profile, as well as the point-to-point TL[22], between the PA-B CGBS location and the seaward boundary of the Piltun feeding area[23]. A secondary goal was to experimentally estimate the TL between the PA-B CGBS location and the offshore feeding area.

In order to estimate the TL along a profile, AUARs are deployed at the specified monitoring stations for each profile (e.g. the Orlan and OFA stations for TLP-4). Tonal and broadband acoustic signals are then transmitted from the source locations for each profile. At the beginning or on completion of the transmission, hydrologic measurements were taken with the sonde. The profile was then sailed by the *Academik Oparin* with bathymetric and

---

installation gives a good indication of the sound generated by construction activities.

[22] Point-to point Transmission Loss profiles are point profiles from the proposed PA-B platform location to the feeding areas. Transmission Loss profiles are designed to better characterize the TL from a proposed facility and have multiple source points allowing a range dependent function to be estimated.

[23] The Piltun-S, Piltun and PA-B-20 Monitor stations, A5 and A8 Acoustic stations.

hydrologic measurements being taken along the profile from the TL source locations to the recording station locations.

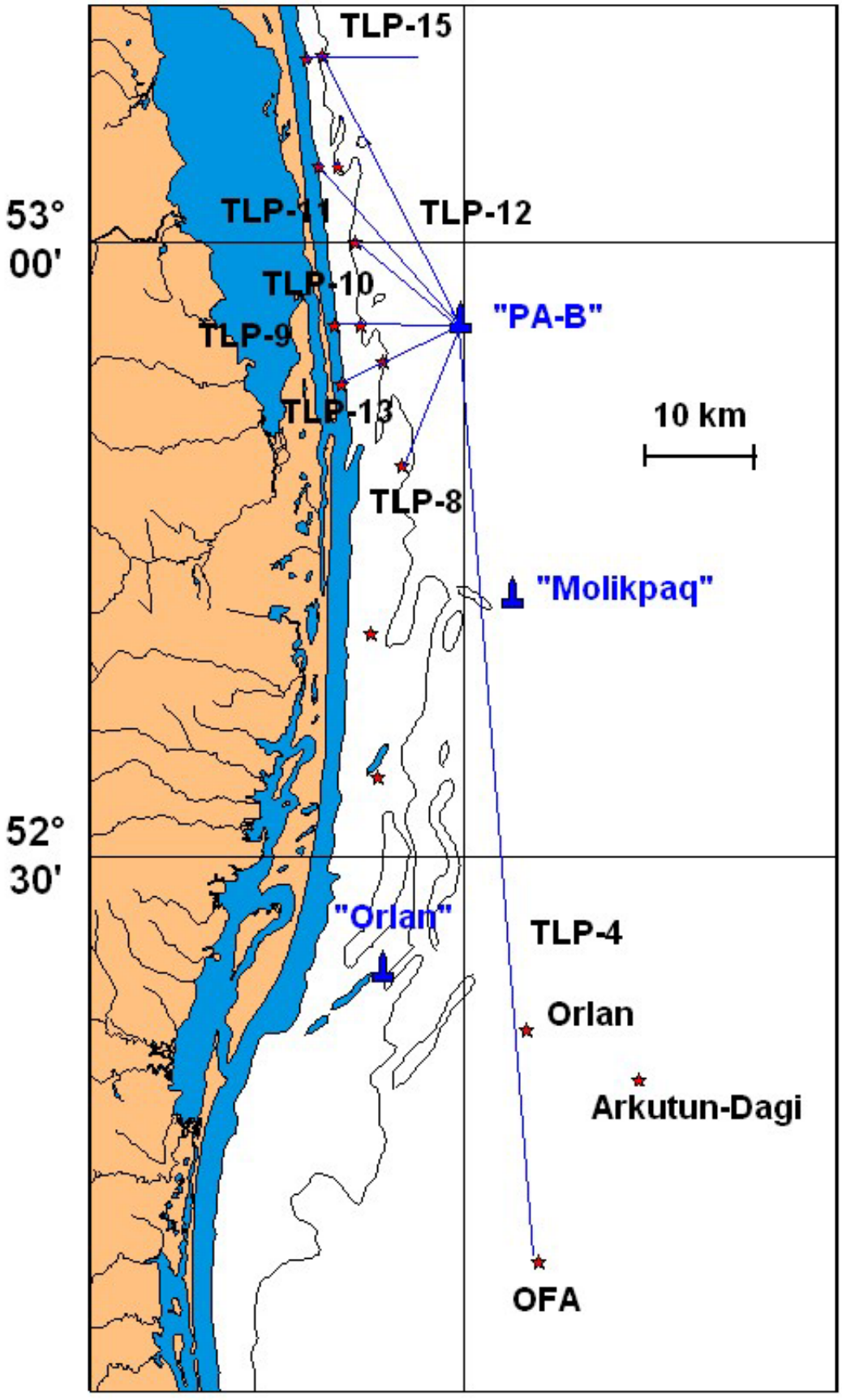

Figure 3.2 - Map of the study area showing the major facilities as well as the AUAR deployment locations for the TL experiments and the profiles surveyed.

One drawback with this methodology in previous seasons was that the sensitivity of the AUARs was high[24] and the acoustic signature of the *Akademik Oparin* when it was nearby could exceed the dynamic range of the systems. Mini-AUARs were therefore additionally deployed at each station, and due to their lowered sensitivity, provided accurate measurements when the source was less than 4 km from the station[25]. When using the mini-AUARs for near-field measurements the following methodology was employed. The mini-AUAR was deployed and the GPS coordinates of its hydrophone were logged. The *Akademik Oparin* deployed its LF transducer at a depth of 10 m generating a 14 Hz tonal signal with harmonics as it drifted. The distance from the transducer to the hydrophone was tracked over time using GPS, allowing plots of near field attenuation vs. range to be constructed for distances up to 1 km.

3.2.1 Analysis of TL profile TLP-4

Experimental TL profile TLP-4 is 85 km long starting at the PA-B platform location and extending through the Orlan monitor station to the center of the offshore feeding area (OFA monitor station). Figure 3.3 is a schematic map showing the layout of profile TLP-4 and the bathymetry along the profile. There are 12 source locations (A, B, C, D, E, F, G, H, I, J, K, and L) along the profile. In addition to AUARs, mini-AUARs were also deployed at the Orlan and OFA stations, recording while signals were transmitted at source locations A, B, C, F, G and H.

Figure 3.4 shows an example of data obtained using mini-AUARs. The plots illustrate the variation in the intensity *I(r)* of 14 Hz and 28 Hz continuous wave tonal signals produced by the LF transducer deployed at 10 m from the *Akademik Oparin* as it drifted away from the mini-AUARs deployed at the OFA monitoring station (Figure 3.4(a) - CW-28Hz) and Orlan monitoring station (Figure 3.4(b) - CW-14Hz). It can be seen from Figure 3.3 that the water depth at the OFA monitor station is 43 m; acoustic energy could therefore be carried by two coupled normal modes as H≈λ. Efficient transmission illustrated by Figure 3.4(a), where the relative TL $\Delta I = I_{(200m)} - I_{(800m)} \approx 9$ dB. The water depth at the Orlan monitor station is 33 m, 14 Hz acoustic energy has a 100 m wavelength so as the first mode cannot exist when $H \leq \frac{\lambda}{2}$, then acoustic energy at this frequency cannot be transferred into the water column.

[24] The gain of the AUARs was set to record low level ambient or anthropogenic acoustic signals.
[25] Distances of less than 1 km are of special interest for TL at infrasonic (below 20 Hz) frequencies.

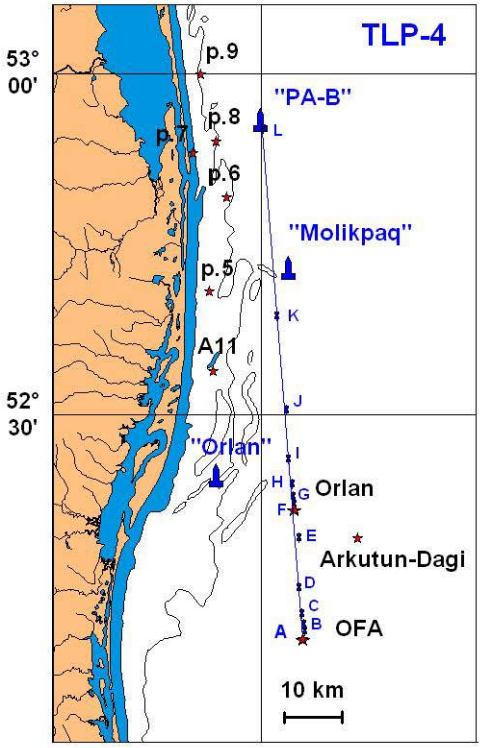

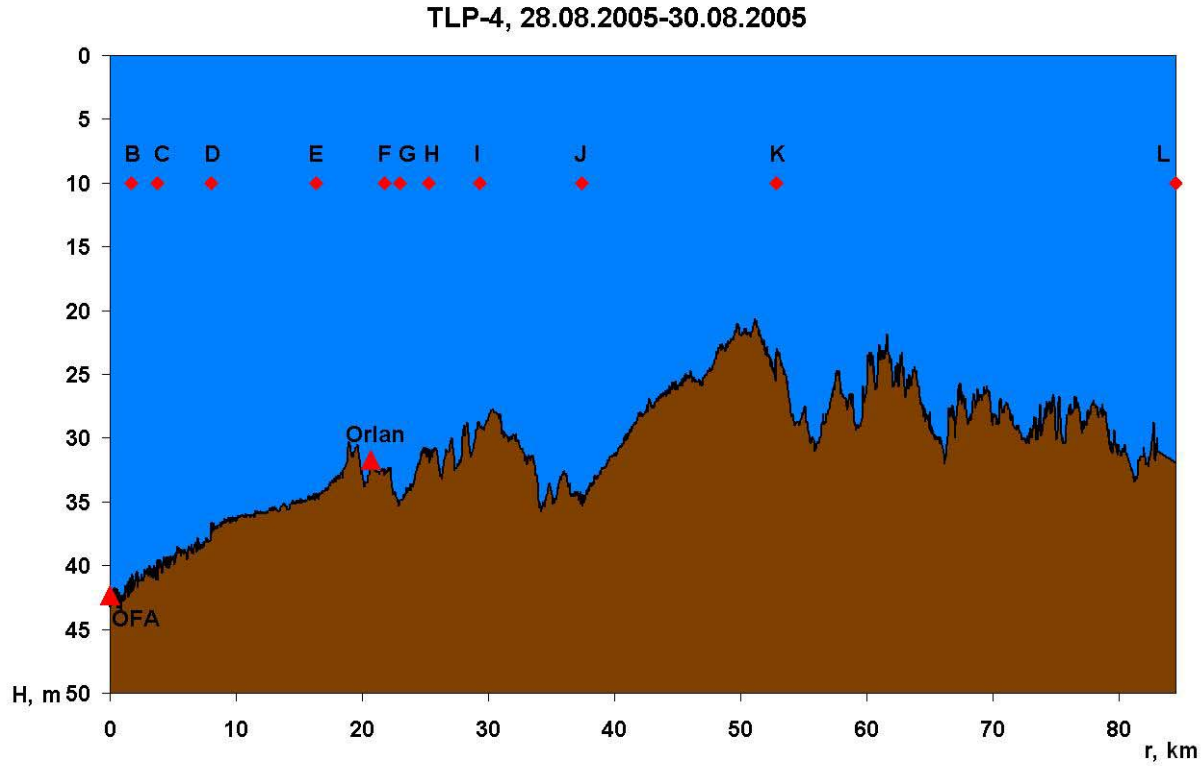

Figure 3.3 - TL profile TLP-4 from the PA-B CGBS location to the Orlan and OFA monitor stations. (a) Schematic map showing the experimental layout (b) bathymetry along the profile as well as the source, and receiver locations.

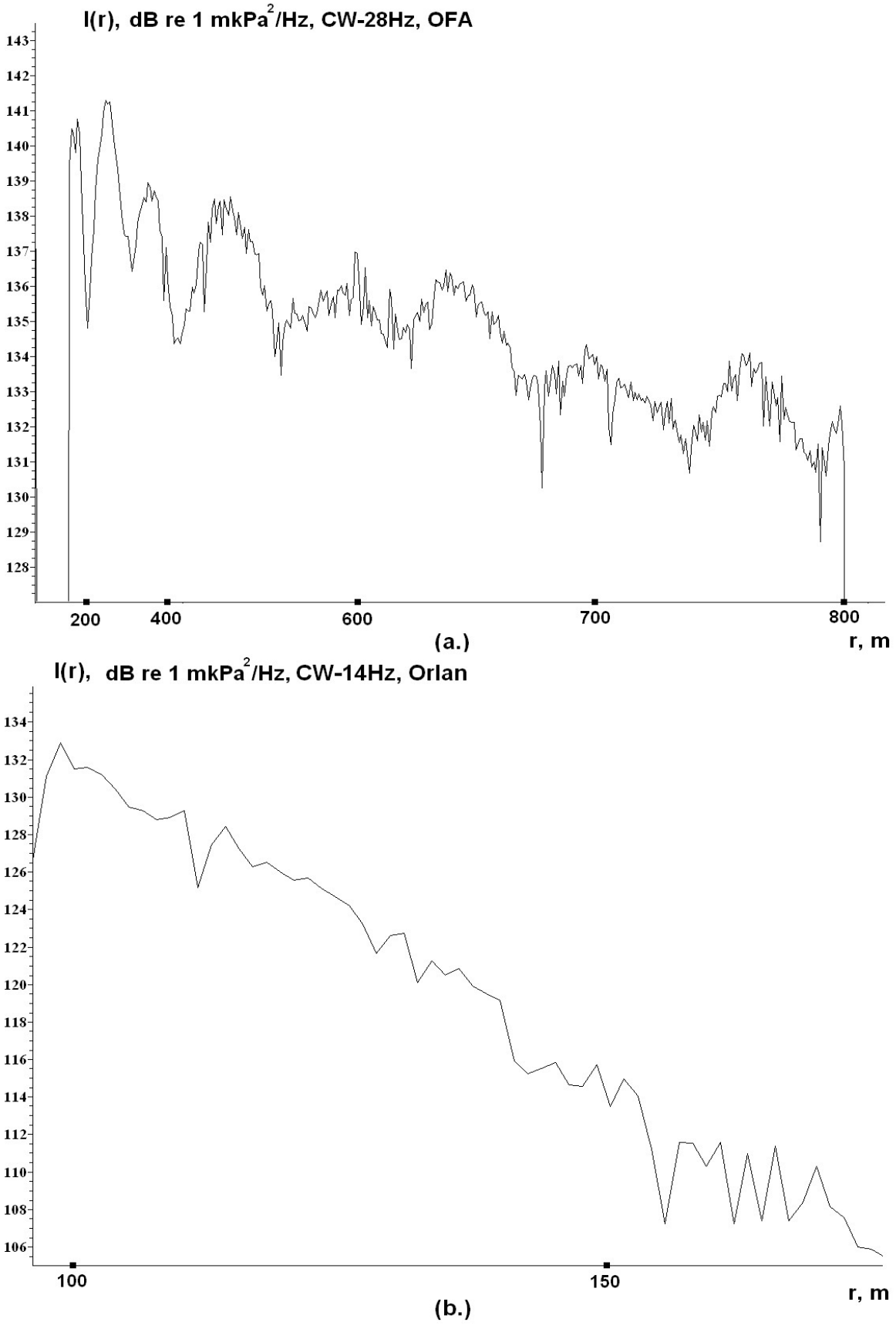

Figure 3.4 – Plots showing the variation of intensity with range to the source (*I(r)*)for two tonal signals. (a) 28 Hz CW tonal signal at the OFA monitor station (43 m depth) and (b) 14 Hz CW tonal signal at the Orlan monitor station (33 m depth).

This transmission is clearly shown by Figure 3.4(b), where the relative TL $\Delta I = I_{(100m)} - I_{(150m)} \approx$ 19 dB. It can however propagate as seismic (elastic) waves in the sub-bottom.

TL profile TLP-4 was acquired in several stages due its length (28-30 August and 14 September). Figure 3.5 gives the frequency dependent TL results for ten of the source locations (A to C and E to K)[26]. Figures 3.6-3.8 give the hydrology for the time periods during which profile TLP-4 was acquired. Figure 3.9 shows the variation in the hydrological parameters with time at location TLP-4D. Vertical profiles of sound velocity *C(z,t)* and temperature *T(z,t)* were acquired with the hydrologic sonde each hour for 12 hours (half a daily tide cycle) from a vessel anchored at source location TLP-4D. Figure 3.9 illustrates the variation in the temperature profile with time *T(z,t)* from 23:00 on 29 August to 01:30 on 30 August and shows that the surface tide was accompanied by a solitary non-linear tidal internal wave approx 6 m high. This tidal internal wave drove the seasonal pycnocline from 10 to 16 m; this phenomenon is common for the shelf areas of tidal seas. Tidal currents in this area of the NE Sakhalin shelf cause surface currents to flow towards the shore and bottom currents from the shore. Figure 3.9 also displays that from 03:00 to 05:00 on the 30th August the water below 20 m was approx 1°C warmer, probably resulting from the flow of warm bottom waters from shallow areas. Low tides lead to the opposite effect, cold waters from the Sea of Okhotsk flow into the shallow areas near bottom and the surface flow direction is away from the shore.

3.2.2 Analysis of point-to-point TL profile TLP-8

Figure 3.2 shows the location of point-to-point TL profile TLP-8. The source location was the location of the PA-B CGBS and the receiving location the Piltun (20 m) acoustic station approximately to the east of the mouth of Piltun Bay. Figure 3.10 gives the hydrology (sound velocity *C(z,t),* temperature *T(z,t)* and salinity *S(z,t)*) acquired on 21 August 2005 prior to transmission from the PA-B location. Figure 3.11 gives the frequency dependent TL results between the PA-B platform location and the Piltun acoustic station.

3.2.3 Analysis of point-to-point TL profile TLP-9

Figure 3.2 shows the location of point-to-point TL profile TLP-9. The source location was the location of the PA-B CGBS and the receiving locations the A8 (20 m) and A7 (10 m)

[26] The TL is the difference in intensity between the source reference and the receiver. Although dimensionless the TL is for intensity not amplitude

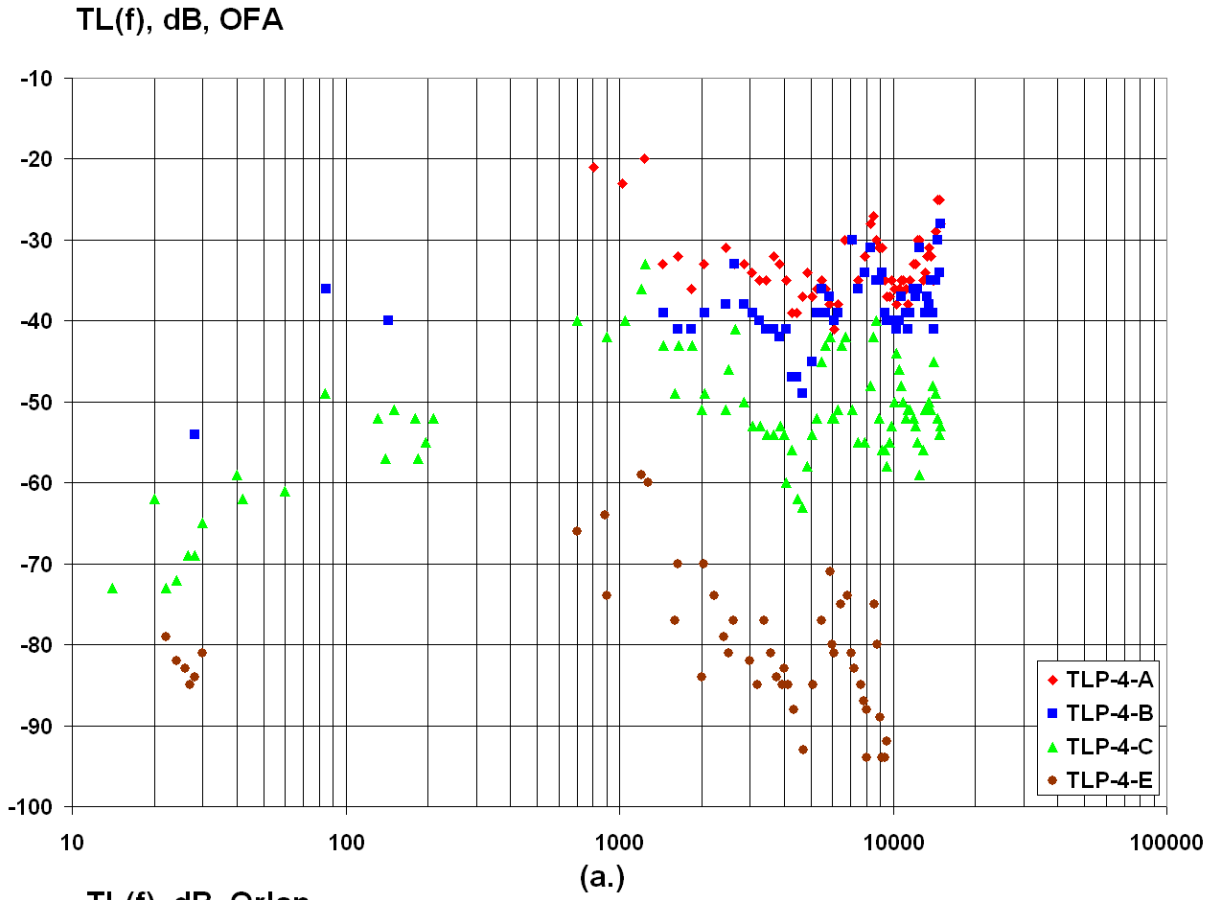

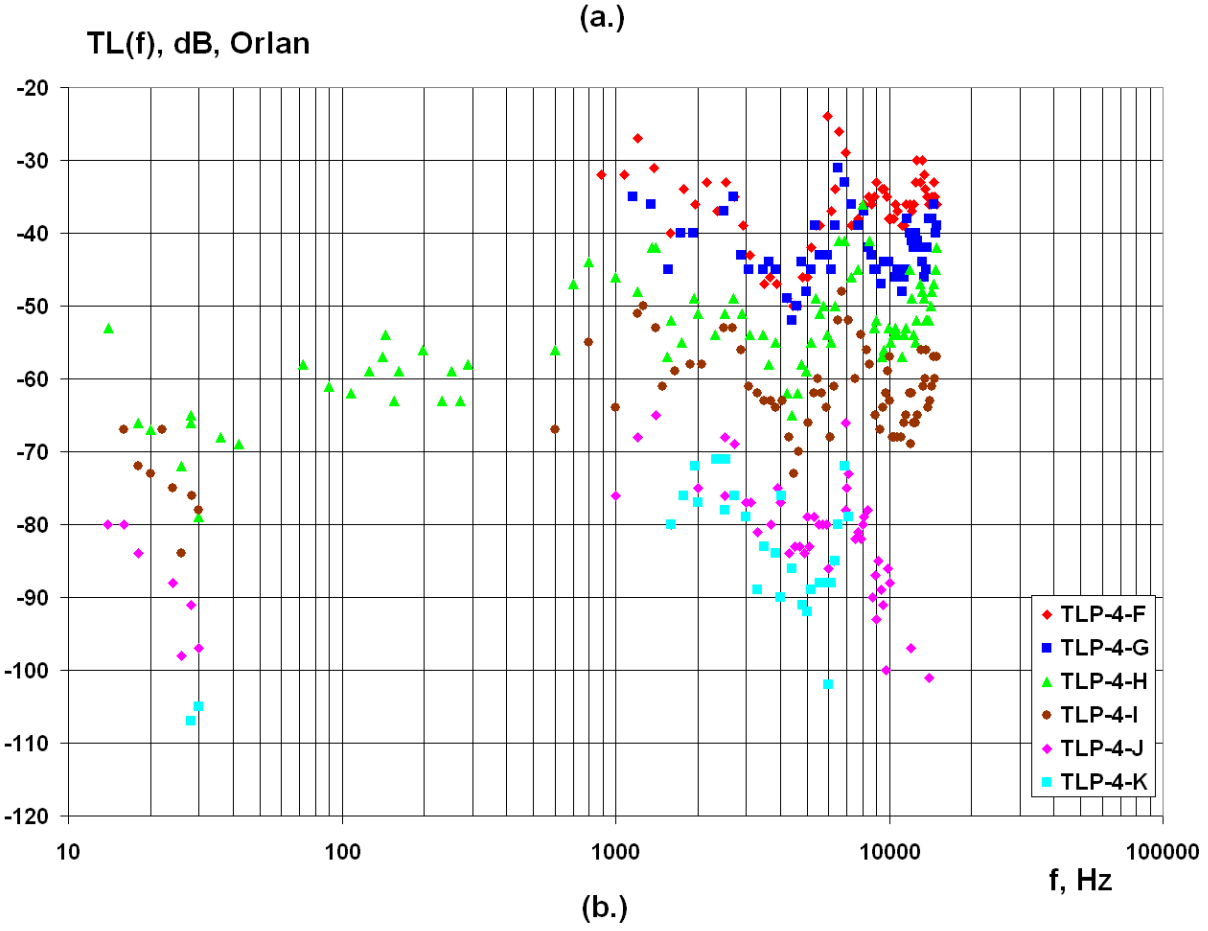

Figure 3.5 – TLP-4: Frequency dependent TL plot showing the results for all the source locations (in different colors) (a) OFA and (b) Orlan monitor stations.

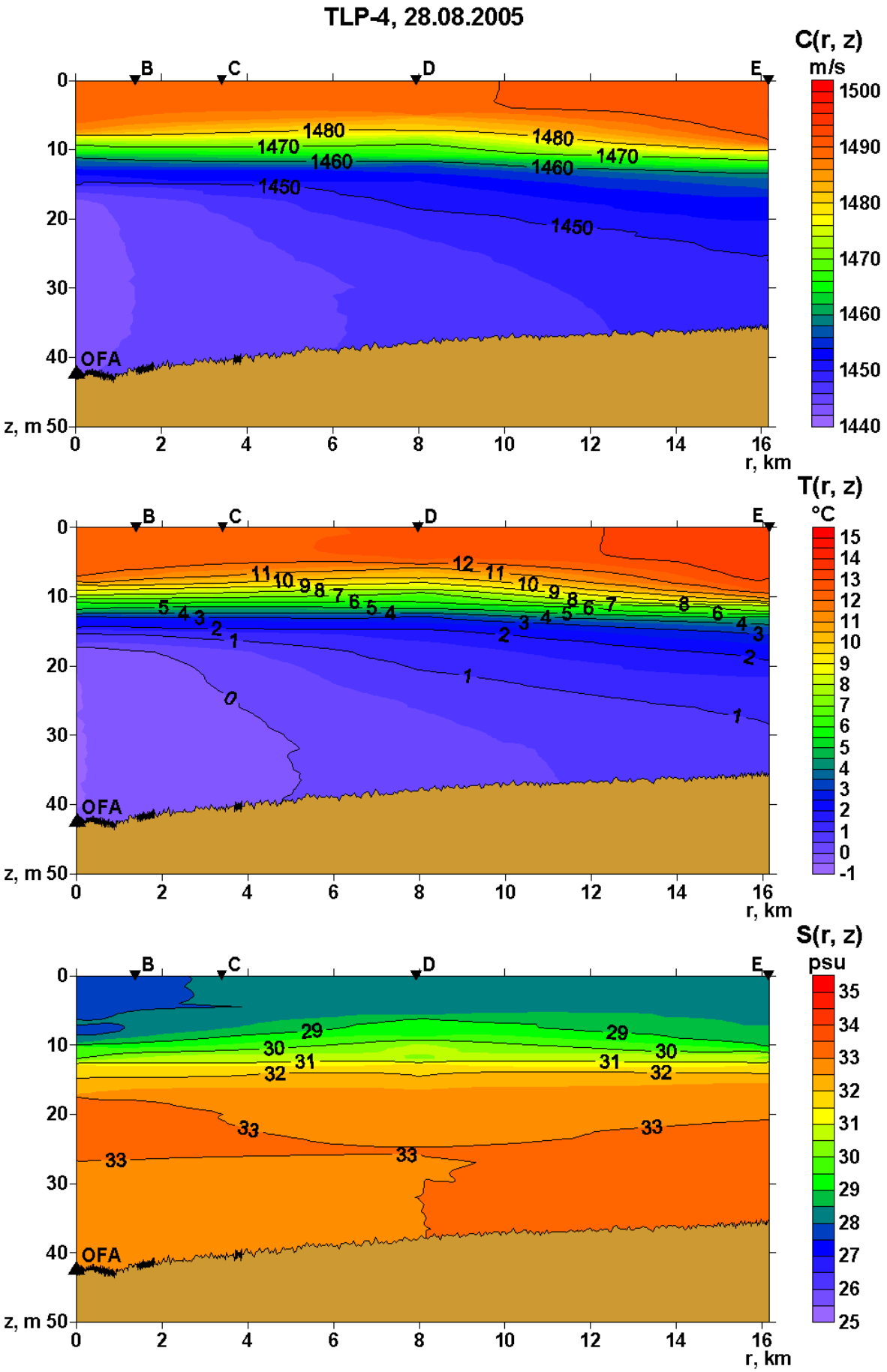

Figure 3.6 - TLP-4: Bathymetry and hydrologic parameters (velocity *C(z,r)*, temperature *T(z,r)*, and salinity *S(z,r)* acquired on 28 August 2005.

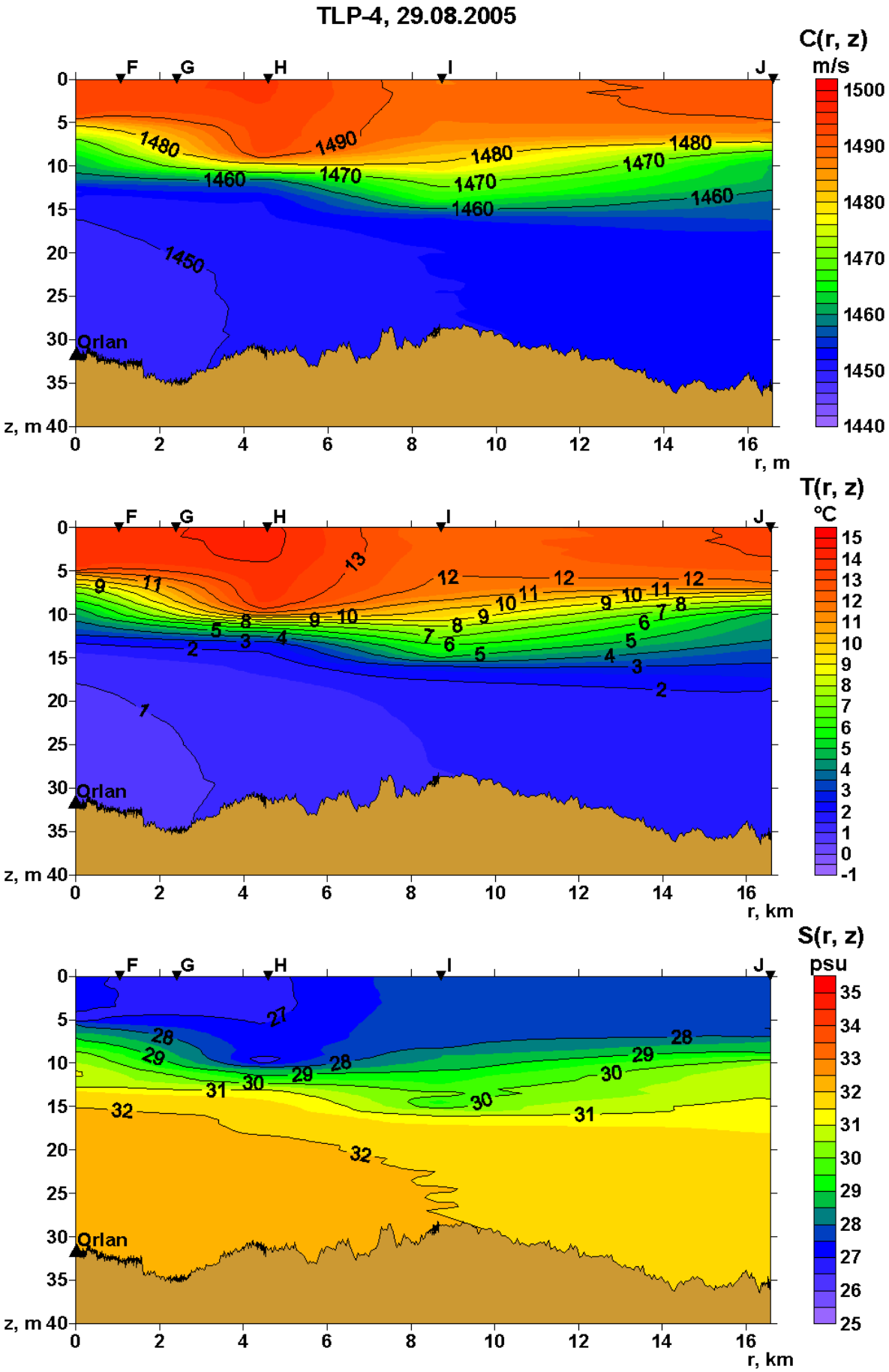

Figure 3.7 - TLP-4: Bathymetry and hydrologic parameters (velocity *C(z,r)*, temperature *T(z,r)*, and salinity *S(z,r)* acquired on 29 August 2005.

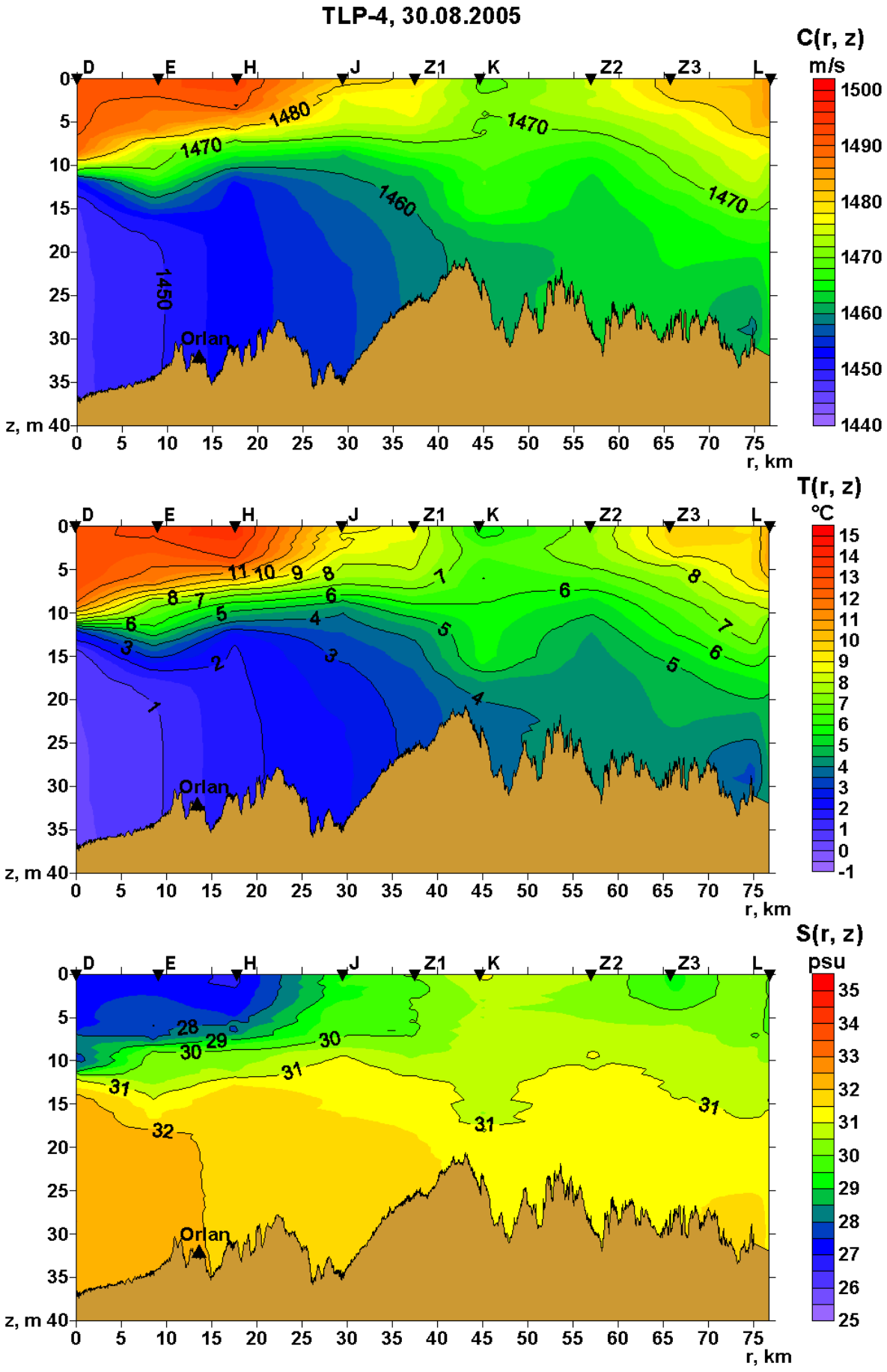

Figure 3.8 - TLP-4: Bathymetry and hydrologic parameters (velocity *C(z,r)*, temperature *T(z,r)*, and salinity *S(z,r)* acquired on 30 August 2005.

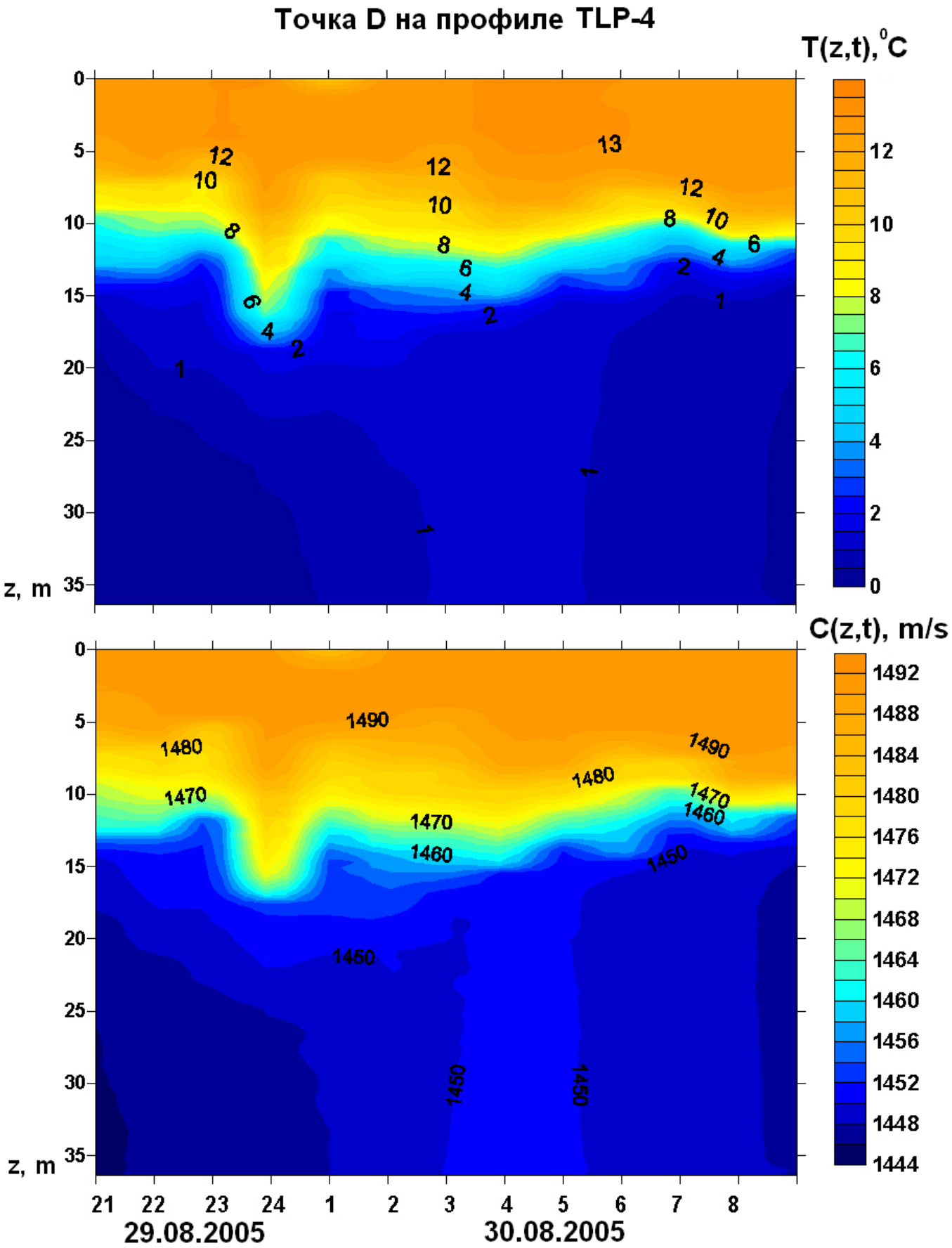

Figure 3.9 - TLP-4: Variations in the sound velocity *C(z,t)* and temperature *T(z,t)* profiles acquired from the *Akademik Oparin* when anchored at source location TLP-4D.

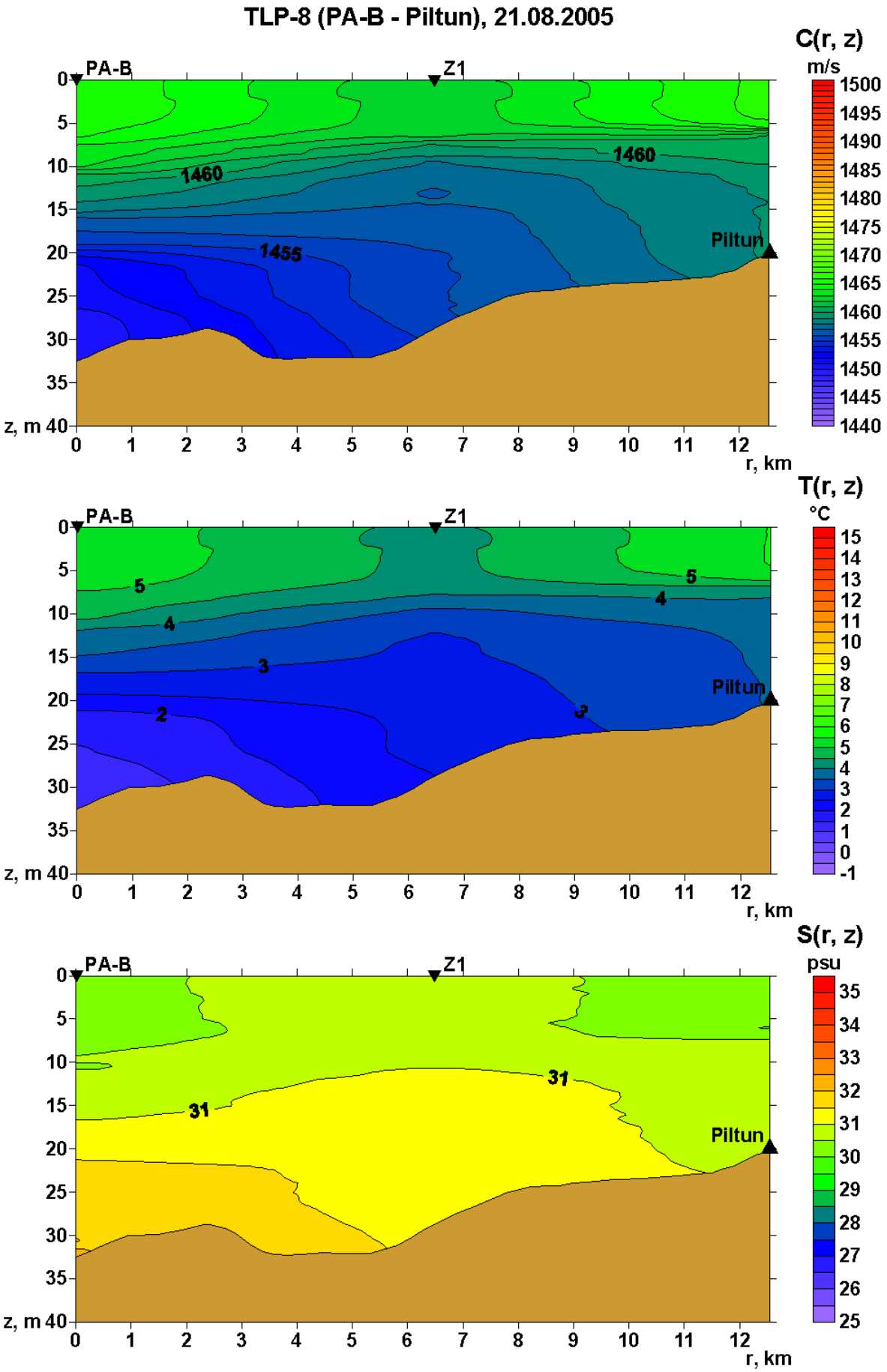

Figure 3.10 - TLP-8: Bathymetry and hydrologic parameters (velocity *C(z,r)*, temperature *T(z,r)*, and salinity *S(z,r)* acquired on 21 August 2005.

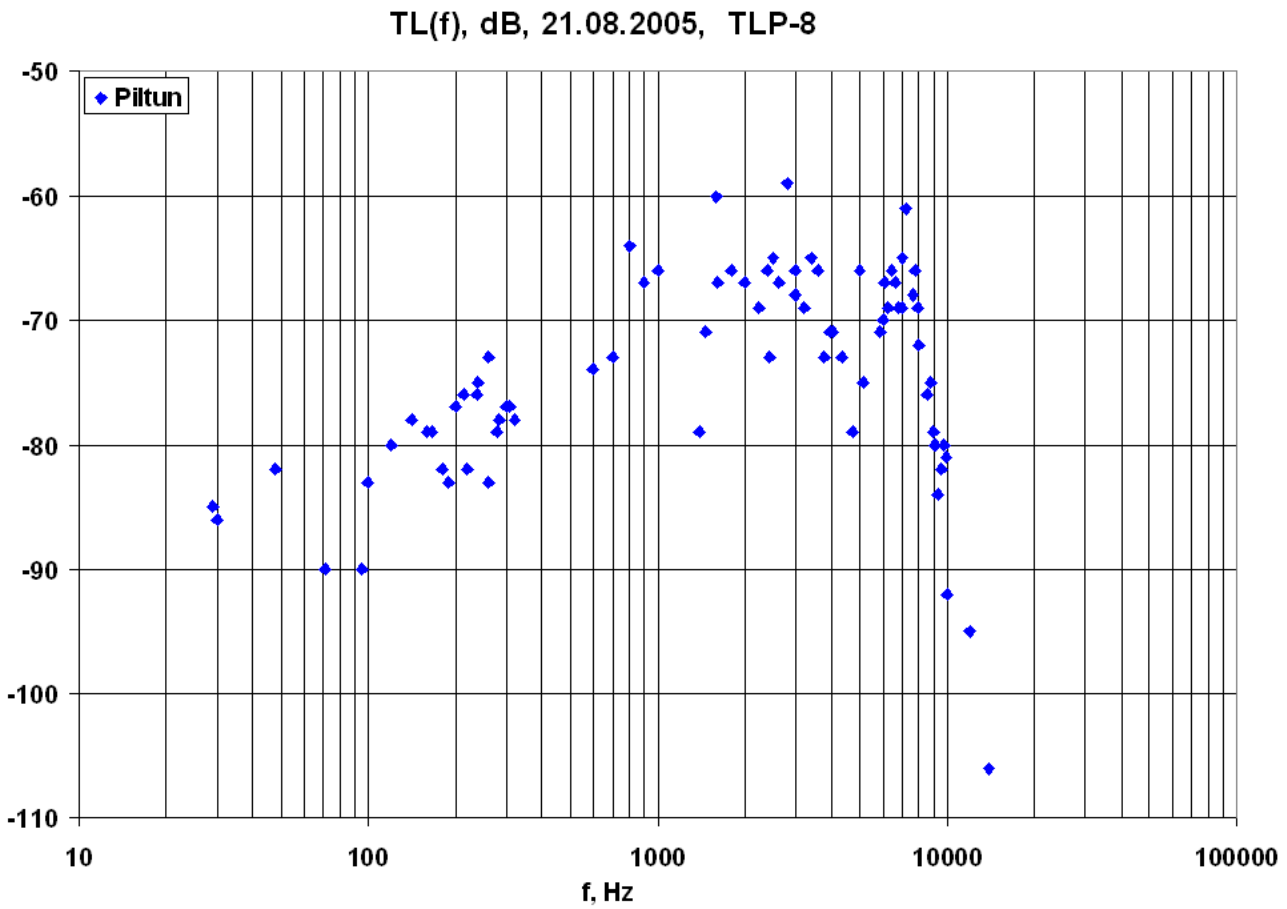

Figure 3.11 – TLP-8: Frequency dependent TL plot showing the results for the Piltun acoustic station.

acoustic stations approximately to the west of the PA-B CGBS location; the profile is approximately perpendicular to the shoreline. Figure 3.12 gives the hydrology (sound velocity *C(z,t),* temperature *T(z,t)* and salinity *S(z,t)*) acquired on 30 August 2005 prior to transmission from the PA-B CGBS location. Figure 3.13 gives the frequency dependent TL results between the PA-B CGBS location and the two acoustic stations.

3.2.4 Analysis of point-to-point TL profile TLP-10

Figure 3.2 shows the location of point-to-point TL profile TLP-10. The source location was the location of the PA-B CGBS and the receiving location the Odoptu-PA-B acoustic station (20 m). Figure 3.14 gives the hydrology (sound velocity *C(z,t),* temperature *T(z,t)* and salinity *S(z,t)*) acquired on 21 August 2005 prior to transmission from the PA-B CGBS location. Figure 3.15 gives the frequency dependent TL results between the PA-B CGBS location and the Odoptu-PA-B acoustic station.

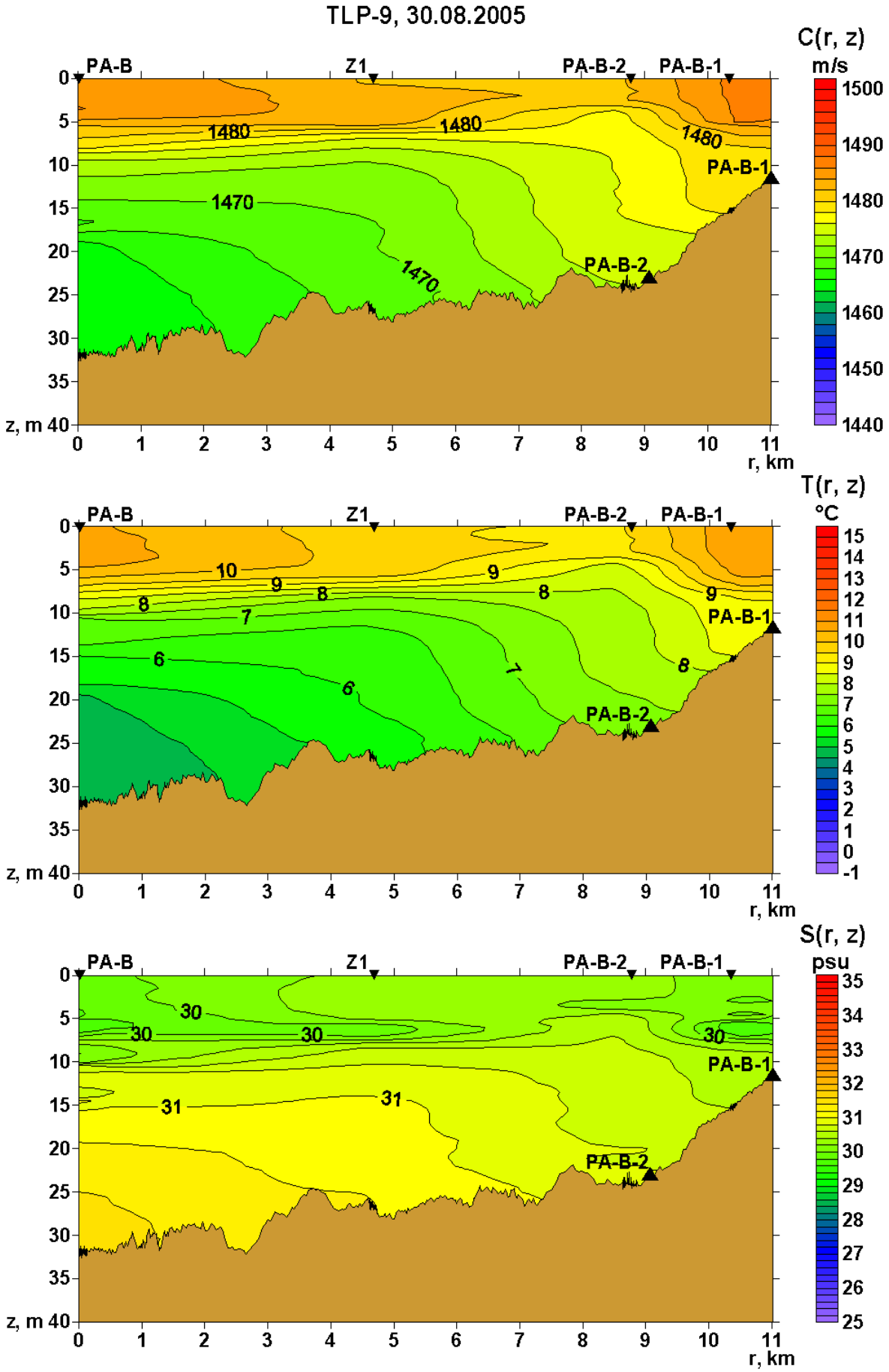

Figure 3.12 - TLP-9: Bathymetry and hydrologic parameters (velocity *C(z,r)*, temperature *T(z,r)*, and salinity *S(z,r)* acquired on 30 August 2005.

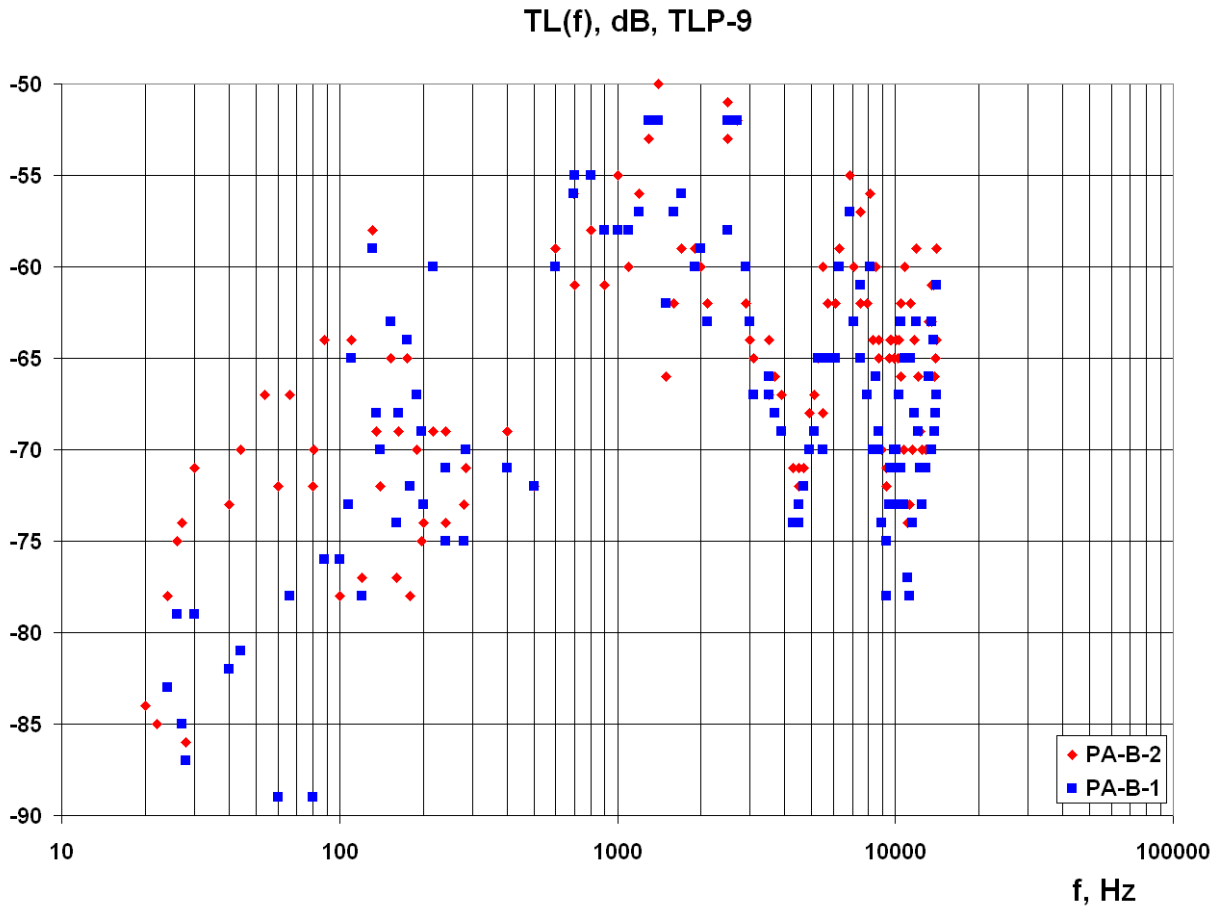

Figure 3.13 – TLP-9: Frequency dependent TL plot showing the results for both the receiver locations (in different colors).

3.2.5 Analysis of point-to-point TL profiles TLP-11 and TLP-12

Figure 3.2 shows the location of point-to-point TL profiles TLP-11 and TLP-12. The source location was the location of the PA-B CGBS and the receiving locations the Odoptu-S-10 monitor station (10 m) (TLP-11) and the Odoptu-N-20 monitor station (20 m) (TLP-12). Figure 3.16 (TLP-11) and Figure 3.17 (TLP-12) give the hydrology (sound velocity *C(z,t),* temperature *T(z,t)* and salinity *S(z,t)*) acquired along the two profiles on 21 August 2005 prior to transmission from the PA-B CGBS location. Figure 3.18 gives the frequency dependent TL results between the PA-B CGBS location and the two monitor stations.

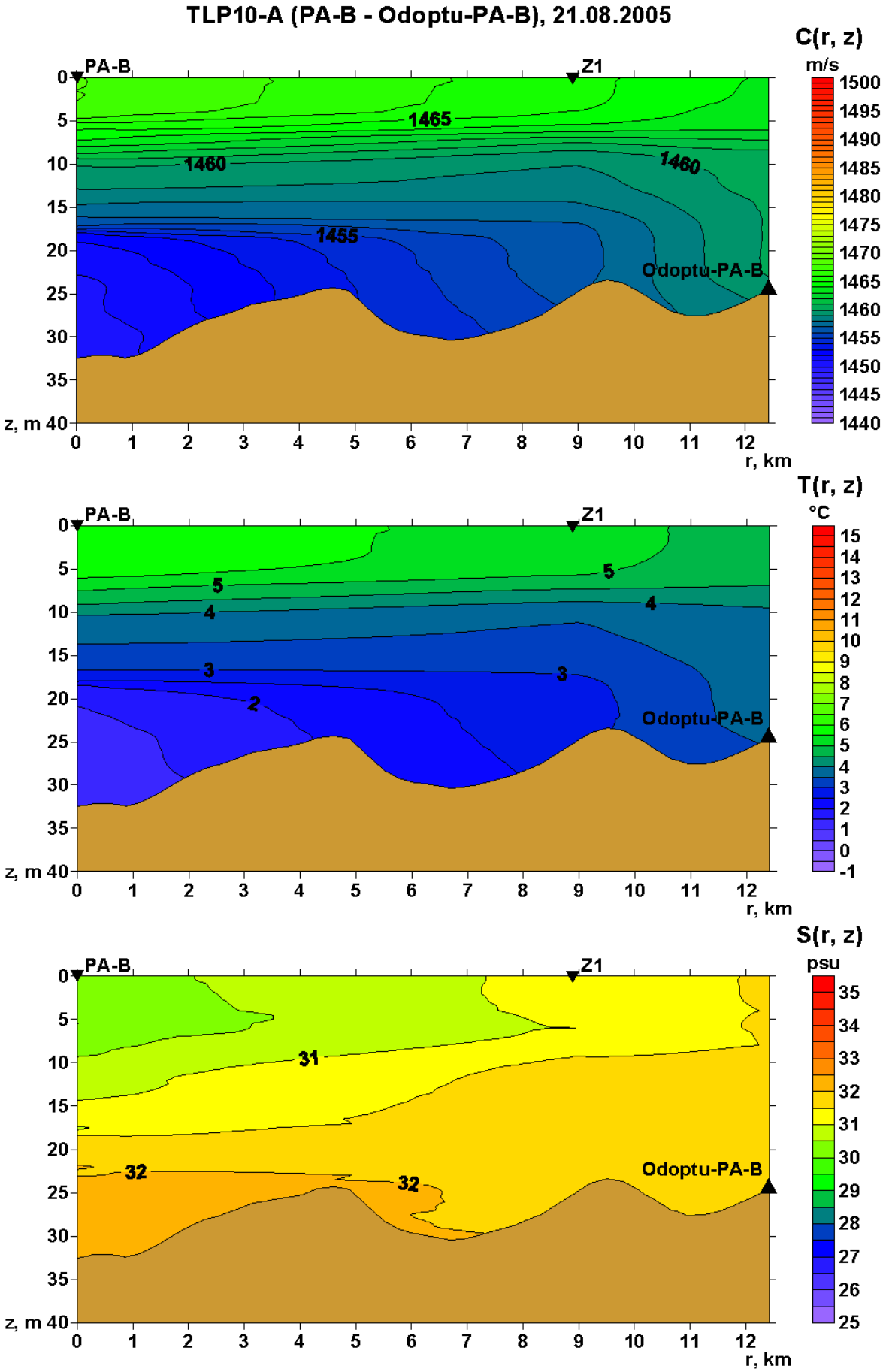

Figure 3.14 - TLP-10: Bathymetry and hydrologic parameters (velocity *C(z,r)*, temperature *T(z,r)*, and salinity *S(z,r)* acquired on 30 August 2005.

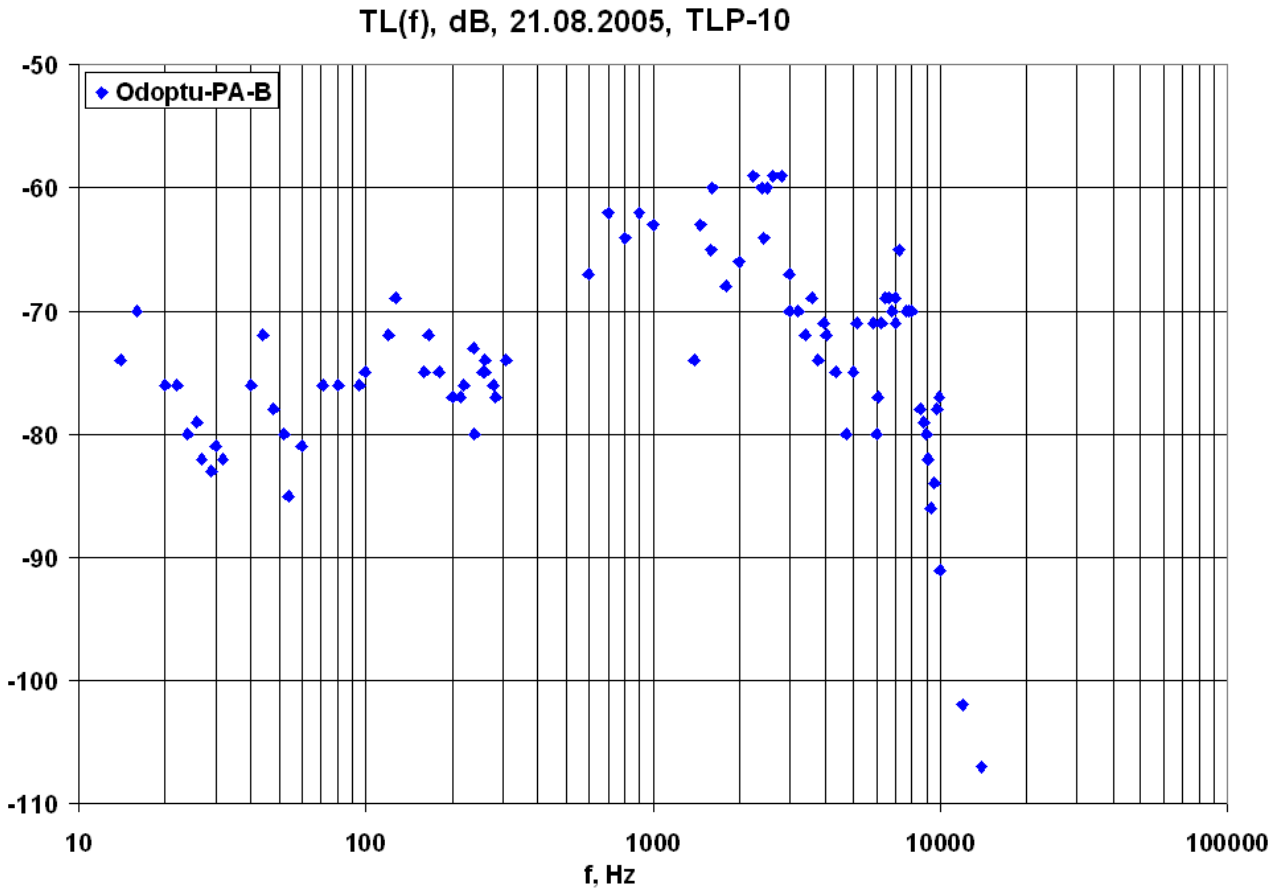

Figure 3.15 – TLP-10: Frequency dependent TL plot showing the results for the Odoptu-PA-B monitor station.

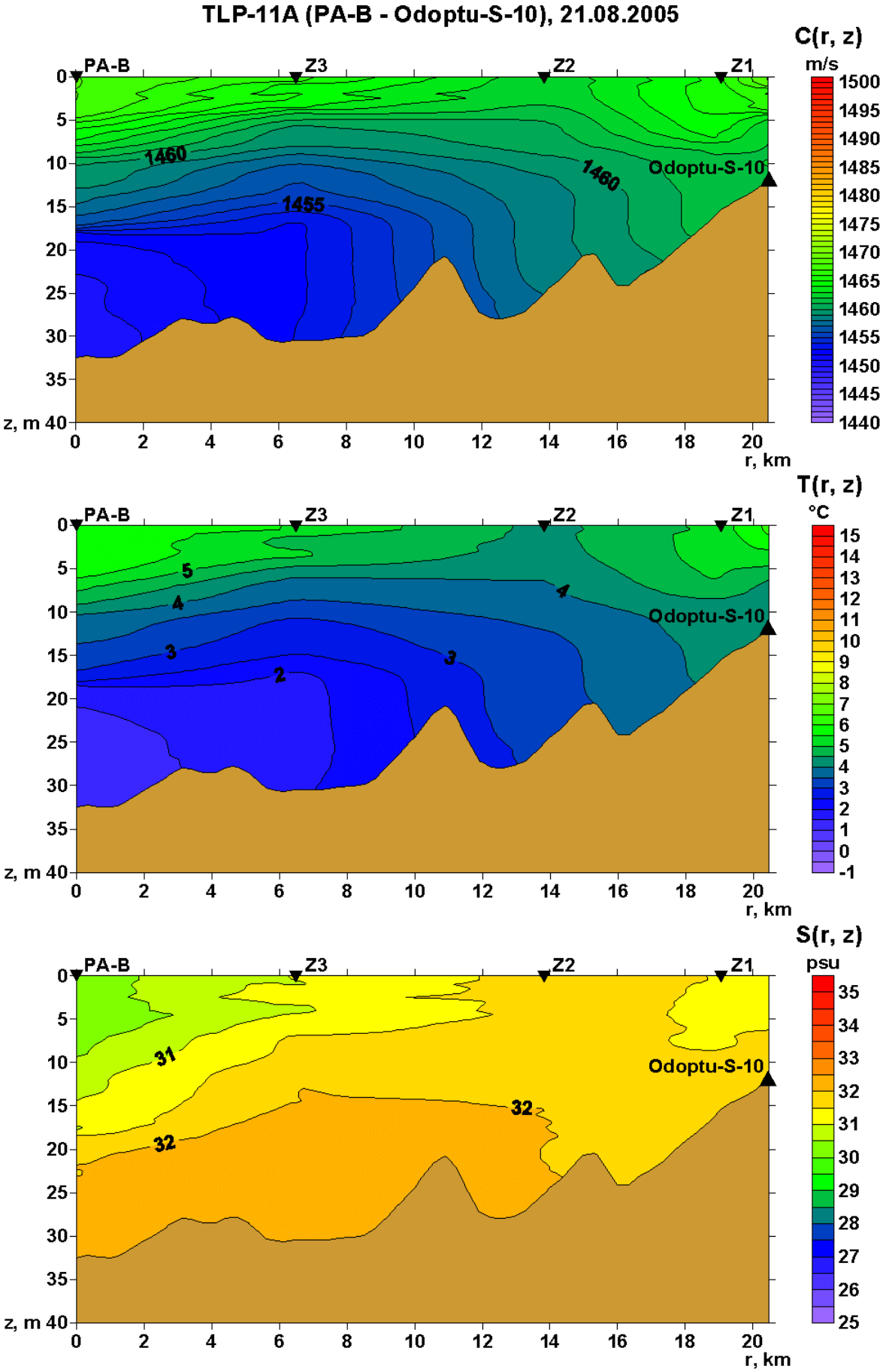

Figure 3.16 - TLP-11: Bathymetry and hydrologic parameters (velocity *C(z,r)*, temperature *T(z,r)*, and salinity *S(z,r)* acquired on 30 August 2005.

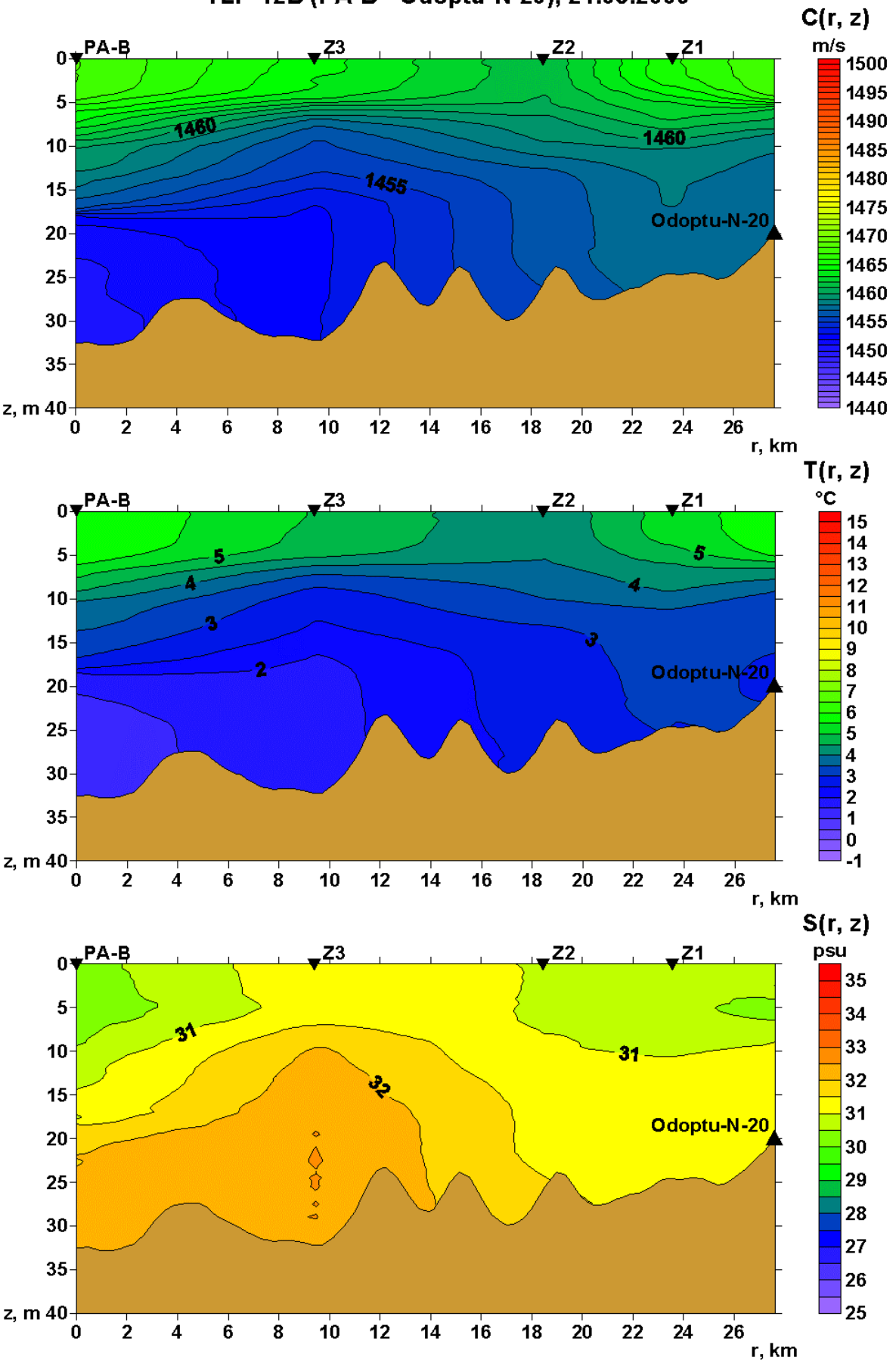

Figure 3.17 - TLP-12: Bathymetry and hydrologic parameters (velocity *C(z,r)*, temperature *T(z,r)*, and salinity *S(z,r)* acquired on 30 August 2005.

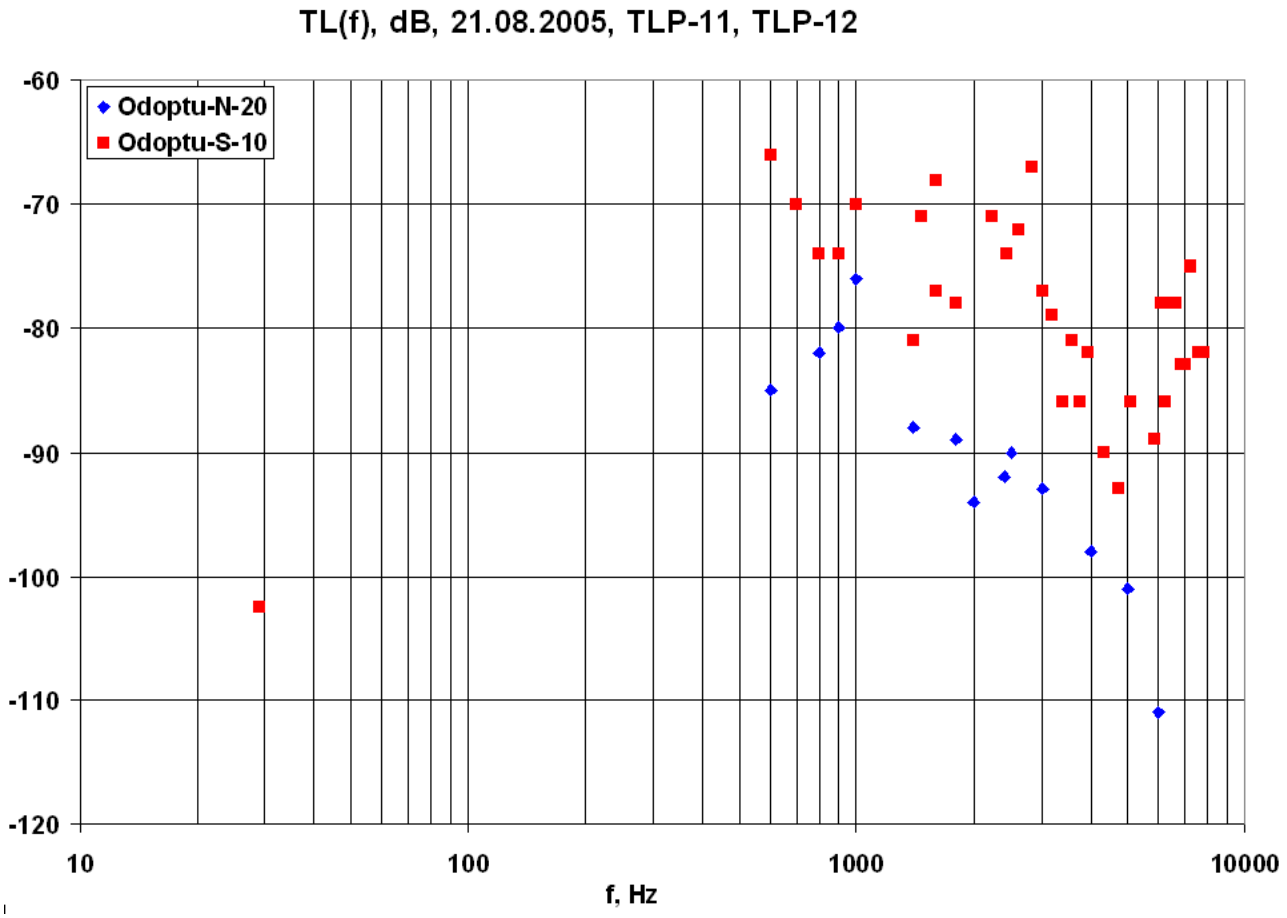

Figure 3.18 – TLP-11 and TLP-12: Frequency dependent TL plot showing the results for both the receiver locations (in different colors).

3.2.6 Analysis of point-to-point TL profile TLP-13

Figure 3.2 shows the location of point-to-point TL profile TLP-13. The source location was the location of the PA-B CGBS and the receiving locations the PA-B-20 (20 m) and PA-B-10 (10 m) monitor stations to the south-west of the PA-B CGBS location. Figure 3.19 gives the hydrology (sound velocity *C(z,t),* temperature *T(z,t)* and salinity *S(z,t)*) acquired on 21 August 2005 prior to transmission from the PA-B location. As can be seen from Figure 3.2 TLP-13 is close to the location of TLP-9 where the hydrology was sampled on 30 August (Figure 3.12). Approximately synchronous acoustic and hydrological measurements were acquired along this profile on 21 August. This data is presented on Figures 3.20 and 3.21. Figure 3.20 gives the frequency dependent TL results between the PA-B CGBS location and the two monitor stations.

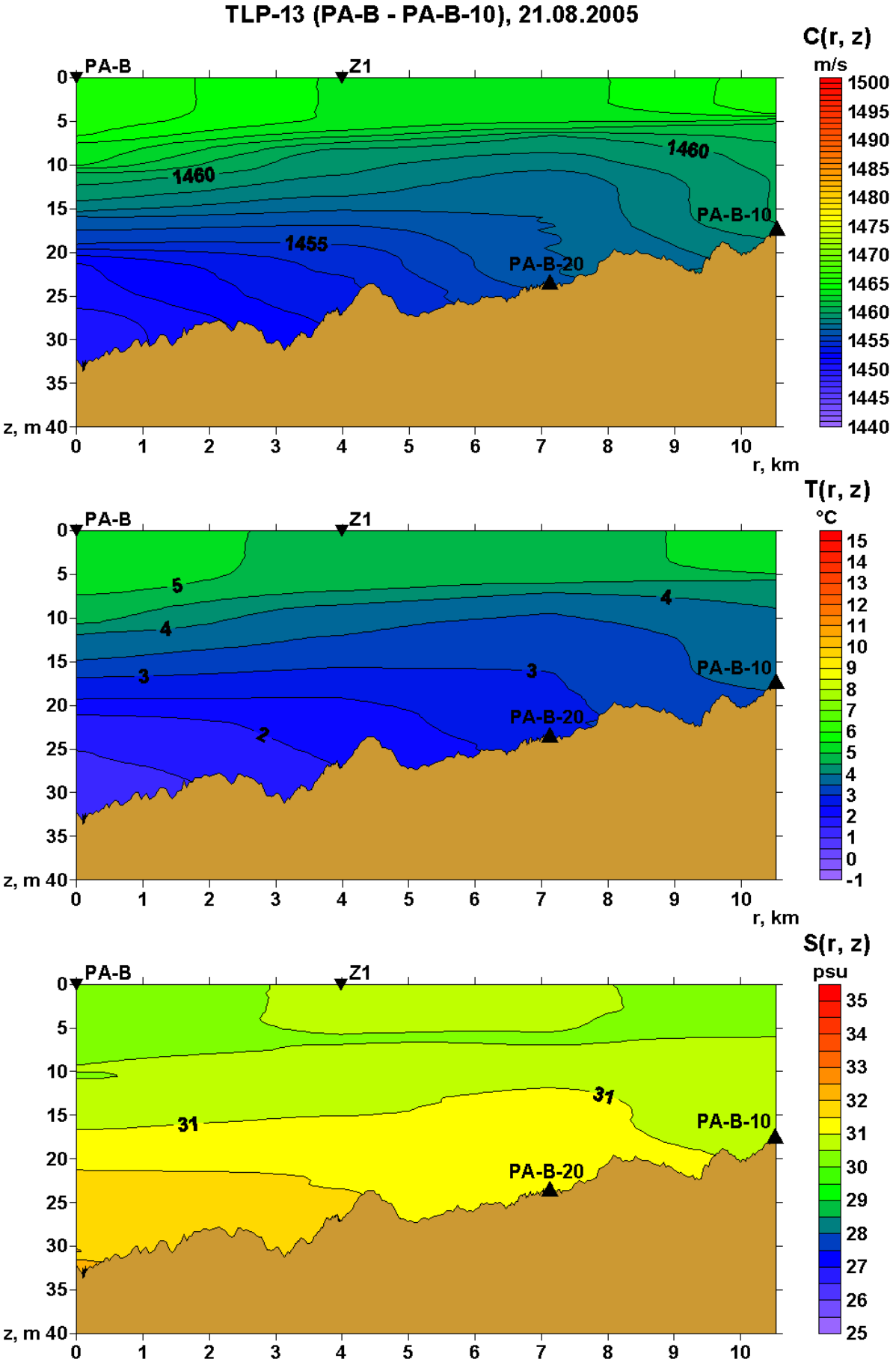

Figure 3.19 - TLP-13: Bathymetry and hydrologic parameters (velocity *C(z,r)*, temperature *T(z,r)*, and salinity *S(z,r)* acquired on 21 August 2005.

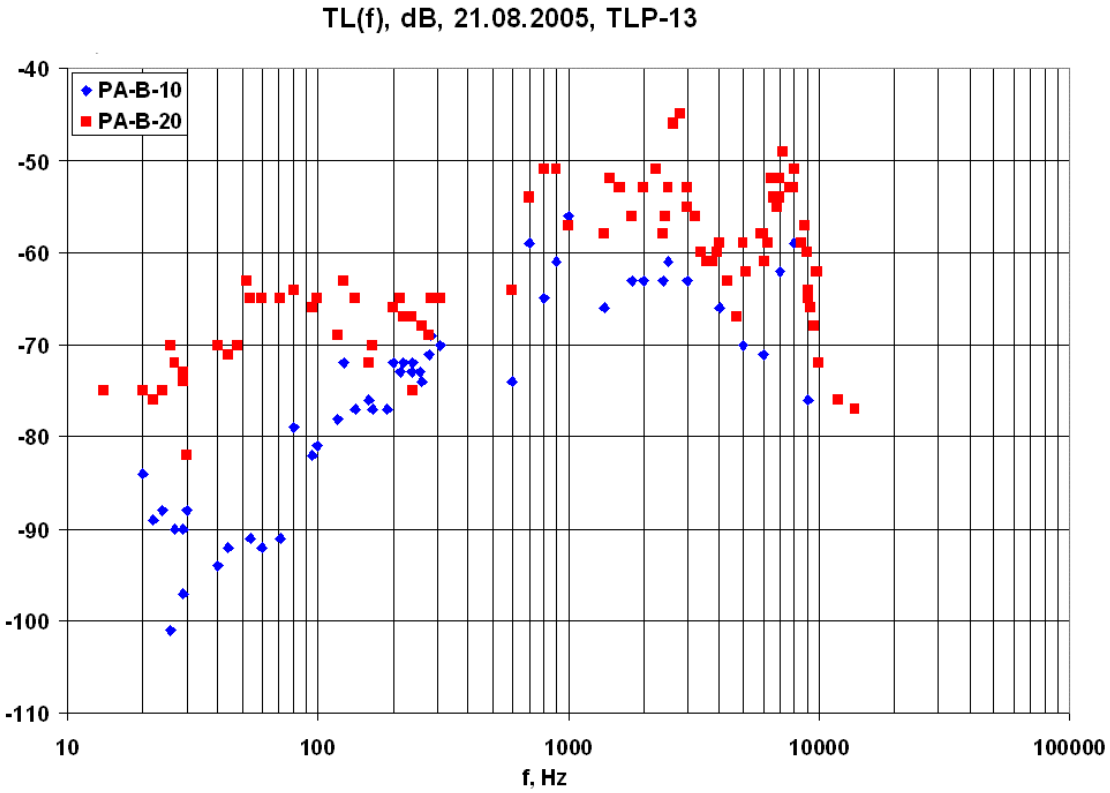

Figure 3.20 – TLP-13: Frequency dependent TL plot showing the results for both the receiver locations (in different colors) (21 August).

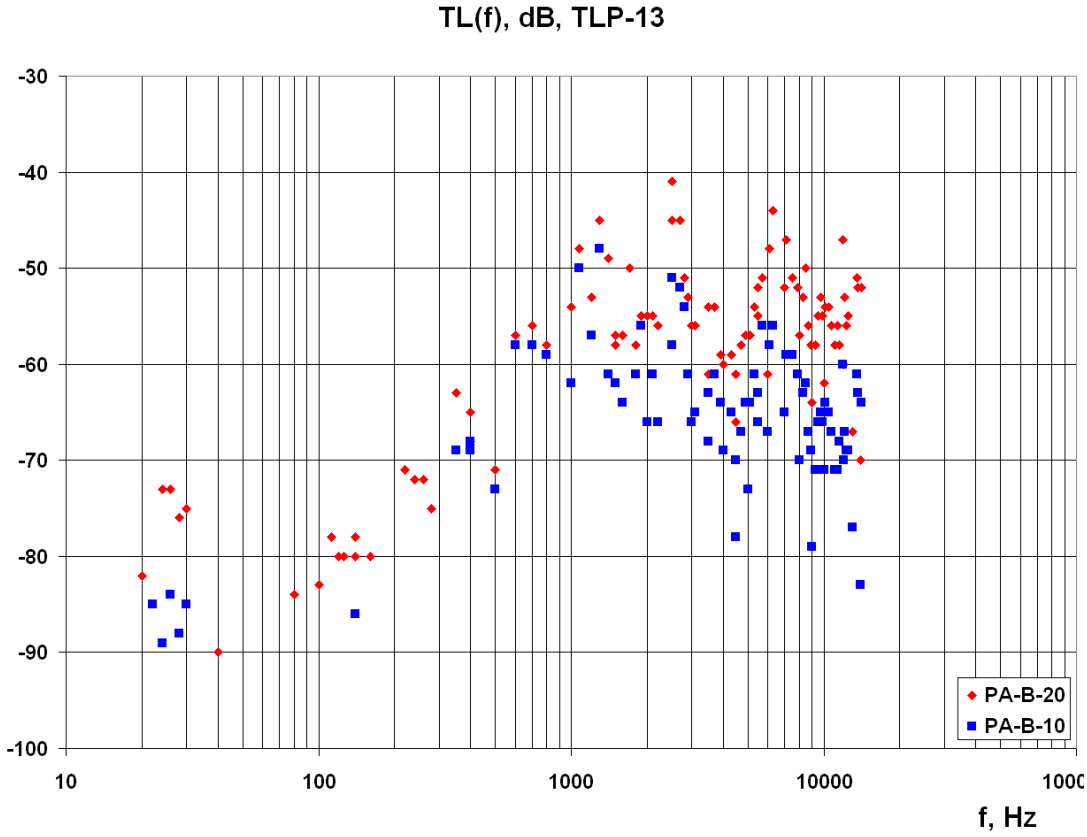

Figure 3.21 – TLP-13: Frequency dependent TL plot showing the results for both the receiver locations (in different colors) (30 August).

The hydrology along profile TLP-13 and nearby TLP-9was significantly different on 21 and 30 August (Figures 3.12 and 3.19), but the TL difference (Figures 3.20 and 3.21) was less than the estimation error expected when obtaining TL from experimental data.

3.3 Analysis of TL from the Odoptu License to the Piltun Feeding Area

Figure 3.22(a) shows acoustic profile TLP-15 acquired on 21-22 September. This profile was oriented east-west, with seven source locations being acquired (TLP15-A, -B, -C, -D, -E, -F, and -G). The data was recorded on the Odoptu-N-10 and Odoptu-N-20 monitor stations. Acoustic signals were generated by the transducers deployed at 10 m depth from the *Academik Oparin*. Figure 3.22(b) displays two sound velocity profiles *C(r,z)* generated from hydrological measurements taken at the source locations on the profile (TLP-15A to G) and back[27]. The sound velocity data acquired on 22 September had a time interval of 91 minutes between the first and last measurements. This is the minimum time required to acquire hydrology data along a 10 km profile using a vessel that enters the Piltun feeding area (source locations TLP-15A and -15B). As wind was light on 21 and 22 of September, the hydrology was stable (Figure 3.22(b)). Figure 3.23 gives the hydrology (sound velocity *C(z,t),* temperature *T(z,t)* and salinity *S(z,t)*) acquired on 21st September 2005.

Figure 3.24 gives the frequency dependent TL results for all seven source locations (LF and HF transducers) for both the Odoptu-N-10 and Odoptu-N-20 monitor stations. To estimate the TL for frequencies below 1 kHz tonal signals produced by the HF transducer and harmonics from the LF transducer were used if the signal levels exceeded the ambient noise level at the receiving point by more than 6 dB.

An experiment conducted on profile TLP-15 during the night of 21 September investigated the impact of tides on the accuracy of TL measurements acquired using broadband FM signals at frequencies of 1-15 kHz. An FM signal with repetition rate of 10 Hz was transmitted for 10 hours using a HF transducer deployed at a depth of 10 m from the *Academik Oparin* when it was anchored at source point TLP-15G (Figure 3.22(a)).

[27] Times of the hydrological measurements: 21st September: TLP-15A 9:36; -15B 10:41; -15C 11:28; -15D 13:37; -15E 14:48; -15F 18:16; -15G 19:04. 22nd September: TLP-15A 9:41; -15B 9:32; -15C 9:20; -15D 9:08; -15E 8:56; -15F 8:39; -15G 8:10.

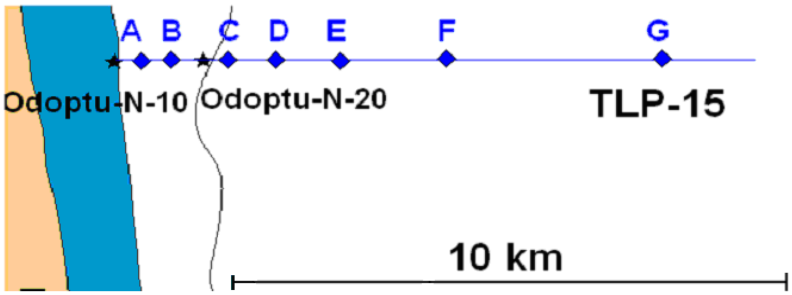

(a.)

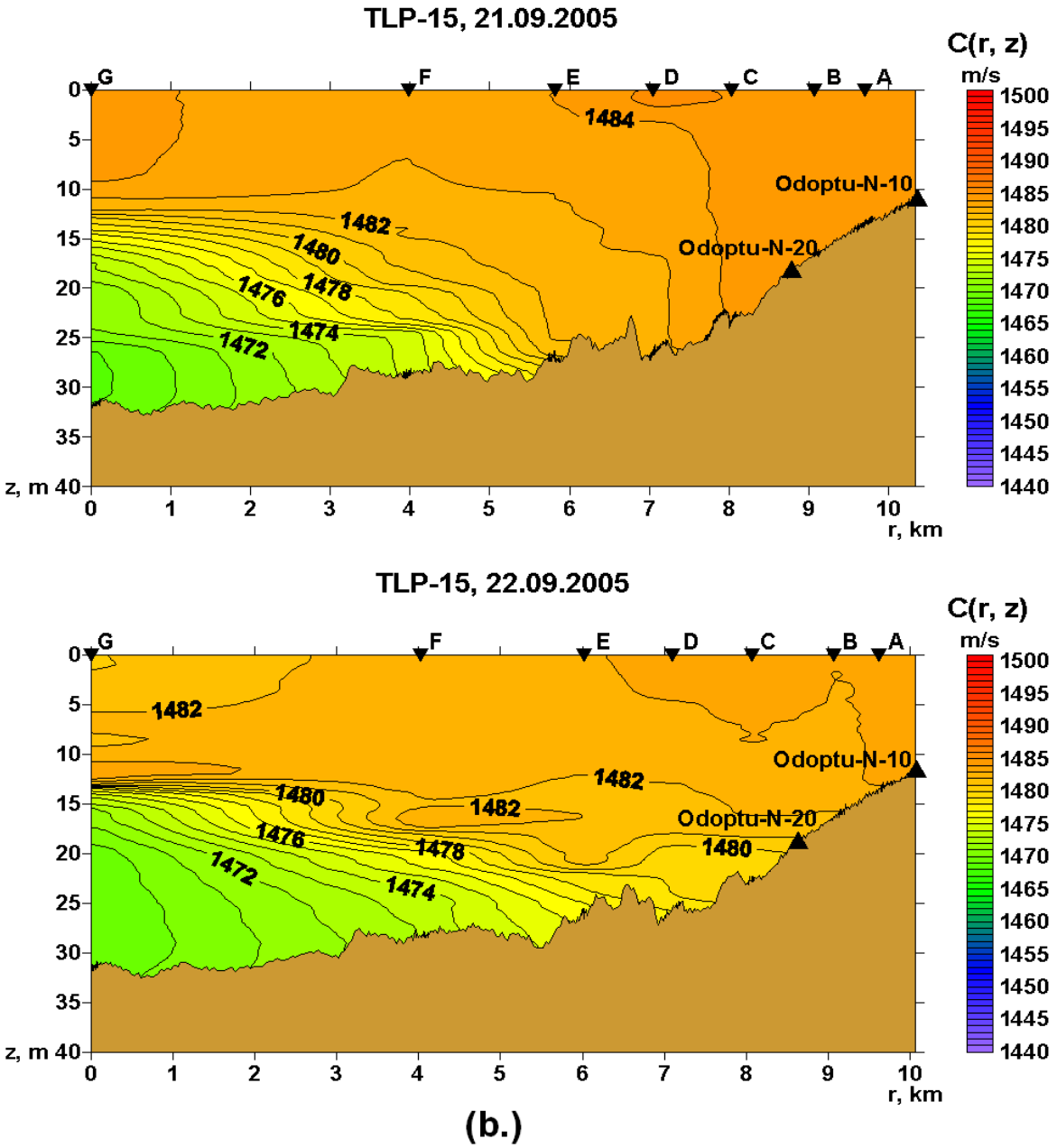

(b.)

Figure 3.22 - TL profile TLP-15 (a) Schematic map showing the experimental layout (b) bathymetry and velocity *C(z,r)* along the profile (on both 21 and 22 September) as well as the source and receiver locations.

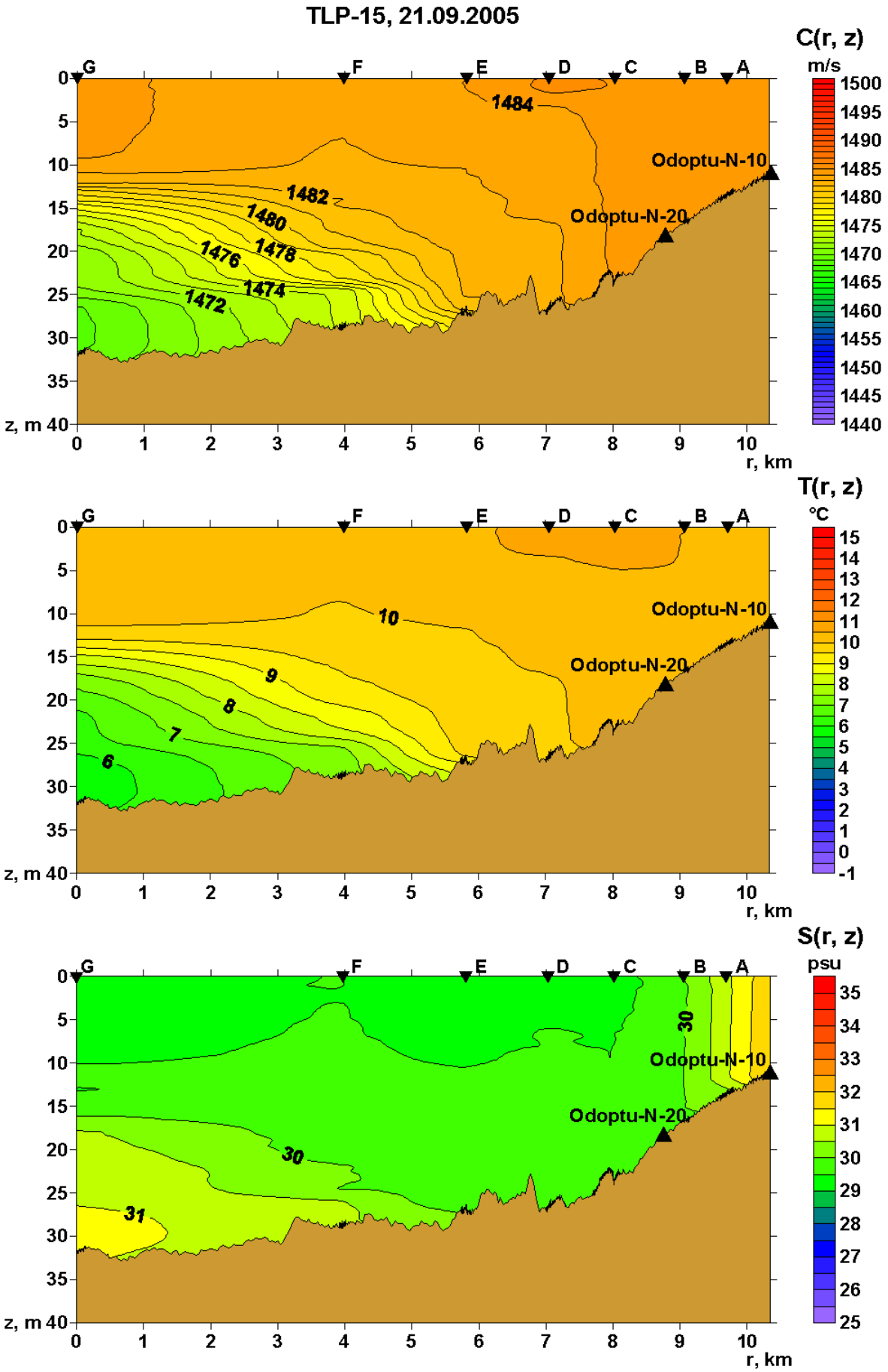

Figure 3.23 - TLP-15: Bathymetry and hydrologic parameters (velocity *C(z,r)*, temperature *T(z,r)*, and salinity *S(z,r)* acquired on 21 September 2005.

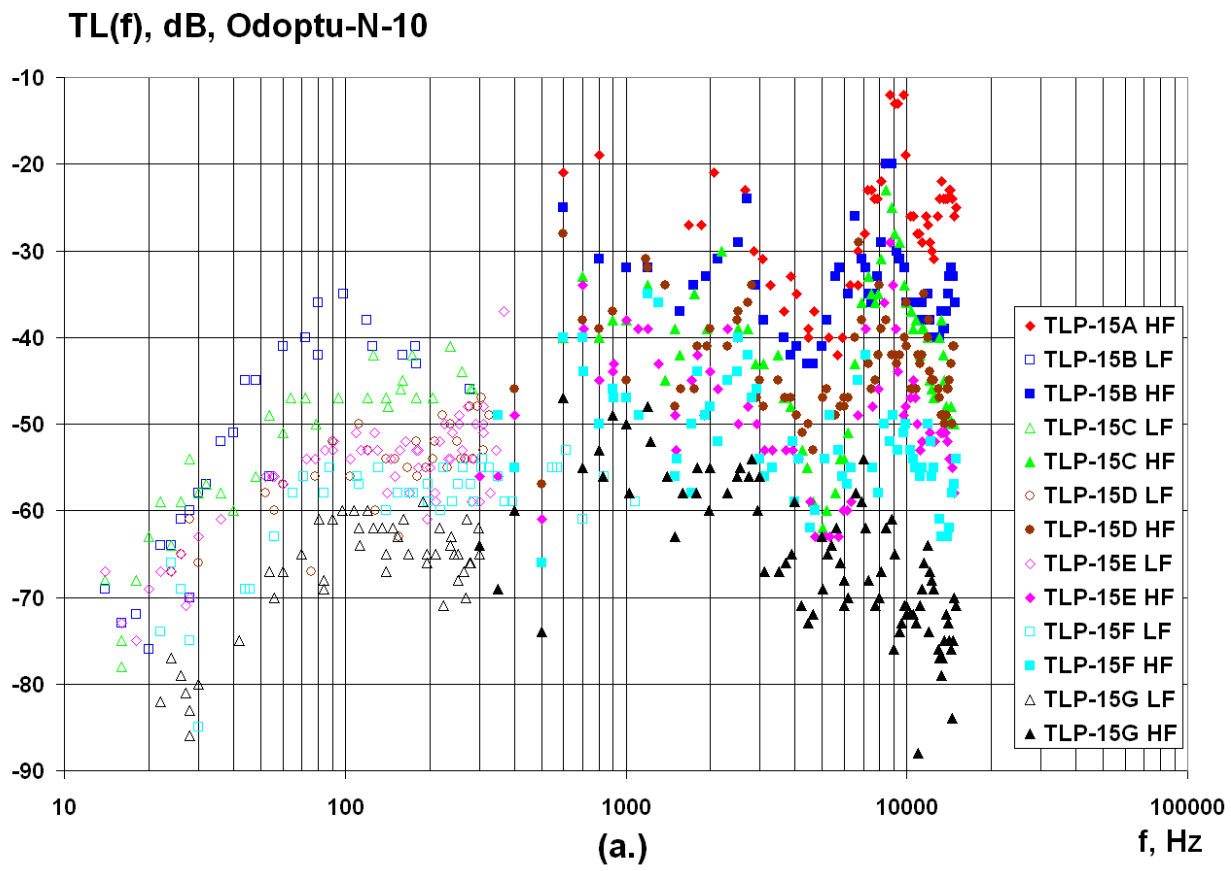

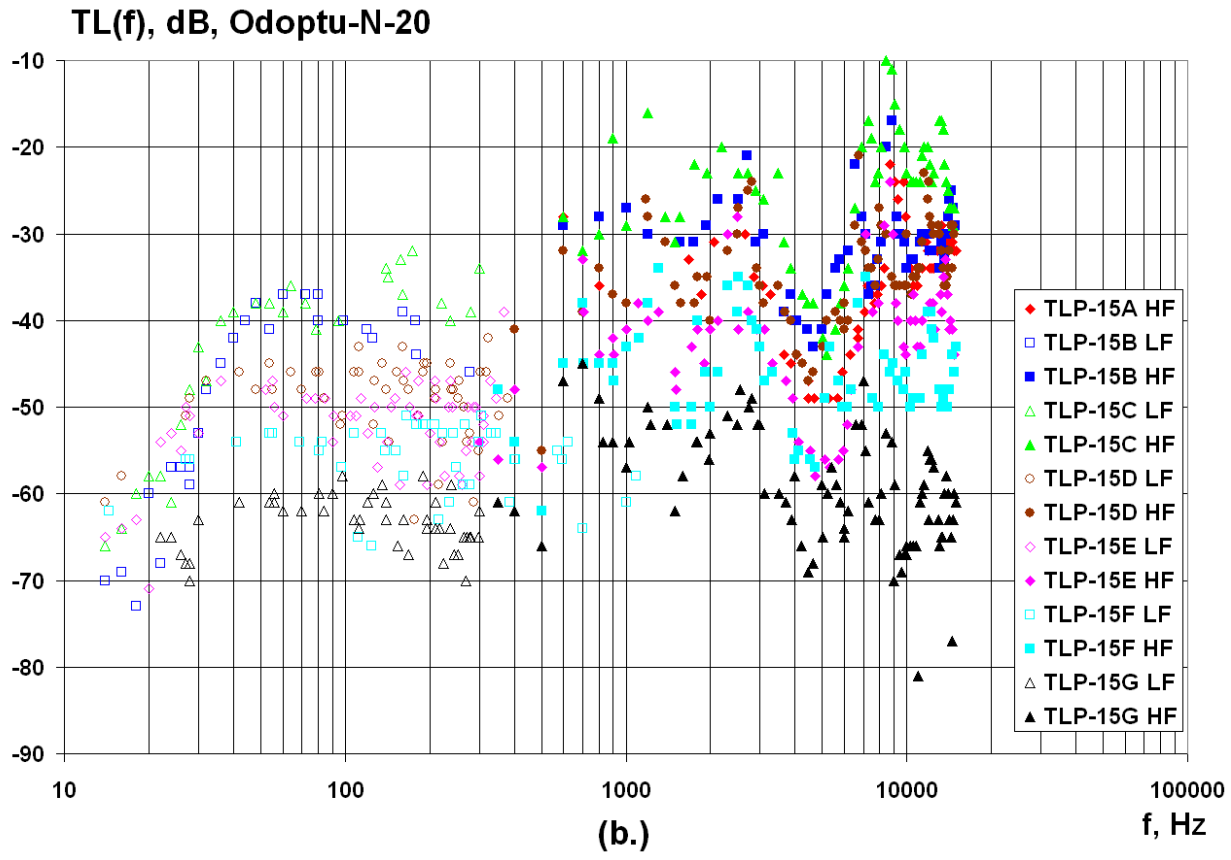

Figure 3.24 - TL profile TLP-15 Frequency dependent TL plot showing the results for both receiver locations (a) Odoptu-N-10 and (b) Odoptu-N-20.

Figure 3.25 shows spectra *G(f)*, and sonograms *G(f,t)* with plots of sound pressure level $D(\Delta f,t)$ computed using data synchronously recorded at monitor stations Odoptu-N-10 and Odoptu-N-20. This figure (Figure 3.25) illustrates that the hydrology and sea level variations along the 10 km profile due to tidal changes result in sound pressure level variations of less than 3 dB in the frequency ranges 1-4.5 kHz, 5-7 kHz, 7-10 kHz and 10-15 kHz (Figure 3.25(b) - $D(\Delta f,t)$: 02:00-07:00 - 22.09.2005).

3.4 Numerical modeling studies along profile TLP-13

This section discusses the results of numerical modeling of the acoustic field produced by a point source deployed at 10 m depth at the PA-B CGBS location along profile TLP-13. The modeling was made using the RAM acoustic modeling code[28]. The objective of the modeling studies was to investigate the suitability of the RAM code for acoustic TL modeling, after adaptation The acoustic field is modeled in a two-layer waveguide with a water column and elastic basement[29]. Figure 3.26 shows the waveguide and its parameters; it also displays the *TL(r,z)* for a 100 Hz source located at a depth of 10 m at location S.

Figure 3.26 illustrates typical sound propagation in a shallow wedge waveguide. Four normal modes are excited at the beginning of the waveguide where the depth is 28 m. The modes carry interfering acoustic energy and due to the shallowing water column, higher modes are absorbed by the seabed, leaving only the first mode to survive by the end of the waveguide. The variation in color on Figure 3.26 demonstrates the interference between the different modes. It is valuable to compare the results of TL field experiments on profile TLP-13 (receiver at Acoustic station PA-B-10) [Kruglov et. al., 2004; Karnauhov et. al., 2005] with numerical modeling that has been calibrated to optimize the elastic parameters of the seabed. This numerical experiment used both a source and receiver deployed at 10m and separated by 10.5 km. Figure 3.27 shows that there is a good match between the numerical modeling and the experimental field data.

[28] The RAM (Range dependent Acoustic Model) acoustic modeling code is capable of computing the acoustic field generated by a point source in a 2D irregular waveguide with an elastic bottom using a PE method.
[29] The currently available version of the software only allows a two-layered irregular waveguide to be modeled.

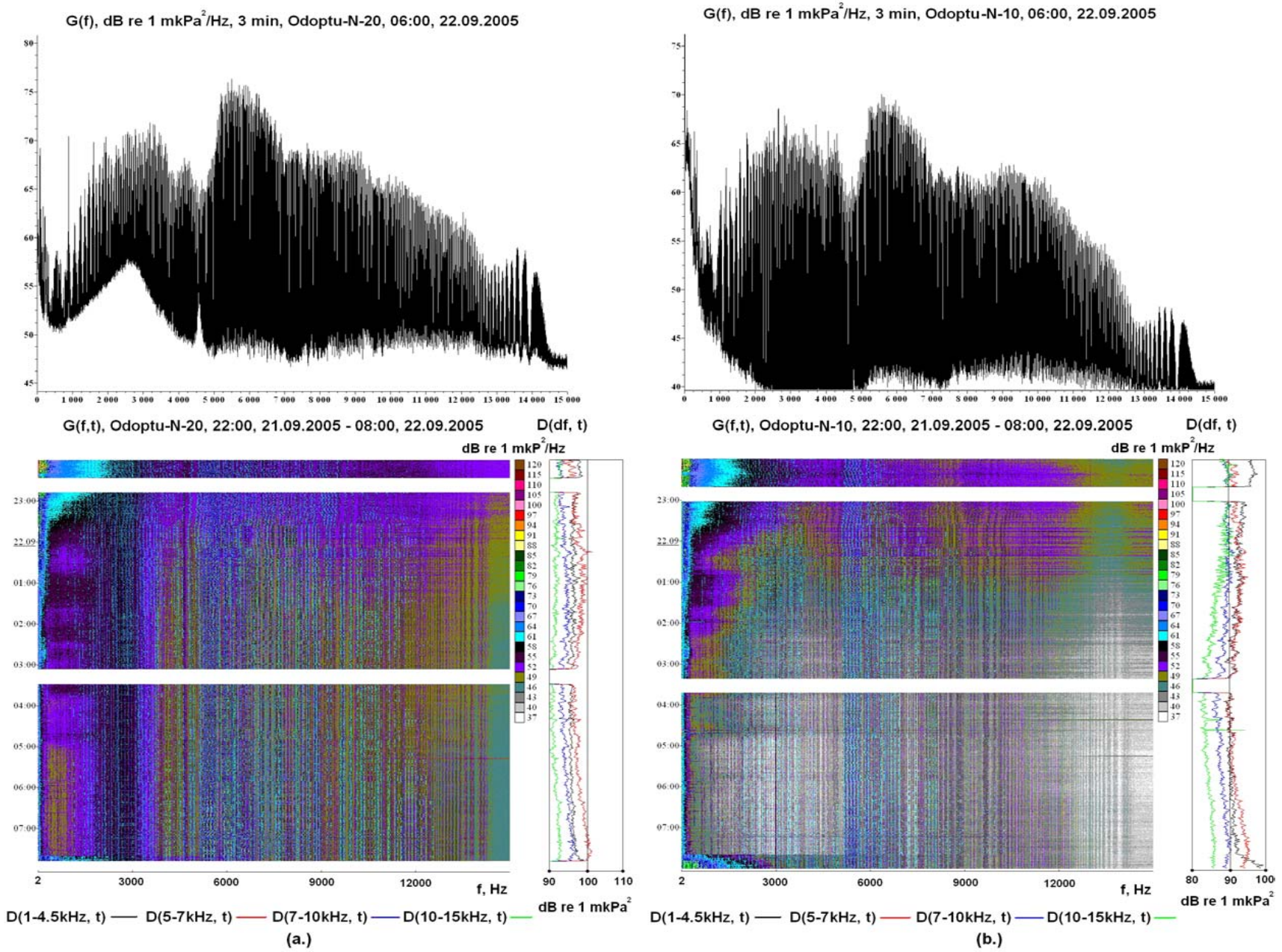

Figure 3.25 – Results of the analysis of data recorded on TL profile TLP-15 during the night of 21 and 22 of September. Broadband FM signals (1-15 kHz) were transmitted for 10 hours by a HF transducer deployed at 10 m from the *Academik Oparin* when it was anchored at source point TLP-15G.

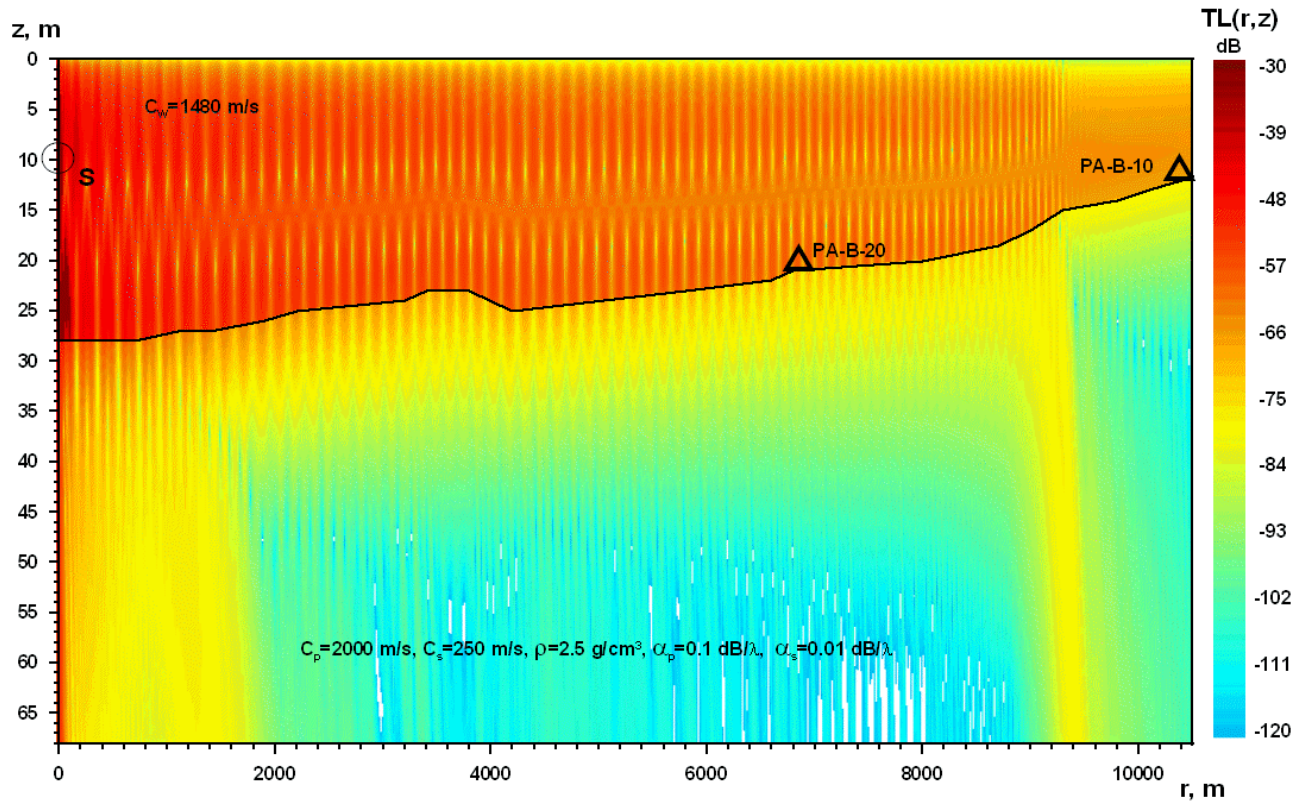

Figure 3.26 – Results of TL numerical modeling of the acoustic field generated by a point source – S (100 Hz) using wide angle parabolic equation modeling code.

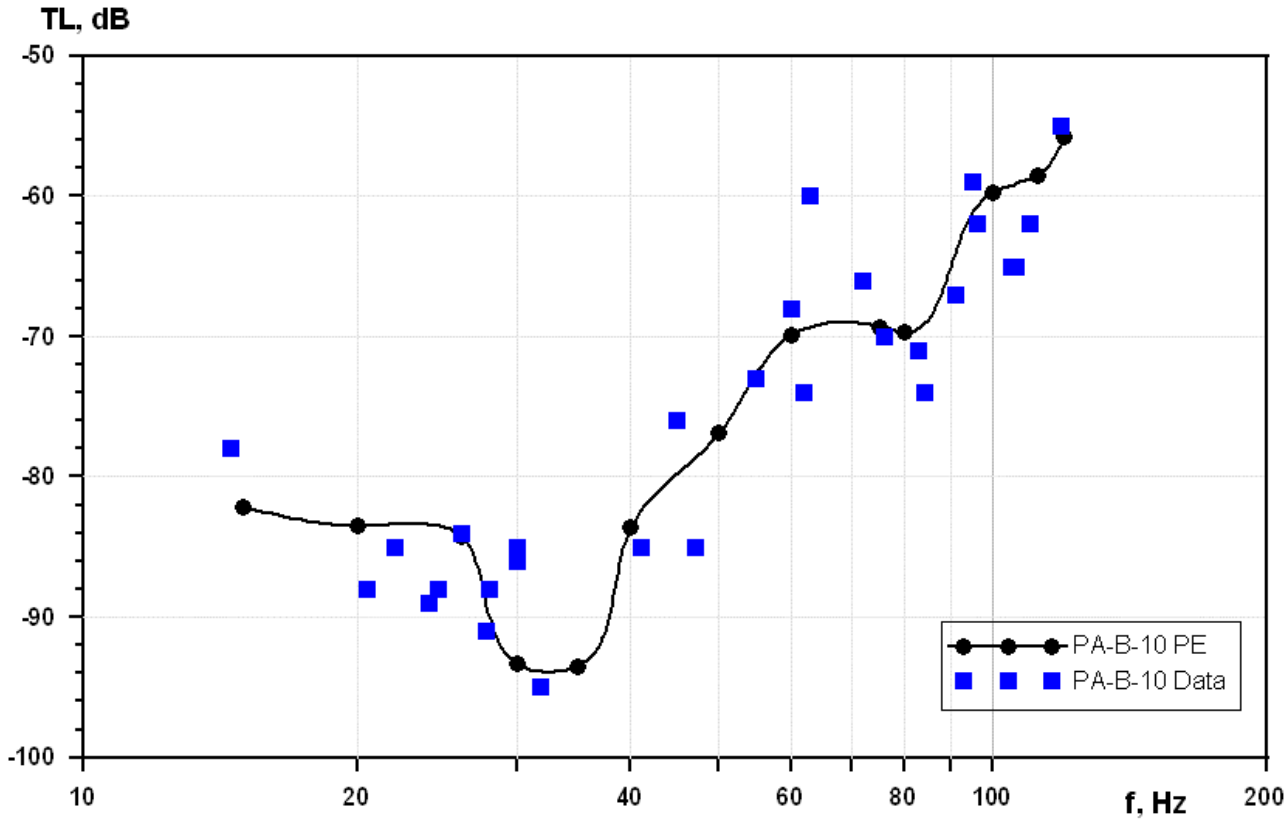

Figure 3.27 – Comparison of frequency dependent TL at the PA-B-10 acoustic station; experimental TL and numerical modeling along profile TLP-13.

4 Analysis of the Acoustic Field Monitored During Oil and Gas Development Activities

This section describes the temporal variation in the average 1-hour sound pressure level recorded at the acoustic monitoring stations during the 2005 field season. As the installation of the SEIC Concrete Gravity Based Structure (CGBS) at the PA-B platform location was the closest activity to the western gray whale feeding area, the majority of the monitoring stations were deployed to effectively monitor this specific offshore activity. Stations were also deployed to monitor the operations associated with the tow and installation of the Orlan platform, the construction of the pipeline from the Orlan platform to the Chayvo OPF and the Molikpaq engineering work.

During the 2005 field season, a real-time acoustic monitoring program was implemented. This real-time monitoring was designed to measure the sound from construction operations so as to minimize the impact on the western gray whale population. The real-time acoustic data transmitted to Piltun lighthouse had a bandwidth of 10 Hz to 5 kHz[30]. The objectives, methodology and data for the real-time acoustic monitoring program are described in volume 1 of this report [Rutenko, 2006].

Data recorded on the six AUARs[31] used for the acoustic monitoring program and processed after the AUARs were recovered had a bandwidth of 1 Hz to 15 kHz. The contribution to the integrated broad band (2 Hz to 15 kHz) sound pressure level from frequencies between 1 Hz and 20 Hz could be significant if flow noise was present on the data. To reduce the acoustic contamination from flow noise a bandwidth of 20 Hz to 15 kHz will be used for this analysis.

4.1 Acoustic monitoring stations and methodology

Six AUARs were deployed to record the acoustic field during the entire field season[32]. Four monitor stations located on the eastern and southern edges of the Piltun feeding area, one station on the north-western edge of the offshore feeding area and one station between the two feeding areas. These broad band acoustic records will be used to identify any anthropogenic sounds associated with SEIC and ENL offshore construction activities.

[30] Four T-AUARs and three analog sonobuoys were deployed for the real-time acoustic monitoring program.
[31] Four T-AUARs and two standard AUARs.
[32] These broad band acoustic recordings were recorded as continuously as operationally feasible during the construction season.

4.1.1 Locations of the monitoring stations

The locations of the acoustic stations used for the monitoring program are plotted in Figure 4.1 and their coordinates are given in Table 1.1. Station PA-B-20 (T-AUAR) was closest to the majority of the PA-B CGBS installation activities and was located to record the highest sound levels generated by these operations. Monitor stations Odoptu-PA-B, Piltun and Piltun-S (T-AUAR) as well as Orlan and A11 (AUAR) were further from the PA-B construction operations. These stations were located to monitor sounds generated from other development activities (e.g. near Molikpaq and Chayvo/Orlan), without being dominated by sounds produced by the CGBS installation.

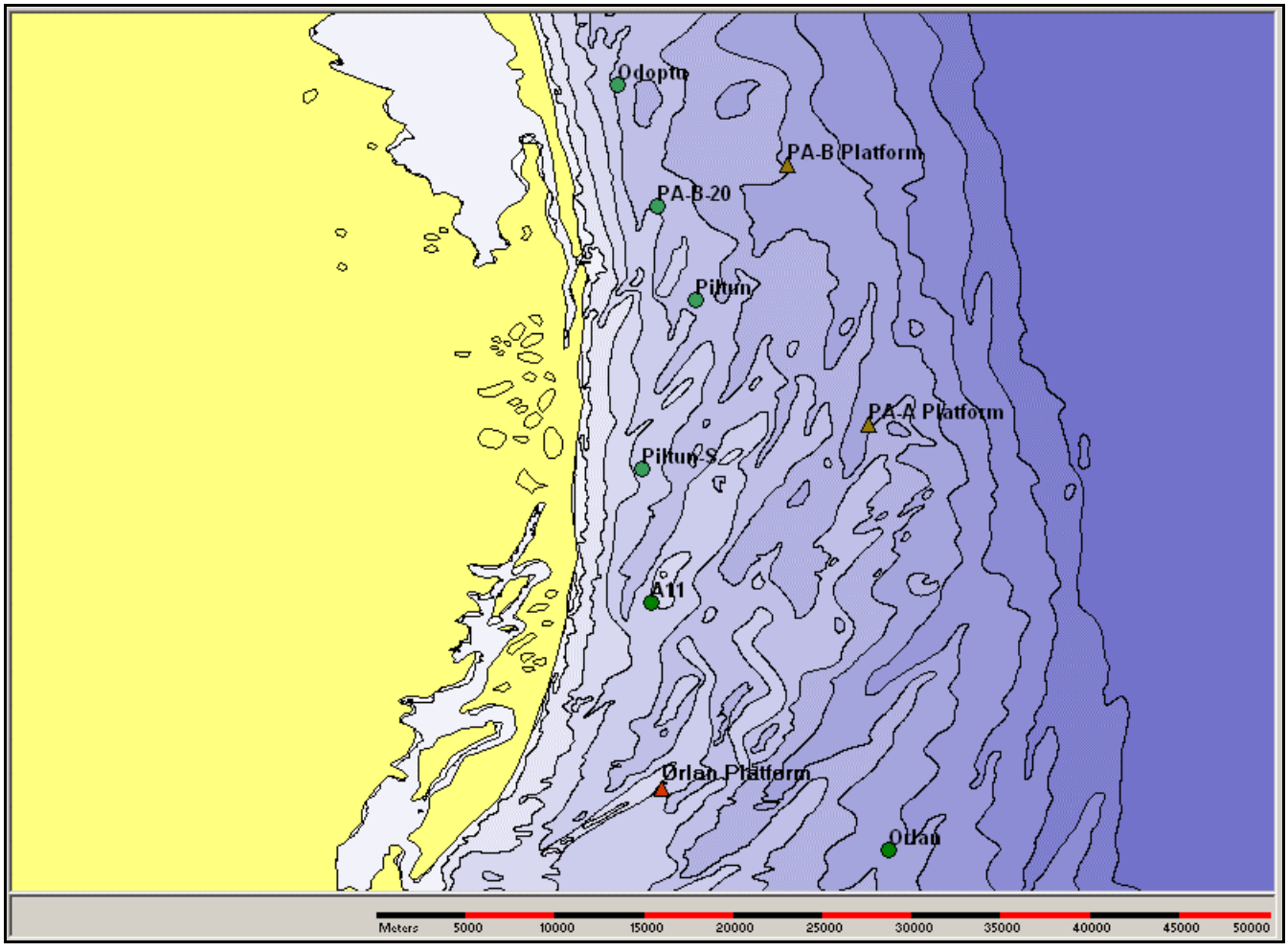

Figure 4.1 - Map of the monitor station locations and PA-B platform CGBS site. The green dots are T-AUAR stations Odoptu-PA-B, PA-B-20, Piltun and Piltun-S, the yellow dots are analog sonobuoy locations ARB2, ARB3 and ARB4.

The six T-AUAR/AUARs were deployed by 13 July to capture background sound levels prior to the start of construction activities. They were in almost continuous operation throughout the construction activities and continued to operate until 26 September. The only gaps in the recording were the periods when the AUARs were being recovered, downloaded and re-deployed. The T-AUAR at the PA-B-20 (#8) station had a mechanical failure for the first deployment (13-23 July)[33], but recorded normally for the remaining four deployments.

4.2 Analysis of the acoustic monitoring data

Figures 4.2 to 4.7 display the average one hour integrated broad band (20 Hz to 15 kHz) sound level values for each of the six stations, calculated from data recorded directly on the T-AUAR/AUARs between mid July and late September. For each of the plots key operational events are annotated. This includes the ENL and SEIC construction activities (yellow boxes – blue (ENL) and red (SEIC) text), weather events (grey boxes) and the acoustic signature of unknown vessels (red boxes with black text (UV)).

At the bottom of the plot the presence of the *Academik Lavrent'ev* or *Academik Oparin* are annotated (blue boxes – text AL and AO). This information is critical to the interpretation of the plots, as when either the *Academik Lavrent'ev* or *Academik Oparin* are near the AUARs[34], the recorded sound pressure level can be much higher. This is clearly illustrated by the high sound pressure levels during deployment and retrieval.

Figure 4.2 shows the time period from 10 to 20 July, during which the Orlan platform was towed in and set down and scour protection commenced. During this time the average sound pressure level at the Orlan station (the closest point to the offshore feeding area) increased by <5 dB and the level seldom exceeded 120 dB re 1 μPa^2. For most of these events the cause was the close approach of the *Academik Lavrent'ev* or an unknown vessel. No significant increase in the acoustic level was noted at the A11 station an acoustic monitoring location half way between the Orlan/Chayvo operations and the southern edge of the Piltun feeding area.

[33] Acoustic data was transmitted via the radio channel, but not recorded on the hard drive of the AUAR.
[34] The *Academik Lavrent'ev* or *Academik Oparin* can be in the area either to maintain the AUARs and sonobuoys, or to conduct biology operations (Photo-ID, benthos sampling or vessel surveys).

Figure 4.3 shows the time period from 21 to 31 July, during which scour protection, dredging and pipe lay operations continued in the Chayvo area and the PA-B CGBS was towed in and set down. During this period the first barge from the sealift operations were received at the temporary Chayvo offloading facilities (22-23 July). No significant increase in acoustic level was noted at the Orlan or A11 monitor stations due to the operations at Chayvo. During the tow in and set down of the PA-B CGBS an increase was noted in the acoustic level at the PA-B-20 monitor station, the station closest to the CGBS location. This increase was within the expected parameters for the CGBS tow in and the results of the real-time monitoring are discussed in greater detail in an SEIC report [Racca and Hannay; 2005]. During this time period there were two storms, these storms generally caused an increase in the acoustic level at all the monitor stations. Because the hydrophone was sometimes moved by wave action during these storms the acoustic data could be more erratic during these times. The barge landing caused a short term increase in the sound levels at the A11 station and a possibly related transient increase in acoustic level at the Orlan station, probably due to a moving vessel.

Figure 4.4 shows the time period from 1 to 15 August, during which dredging and pipe lay operations continued in the Chayvo area and de-rigging and scour protection operations continued in the PA-B area. During this period two more barges were received at the temporary Chayvo offloading facilities. The acoustic levels received during this time were similar to those described earlier. A storm at the end of the period caused an increase in the acoustic levels at all the stations. A number of increases in the sound level due to unknown vessels were noted at this time. From 16 to 31 August (Figure 4.5) operations continued as before and similar sound pressure levels were noted.

Figures 4.6 and 4.7 show the time periods from 1 to 13 and 14 to 26 of September, when monitoring was completed. No significant acoustic levels were reached during this time period except when unknown vessels transited nearby. The landing of barges at the temporary Chayvo offloading facilities sometimes caused a short term increase in the sound levels at the A11 and Orlan stations, but these increases seldom exceeded 120 dB re 1 μPa^2, and if so only for short periods.

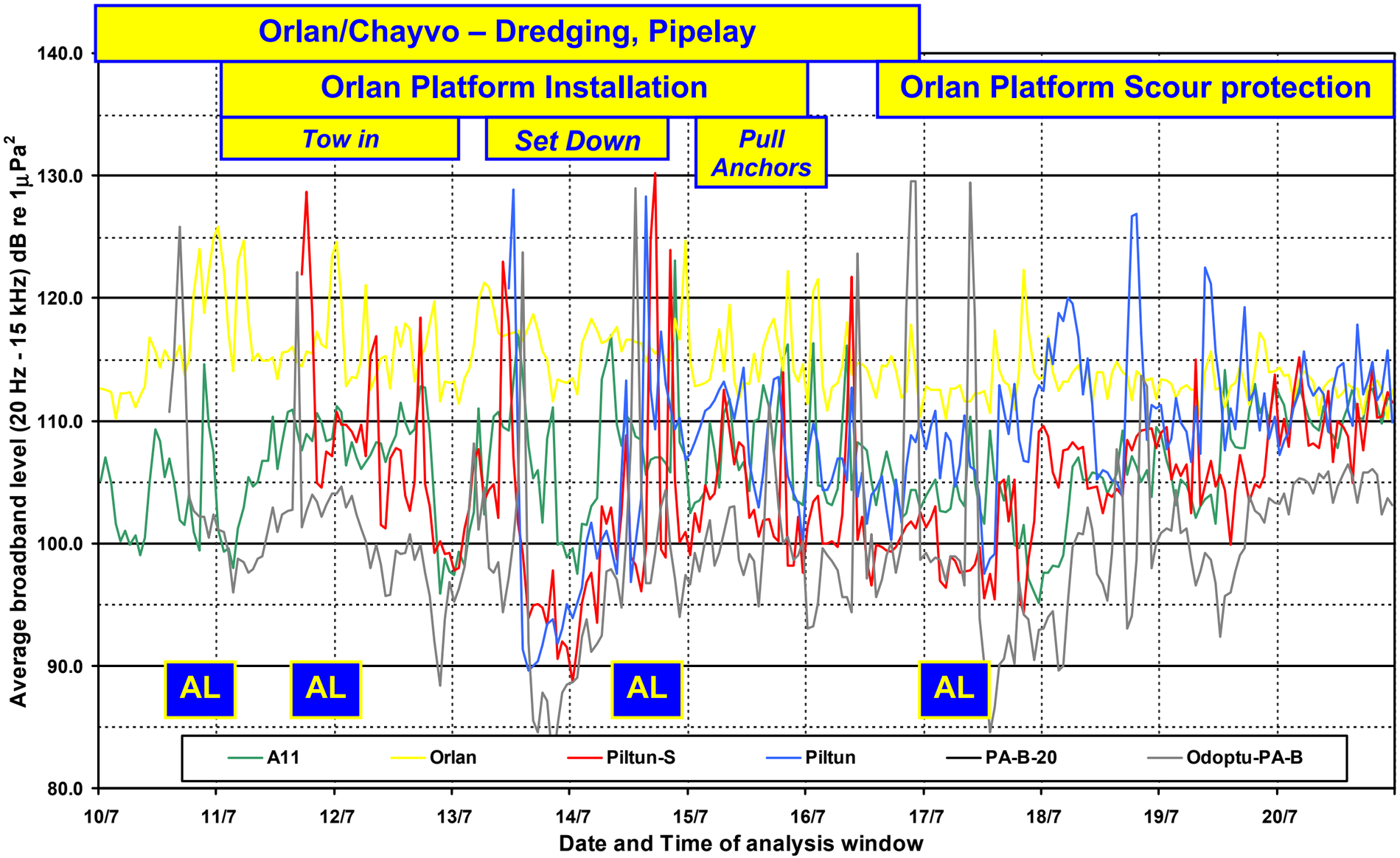

Figure 4.2 – Plot showing the average 1-hour broadband (20 Hz to 15 kHz) received level recorded on the disc of the six T-AUAR/AUARs from 10 to 20 July.

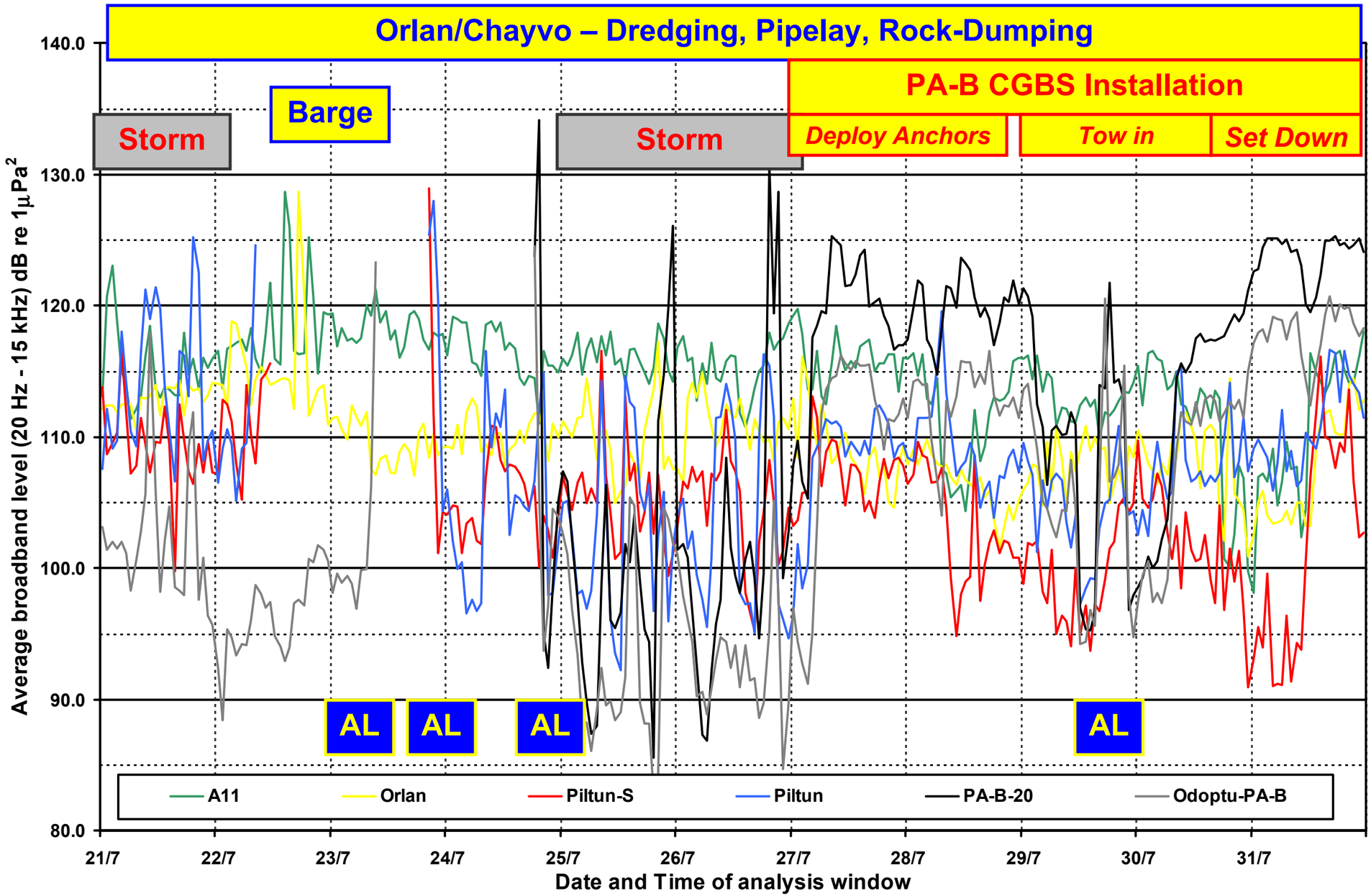

Figure 4.3 – Plot showing the average 1-hour broadband (20 Hz to 15 kHz) received level recorded on the disc of the six T-AUAR/AUARs from 21 to 31 July.

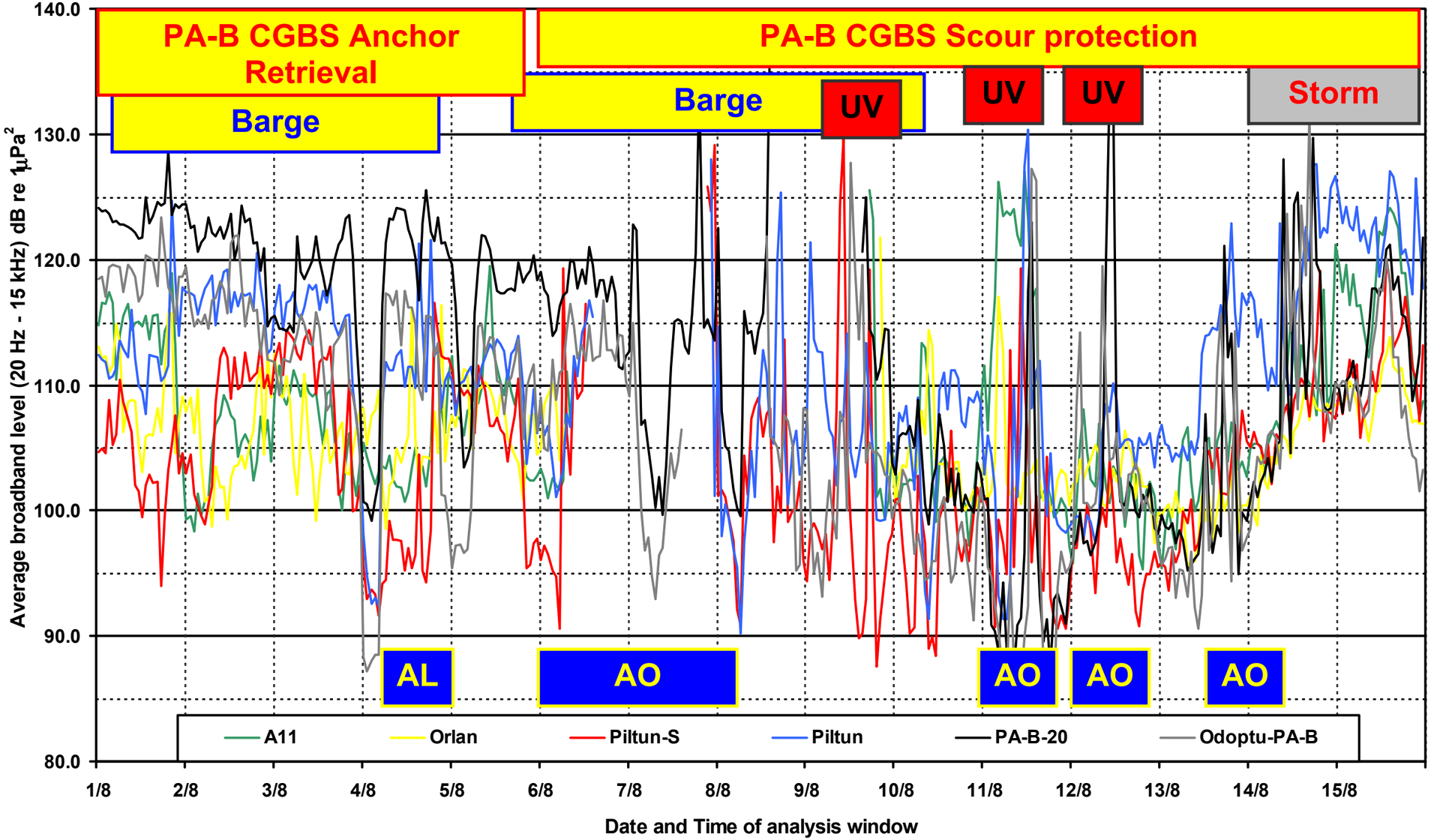

Figure 4.4 – Plot showing the average 1-hour broadband (20 Hz to 15 kHz) received level recorded on the disc of the six T-AUAR/AUARs from 1 to 15 August.

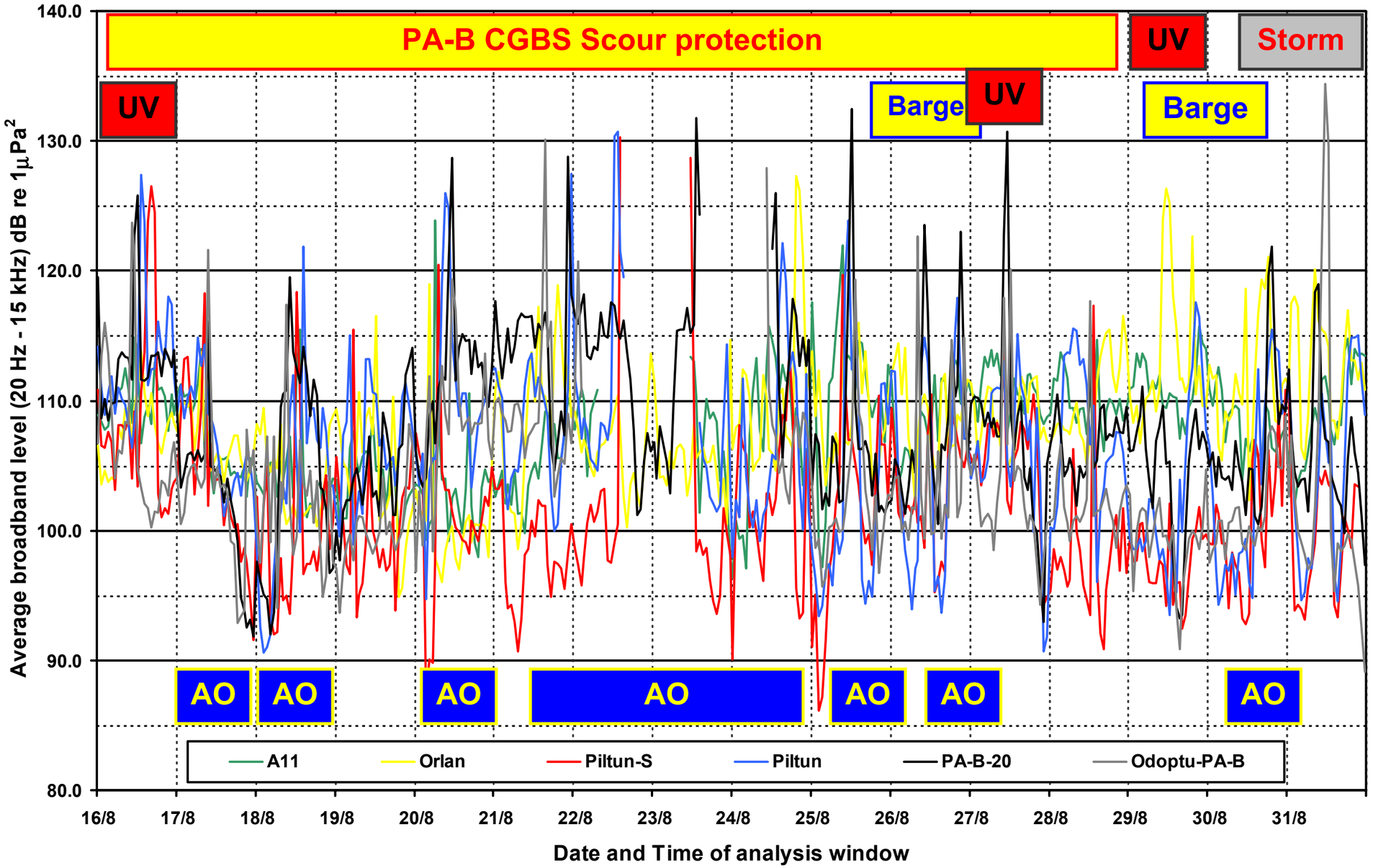

Figure 4.5 – Plot showing the average 1-hour broadband (20 Hz to 15 kHz) received level recorded on the disc of the six T-AUAR/AUARs from 16 to 31 August.

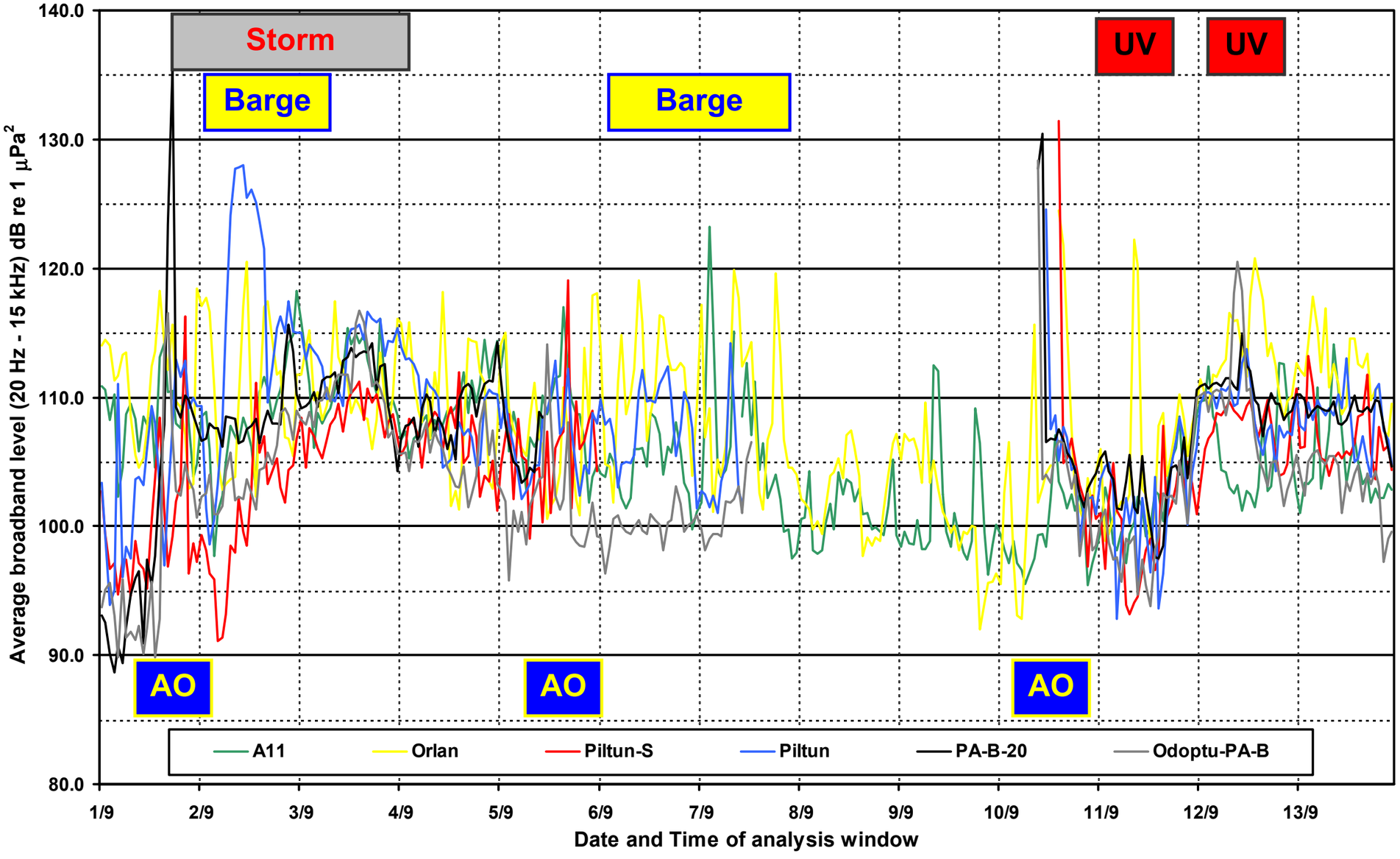

Figure 4.6 – Plot showing the average 1-hour broadband (20 Hz to 15 kHz) received level recorded on the disc of the six T-AUAR/AUARs from 1 to 13 September.

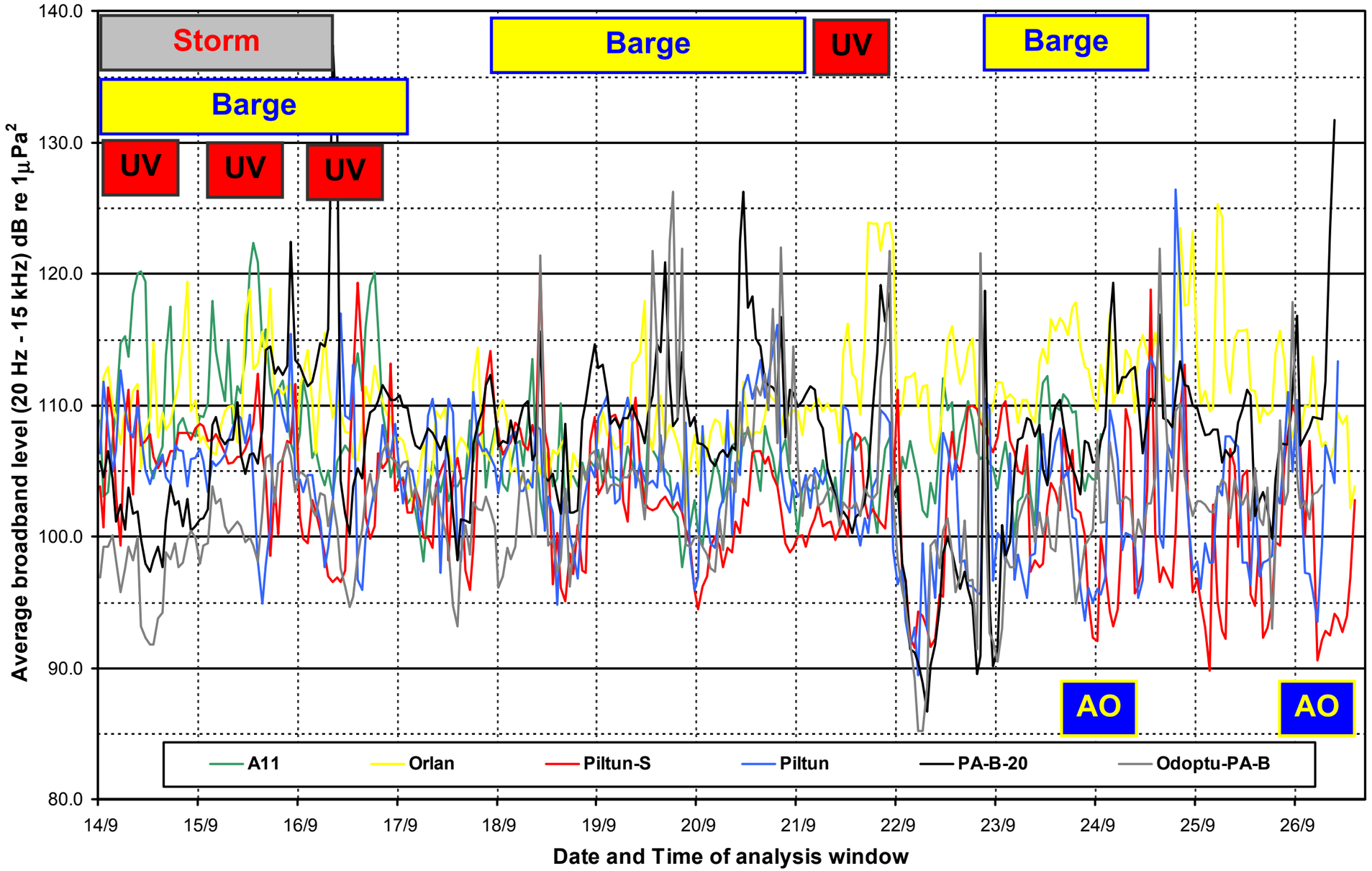

Figure 4.7 – Plot showing the average 1-hour broadband (20 Hz to 15 kHz) received level recorded on the disc of the six T-AUAR/AUARs from 14 to 26 September.

5 Estimation of Exposure Level (EL) at the behavioral observation stations

In order to evaluate whether the oil and gas developments on the NE Sakhalin shelf will have any effect on gray whale behavior it important to estimate the total acoustic exposure of the area near the behavioral observation stations during and prior to the period of observation [Gailey et.al., 2005][35]. During the 2005 field season six behavioral stations on the coast were occupied by biologists. Where possible AUARs were deployed at the 10 m bathymetric contour directly offshore from these land based behavioral monitoring stations to monitor the acoustic levels. The closest relationship between the locations of the behavioral and acoustic monitoring stations is given in Table 5.1 and is shown on Figure 1.3.

Table 5.1 - Relationship between the behavioral and acoustic monitoring stations.

Behavioral station		Acoustic station	
North Station	4	BEH-North	A10
Odoptu Station	2	BEH-Odoptu	A9
Station 07	6	Odoptu-N-10	12
2nd Station	3	Odoptu-S-10	10
1st Station	5	Odoptu-PA-B	9
South Station	1	PA-B-10	7

For the 2005 field season the behavioral and acoustic monitoring stations were synchronously occupied on seventeen days (27 stations)[36]. The behavioral observations are listed in Table 5.2 with their corresponding acoustic observations if available.

[35] Acoustic data near the behavioral stations was analyzed in 10 minute bins and an estimate of the energy in these bins (20-2000 Hz and 20-15000 Hz bandwidths) was given to the behavioral team. It is hoped that a combined analysis of the behavioral data and the acoustic energy in 10 min bins could improve our understanding of the acoustic threshold above which noise starts to affect the behavior of the western gray whales.

[36] At the beginning of the field season two AUARs making sound measurements near two northern behavioral stations (stations A9 and Odoptu-N-10) were lost (presumed stolen). This limited the acoustic teams' ability to conduct monitoring studies near the northern behavioral stations.

Table 5.2 – Relationship between behavioral observation times and acoustic recording at nearby stations.

Date	Behavioral Observations	Acoustic
12-Jul-2005	1st Station	#9
13-Jul-2005	South Station (11:00-15:00) / 1st Station	#7, #9
14-Jul-2005	2nd Station (08:00-16:30) / Station 07 (08:00-16:00)	#10, #12
15-Jul-2005	Odoptu Station (09:45-12:20)	#A10
17-Jul-2005	1st Station	#9
18-Jul-2005	1st Station	#9
24-Jul-2005	Odoptu Station (11:00-5:00)	#A10
26-Jul-2005	South Station (10:49-18:26) / 1st Station (09:10-19:02)	#7, #9
27-Jul-2005	2nd Station (09:30-18:30) / Station 07 (10:11-11:40; 15:20-18:00)	#10, #12
29-Jul-2005	South Station (08:00-18:00) / 1st Station (7:40-18:50)	#7, #9
31-Jul-2005	South Station (08:00-9:00) / 1st Station (07:20-9:00)	#7, #9
6-Aug-2005	South Station (07:10-15:10) / 1st Station (07:07-15:10)	#7, #9
7-Aug-2005	Station 07 (08:16-17:32)	#12
11-Aug-2005	South Station (11:35-18:20) / 1st Station (10:58-18:52)	#7, #9
20-Aug-2005	South Station (07:30-14:00) / 1st Station (07:30-14:00)	#7, #9
25-Aug-2005	1st Station (13:00-18:00)	#9
26-Aug-2005	South Station (11:20-16:40) / 1st Station (10:30-17:00)	#7, #9

5.1 Estimating energy levels at the acoustic monitor stations

To effectively sample the variation in the energy level received at the 10 m contour near to the behavioral monitoring station over time, broad band sound pressure levels were estimated in 1-minute windows and continuous acoustic energy estimates (μPa^2) were made in ten-minute windows[37]. These ten-minute estimates were computed for the target day and the previous three days.

One issue that must be contended with in computing energy estimates is the inclusion of non-real acoustic data into the ten-minute energy estimates. In general there are three different scenarios where non-real acoustic levels are present and would be added to the energy estimate unless otherwise identified and corrected:

- Clipped data where the acoustic level exceeds the maximum input voltage of the recorder. This data can be distorted and will not record the acoustic field with good

[37] 10-minute energy values were estimated for the following frequency ranges and stored digitally: 2 Hz - 15 kHz, 20 Hz - 2 KHz and 20 Hz - 15 kHz.

fidelity. Although this could be due to the presence of an acoustic field greater than expected the most likely cause is mechanical (e.g. the mechanical movement of the hydrophone assembly in a storm, large swell or strong currents).

- Zero data when no data is recorded. The AUAR records to a 1 GB flash disk until it is full, it then stops recording and writes the data to a hard drive. No acoustic data is recorded during this time and the acoustic level is set to zero.
- Non-real acoustic data. Data may be present that while recorded with fidelity does not correctly represent the acoustic field present at the time of recording. An example of this is the high amplitude, low frequency flow noise generated during high tidal current flows.

In order to compensate for these errors a procedure was established where the ten-minute energy estimate is generated from the good samples using the following technique:

1. Average the energy in 10 1-second windows[38]. The energy in each 1-second window is then compared with the average energy in the 10-second window. If the energy in the target 1-second window is larger or smaller by a pre-defined factor than the average of the 10-second windows; then the energy estimate for the target 1-second window is replaced by the previous 1-second value[39].
2. Next compute the energy in 60 ten-second windows. If the energy in any of these 1-second windows is zero the value in the 10-second window is set to zero.
3. Compute the 10-minute energy estimates from the ten-second windows. If any of the ten-second windows are zero replace the value of the 10-minute energy estimate using linear interpolation between the last and next good 10-minute energy estimate.

The windows are time synchronized to the start of the day. For every 10-minute window the total energy (μPa^2) is computed as described above. These energy estimates can be added to make a larger window (e.g. the energy in 6 ten-minute windows makes a one-hour estimate).

Figure 5.1 is a sonogram *G(f,t)* recorded at the PA-B-10 (#7) acoustic monitoring station from 27 July to 13 August 2005. The figure also displays the variation in sound pressure level with time $D(\Delta f,t)$ (equivalent to rms) for five different bandwidths. Station PA-B-10 is located on the 10 m contour directly seaward of the South behavioral station (Figure 1.3). The sonogram quantitatively illustrates variations in the anthropogenic sound levels (bandwidth 2 Hz to 15 kHz) recorded during the PA-B CGBS tow in and set down.

[38] Five windows behind and five ahead of the target window.
[39] The number of replacements is tracked as a QC measure.

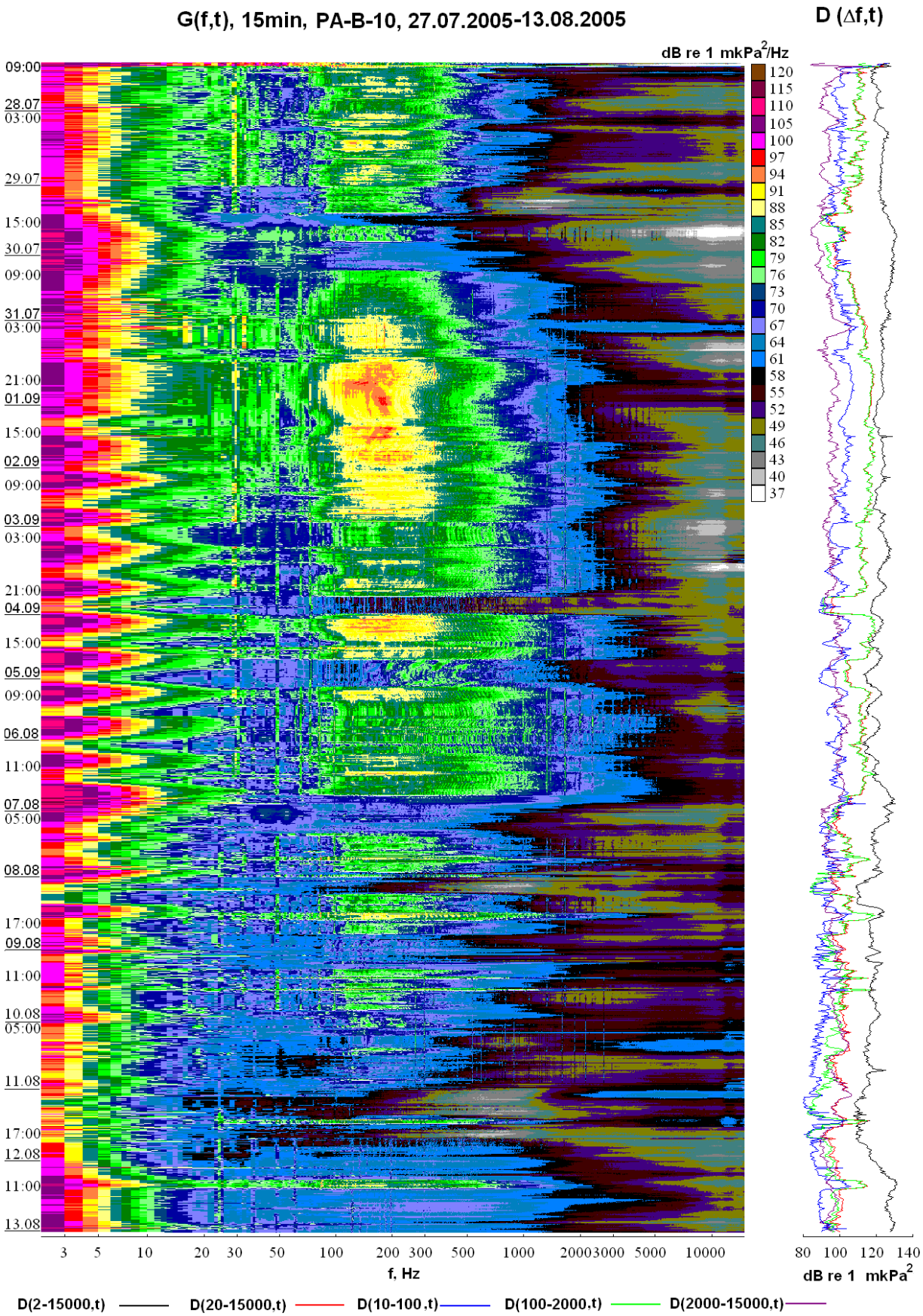

Figure 5.1 - Sonogram *G(f,t)* and plot of the variation of sound pressure level with time *D(Δf,t)* for data recorded at the PA-B-10 monitor stations from 27 July to 13 August 2005.

Behavioral observations were conducted at the South behavioral station on 29 and 31 July and 6 and 11 August. Figure 5.2 gives plots (for 2 frequency bands) showing the variation in energy estimated for these 10-minute windows for the time periods corresponding to the behavioral observations.

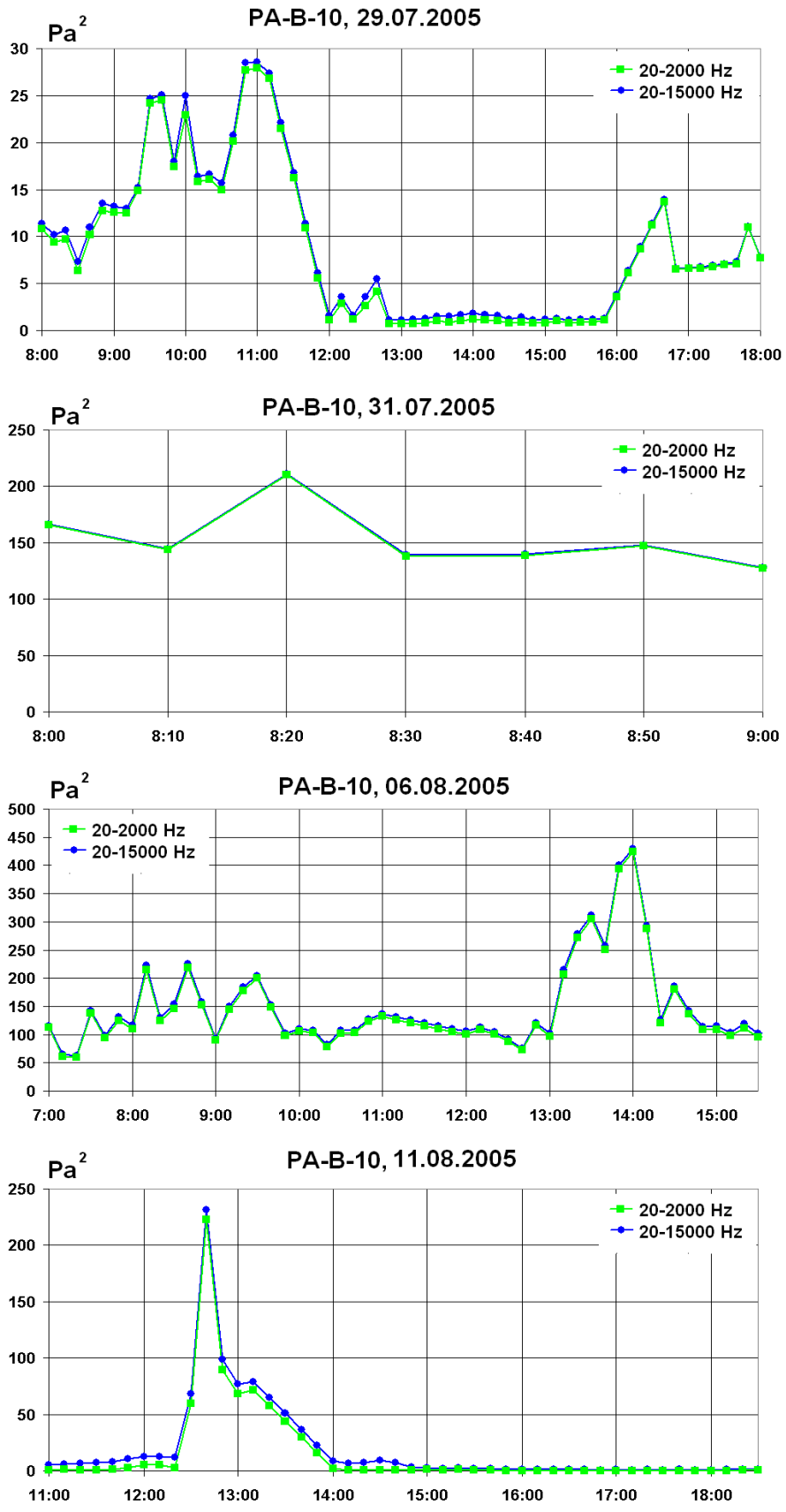

Figure 5.2 - Ten-minute acoustic energy estimates for two frequency bands. The plot is for the PA-B-10 (#7) Monitor station on days (between 27 July and 13 August) 2005 when synchronous observations were being made at the South behavioral station.

6 Acoustic Signatures of the *Academik Lavrent'ev and Oparin* and Photo-ID Zodiac

During the 2005 field season the acoustic studies were conducted from two research vessels the *Academik Lavrent'ev* (20 June to 5 August) and her sister ship the *Academik Oparin* (5 August to 7 October), these vessels were also used to accommodate the biology teams (Benthic, Marine Mammal Observers (MMO) and Photo-ID). The Photo-ID and benthic teams used a zodiac with a four-stroke outboard motor (40 hp). The acoustic signatures of two of the vessels involved in the expedition (*Academik Oparin* and principal Photo-ID zodiac (two-stroke and four-stroke outboard motors) were measured during the 2004 expedition while employed in operations related to biological and acoustical studies in the Piltun and offshore feeding areas [Karnauhov, 2005]. However, the AUARs used for these measurements were too sensitive and were overdriven by the vessel when at close range[40]. Comparative analysis of the acoustic output of the two-stroke and four-stroke zodiac outboard motors revealed that both the narrow and broadband noise from the two-stroke outboard motor was more then 15 dB higher than that produced by the four-stroke outboard motor. The experiment also suggested that a zodiac sailing at 25 km/h was quieter than one sailing at 7 km/h. In 2005 the Photo-ID team used only four-stroke outboard motors; the acoustic output for these outboard motors was investigated at different operational speeds in calm weather. Additionally, additional measurements of the acoustic footprint of the *Academik Oparin* were conducted while it conducted hydrological sampling on TL profile TLP-15.

6.1 Acoustic measurements of the research vessel *Academik Oparin*

The acoustic signature of the *Academik Oparin* was recorded while it was acquiring TL profile TLP-15. Figure 6.1(a) is the map giving the locations p1 and p2 of mini-AUARs used during the experiment. Additionally, Figure 6.1(a) shows the vessel locations with distances to p1 and p2 and vessel speed. The experiment was conducted on the morning of 22nd September as the *Academik Oparin* was profiling TLP-15 sampling the hydrology at source locations TLP-15F, E, D, C, B, and A. Figure 6.2(b) displays sonograms *G(f,t)* and the variation in sound pressure level with time $D(\Delta f,t)$ for two different bandwidths (2 Hz -15 kHz and 20 Hz -15 kHz). It can be seen from Figure 6.2 that the noise generated when the *Academik Oparin* was slowing down or drifting with an operational engine exceeded that generated as the *Academik Oparin* was sailing.

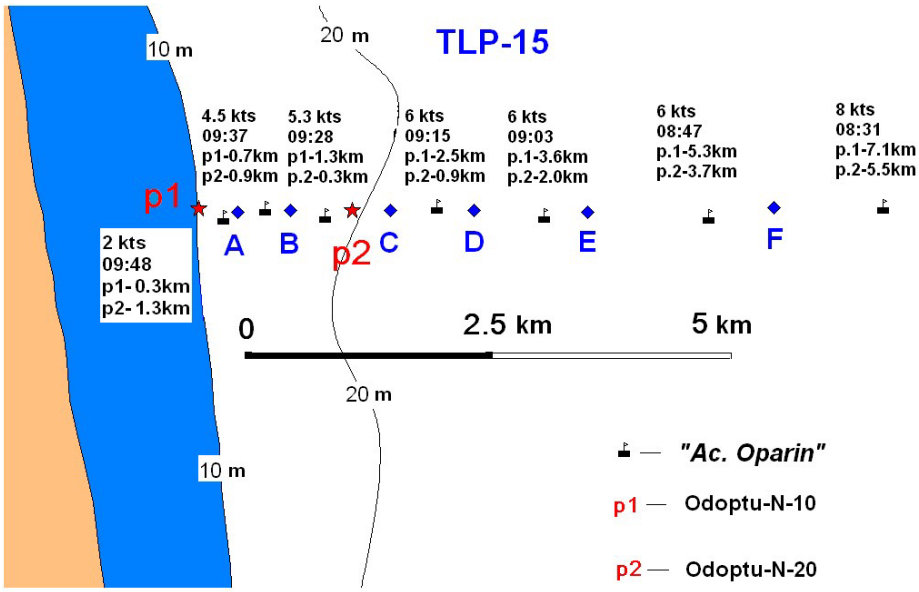

(a.)

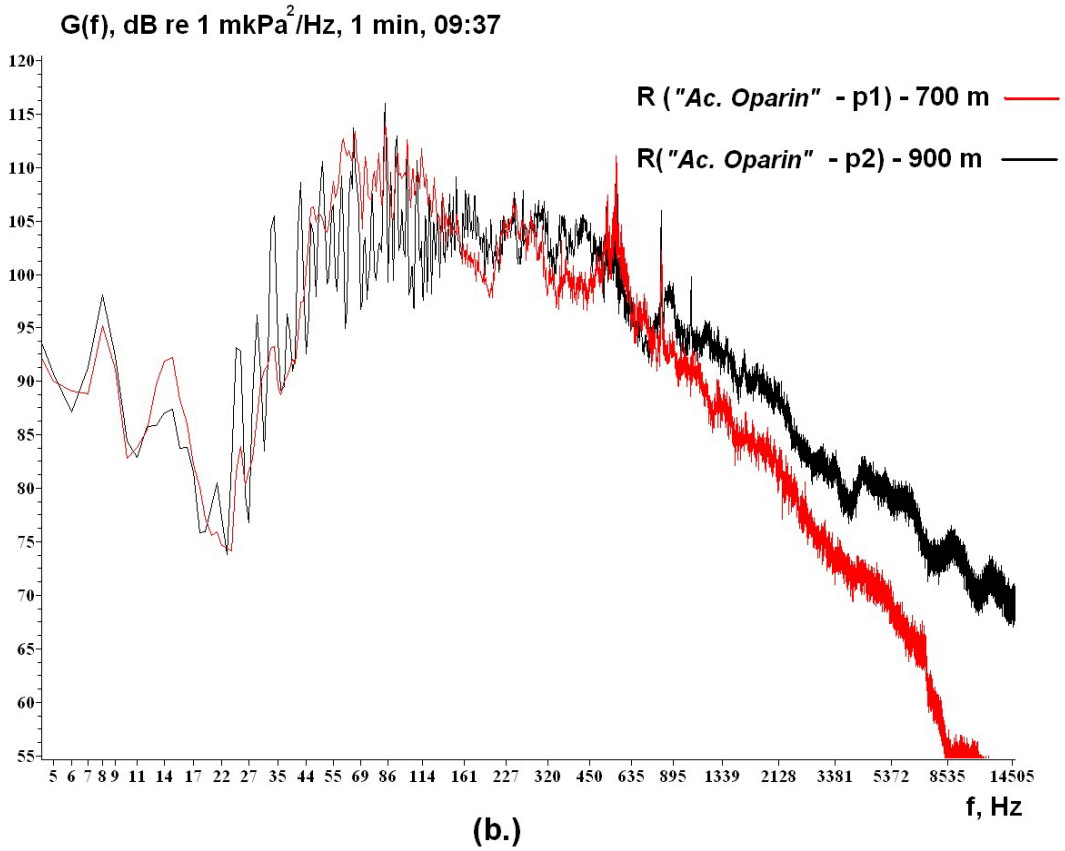

(b.)

Figure 6.1 – (a) Experimental schematic giving the locations of the *Academik Oparin* as it acquired TLP-15 (b) Spectra G(f) recorded at locations p1 and p2 as *the Academik Oparin* sailed at 4.5 knots at location '09.37'.

[40] The gain of the AUARs was set to record low level ambient or anthropogenic acoustic signals.

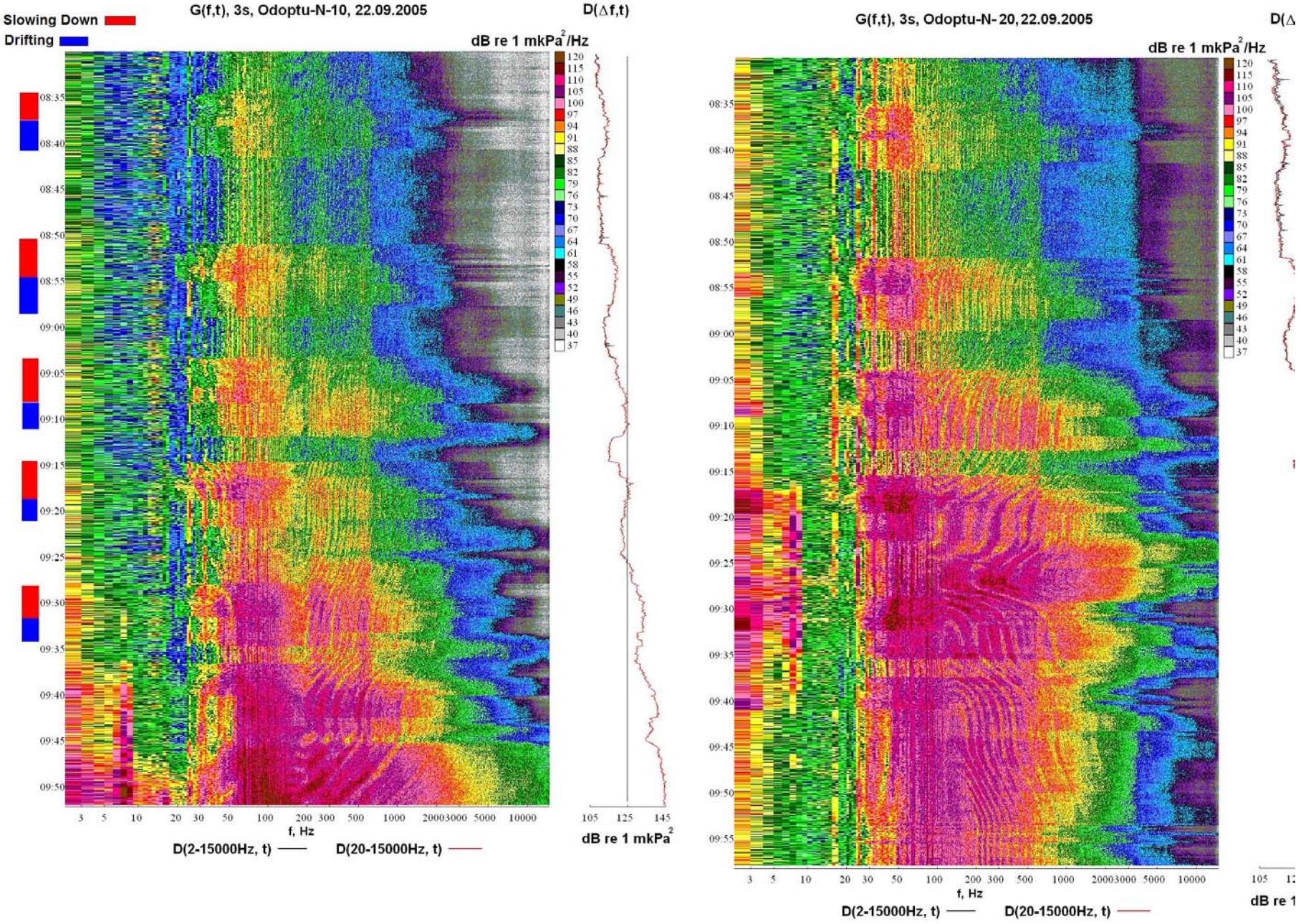

Figure 6.2 - Sonogram *G(f,t)* and plot of the variation of sound pressure level with time *D(Δf,t)* for data recorded at the Odoptu-N-10 and Odoptu-N-20 monitor stations on 22 September 2005.

Figure 6.1(b) shows spectra *G(f)* recorded at points p1 and p2 as the *Academik Oparin* sailed at 4.5 knots from p2 to p1 at location '09.37', a location equidistant from both the receiving points. Figure 6.2(b) also demonstrates that the acoustic level is higher behind the vessel (p2) than ahead of it, especially for broadband acoustic energy above 1 kHz.

Figures 6.3 and 6.4 show power spectral density plots *G(f)* that can be used to quantitatively characterize the sound levels generated by the *Academik Oparin* as it sailed away from the coast. As the measurements at p1 and p2 were synchronous (spectra were averaged over 1 min) they can be used to estimate the acoustic propagation and TL for sound propagating into the inshore area.

6.2 Acoustic measurements of the primary Photo-ID Zodiac

Gray whale Photo-ID surveys have been conducted by a specially trained team from IBM led by Dr. Y.M. Yakovlev since 2002 [Яковлев; 2003]. Since the 2004 field season a 3.8 m Zodiac with a 4-stroke 40 hp engine was used to reduce the acoustic signature of the Photo-ID zodiac and minimize any impact on western gray whales due to Photo-ID studies[41]. In 2005 a hydrophone was deployed from a zodiac while the Photo-ID zodiac sailed past it at 19 and 6 knots. The Photo-ID zodiac then maneuvered, approaching the acoustic boat as if the goal was to photograph a gray whale. Figure 6.5(a) displays sonograms *G(f,t)* and plots of the variation of sound pressure level with time *D(Δf,t)* recorded during this experiment. Figure 6.5(b) gives power spectral density plots recorded as the zodiac sailed at different speeds (19 and 6 knots). Figure 6.5 demonstrates that a zodiac moving at 19 knots produces a lower level of underwater noise than when sailing at 6 knots. It is possible that the outboard motor transmits less noise into the water than the hull of the zodiac. At lower speeds the outboard motor vibrates at frequencies close to the resonant frequency of the zodiac hull, this vibration couples into the water better than the vibration of the outboard motor. Figure 6.5(b) displays a resonant peak at approximately 68 Hz, this reaches a level of 130 dB re 1 μPa^2/Hz more than 20 dB higher than the acoustic levels below 85 Hz generated by a zodiac sailing at 19 knots.

[41] Scientific protocols have indicated that a 4-stroke outboard motor is quieter than a 2-stroke outboard motor.

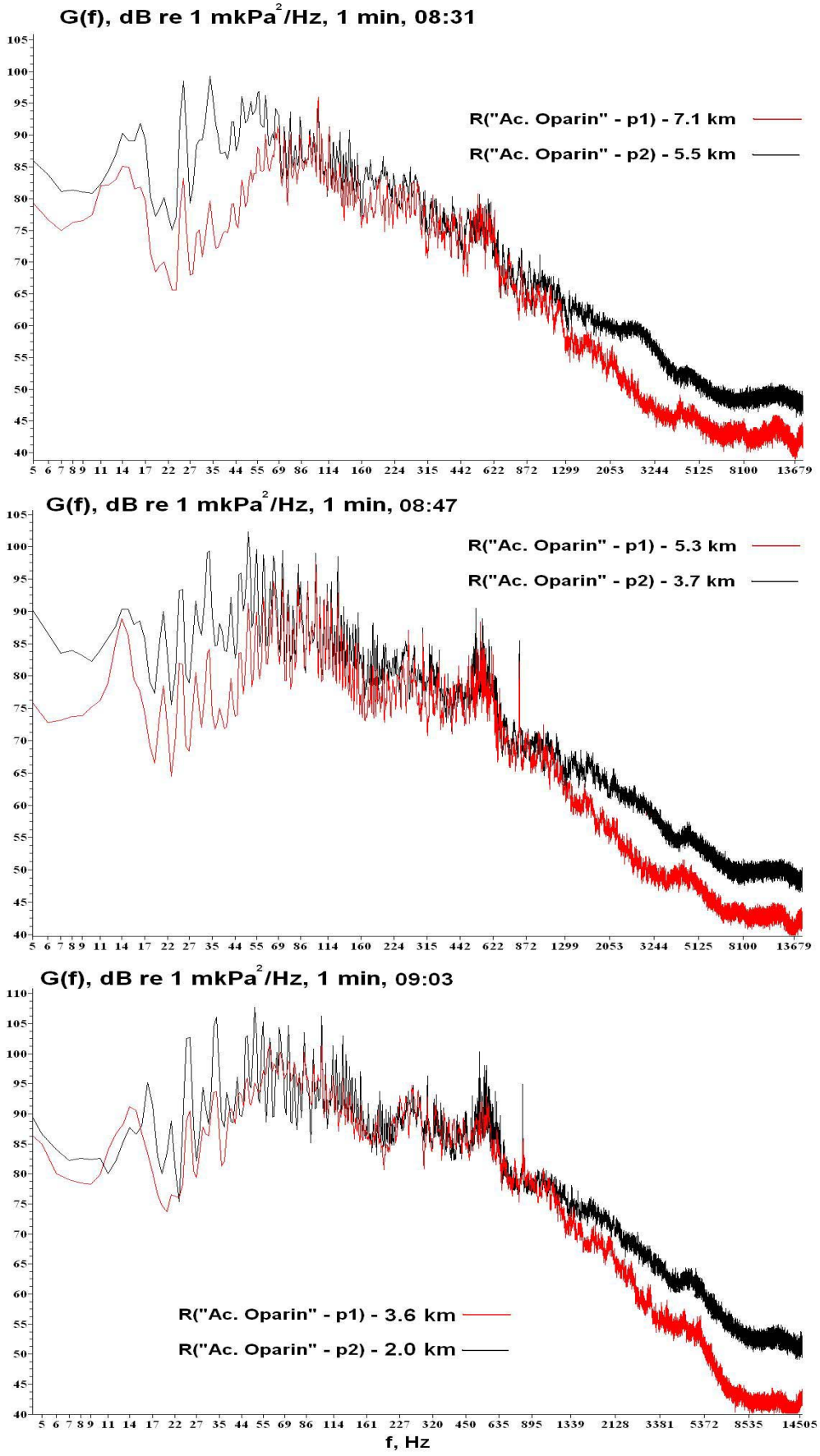

Figure 6.3 - Acoustic signature of the *Academik Oparin* recorded at locations p1 and p2 as the vessel sailed along TL profile TLP-15.

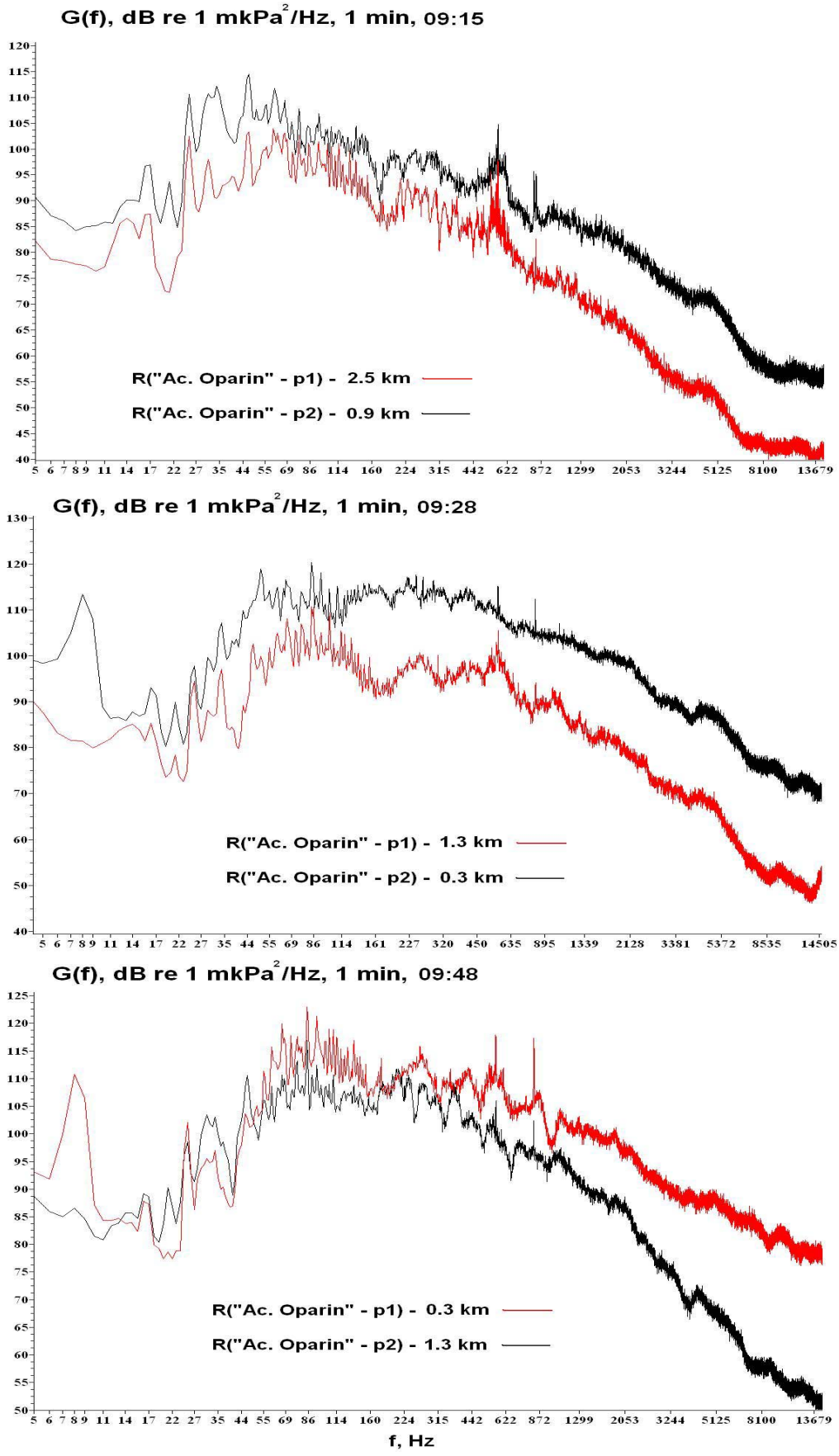

Figure 6.4 - Acoustic signature of the *Academik Oparin* recorded at locations p1 and p2 as the vessel sailed along TL profile TLP-15.

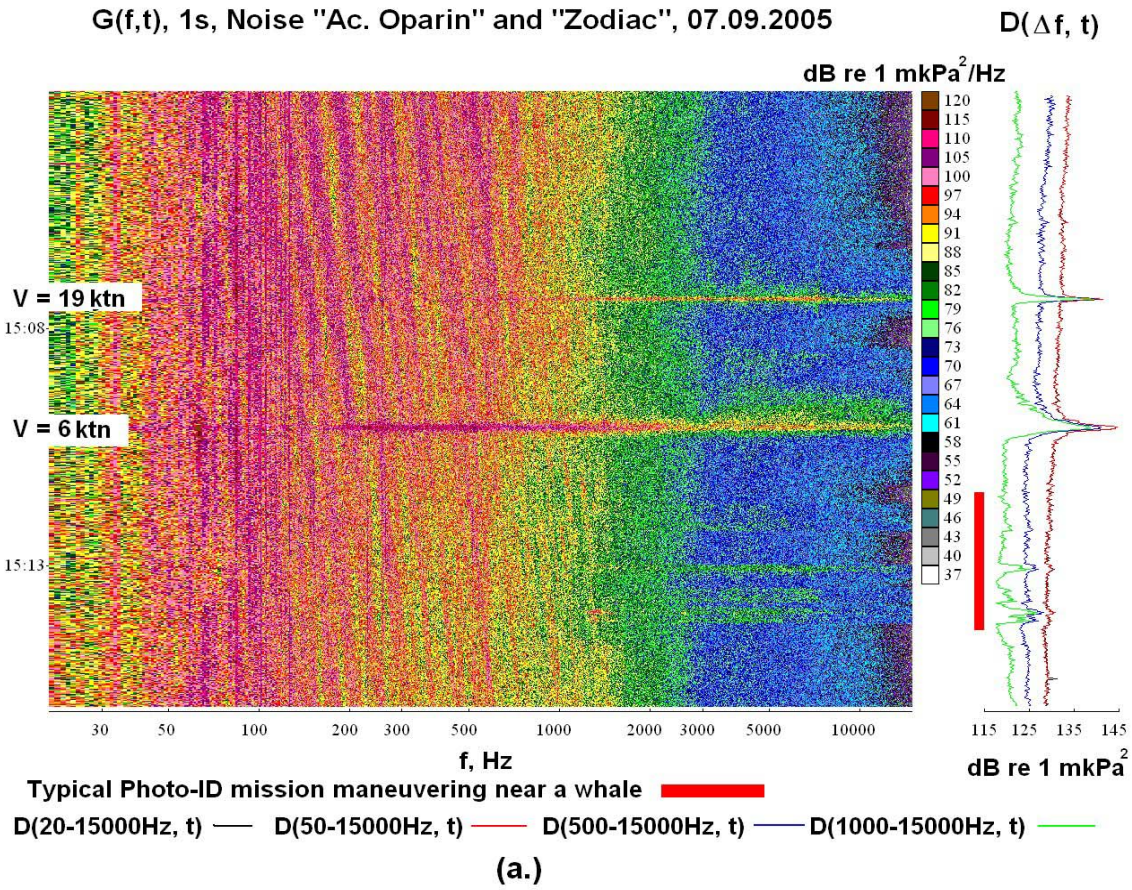

(a.)

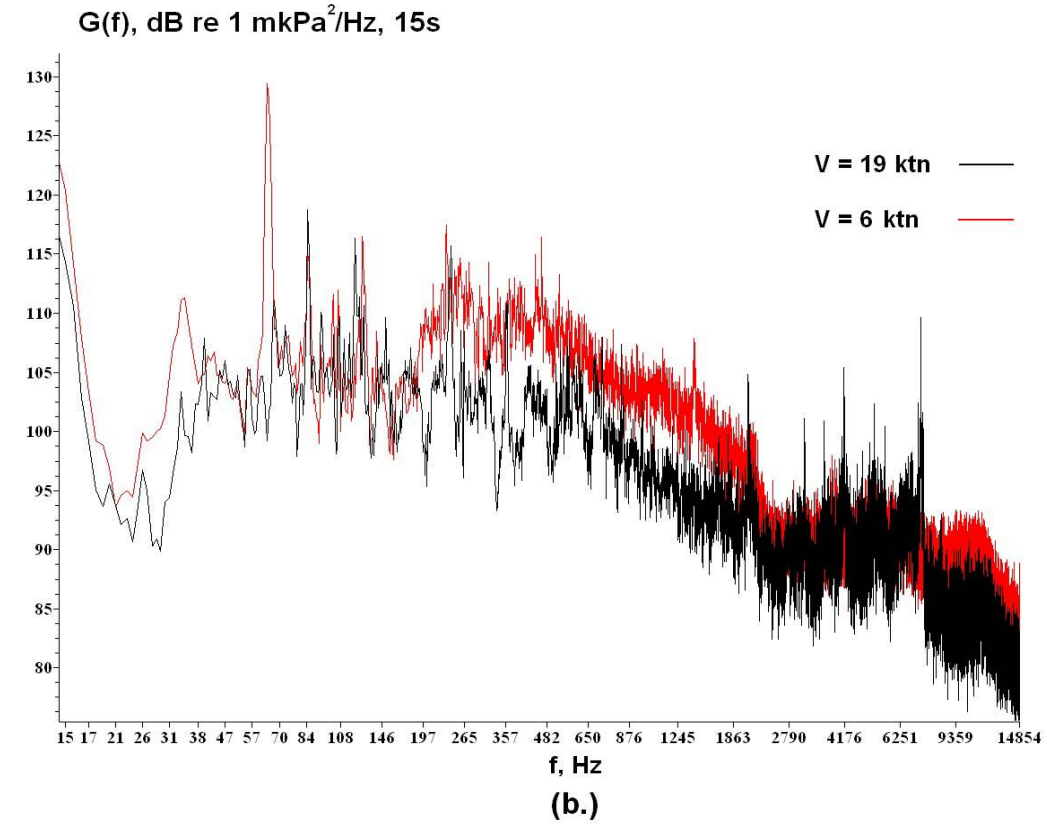

(b.)

Figure 6.5 - (a) Sonogram *G(f,t)* and (b) Spectra *G(f)* of data recorded as the Photo-ID zodiac was replicating a Photo-ID mission on the acoustic zodiac.

7 Bathymetric and Hydrologic Studies on the NE Sakhalin Shelf

This section presents the analysis of bathymetric and hydrological measurements performed during the 2005 field season. Bathymetric and hydrological measurements conducted during the 2004 field season are also used to explain the spatial distribution and variation in the temperature *T(r,z)* and salinity fields *S(r,z)* observed in the study area. In addition, the results of studies by other authors in the area in question and numerical simulation results are included. This data will be used to build acoustic models which will be used to model the acoustic fields generated by known sources and analyze the impact of bathymetry and hydrology on the propagation of these fields. The data will also be used to investigate the impact of temperature and salinity variations on benthos development.

7.1 Spatial and temporal variation of the key hydrological characteristics of the area

Oceanological studies were performed in an area from 51.36°N to 53.6°N and 143.1°E to 143.7°E (Figure 7.1). Overall, these observations extended over an area stretching from Nabil Bay to Okha along the NE coast of Sakhalin Island; this area of the Sea of Okhotsk extends approximately 200 km from its northern to southern edge. The shelf zone in this area is characterized by broad shallows, mostly with a sandy floor and patches of finer silty sand deposits near Chayvo and Niyskiy bays [Бровко et. al., 1999].

Several hydrological surveys and individual transects, both parallel to and perpendicular to the shore were completed in 2005 under different tidal phases and meteorological conditions. It is well known that in the study area, located on the shallow-water shelf at the western edge of the circular cyclonic flow of the Sea of Okhotsk, hydrological conditions are determined by the effects of wind and tides. The prevailing winds are southerly winds in the summer and northerly and northwesterly winds in the fall. In the presence of high wind speeds in coastal waters, Ekman (wind driven) currents are typically observed, with a characteristic current divergence of 90 degrees to the right of the wind direction [Леонтьев, 2001; Попудрибко et. al., 1998]. The East Sakhalin Current, one of the major components of the circulation of the Sea of Okhotsk, intensifies in the fall (starting in the second half of September); this intensification is associated with a rearrangement of atmospheric circulation and the prevalence of northerly winds.

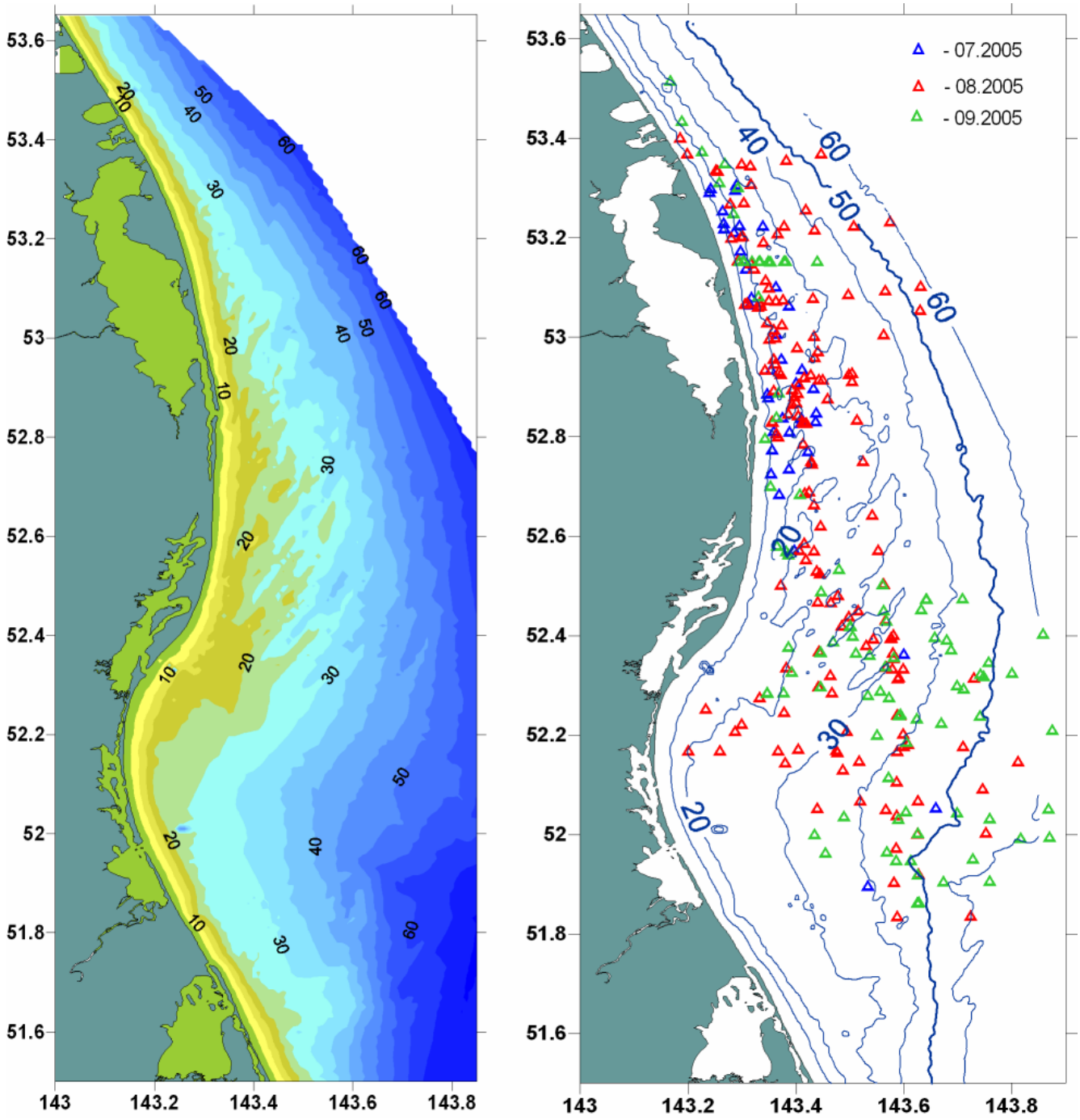

Figure 7.1 - Map of the NE Sakhalin Shelf showing (a) the bathymetry of the study area and (b) locations where vertical hydrologic profiles were acquired.

This current is created by the discharge of water from the Amur River into the bordering Amur firth and then into Sakhalin Bay. During the spring and summer-fall floods, the discharge from the Amur River passes through the north channel of the Amur firth into Sakhalin Bay of the Sea of Okhotsk, part of the discharge is carried beyond the northern end of Sakhalin Island. The water is then drawn into the flow of the East Sakhalin Current and flows along the east coast of the island.

The lens of fresh Amur River water is usually separated from the underlying sea water by a sharp density differential [Жабин et. al., 2005]. A characteristic of this water mass is its low salinity, which was as low as 21 psu (Practical Salinity Unit) in the near-shore transect run on 14 July 2005, and shown in Figure 7.2. In comparison, data obtained in Sakhalin Bay of the Sea of Okhotsk in July 2003, showed that this freshening could be traced to a depth of 20 m in the Amur River discharge lens, and the freshest waters (S < 22.5 psu) formed a uniform surface layer about 5 m deep, the water temperature in this surface layer was more than 13°C [Жабин et. al., 2005].

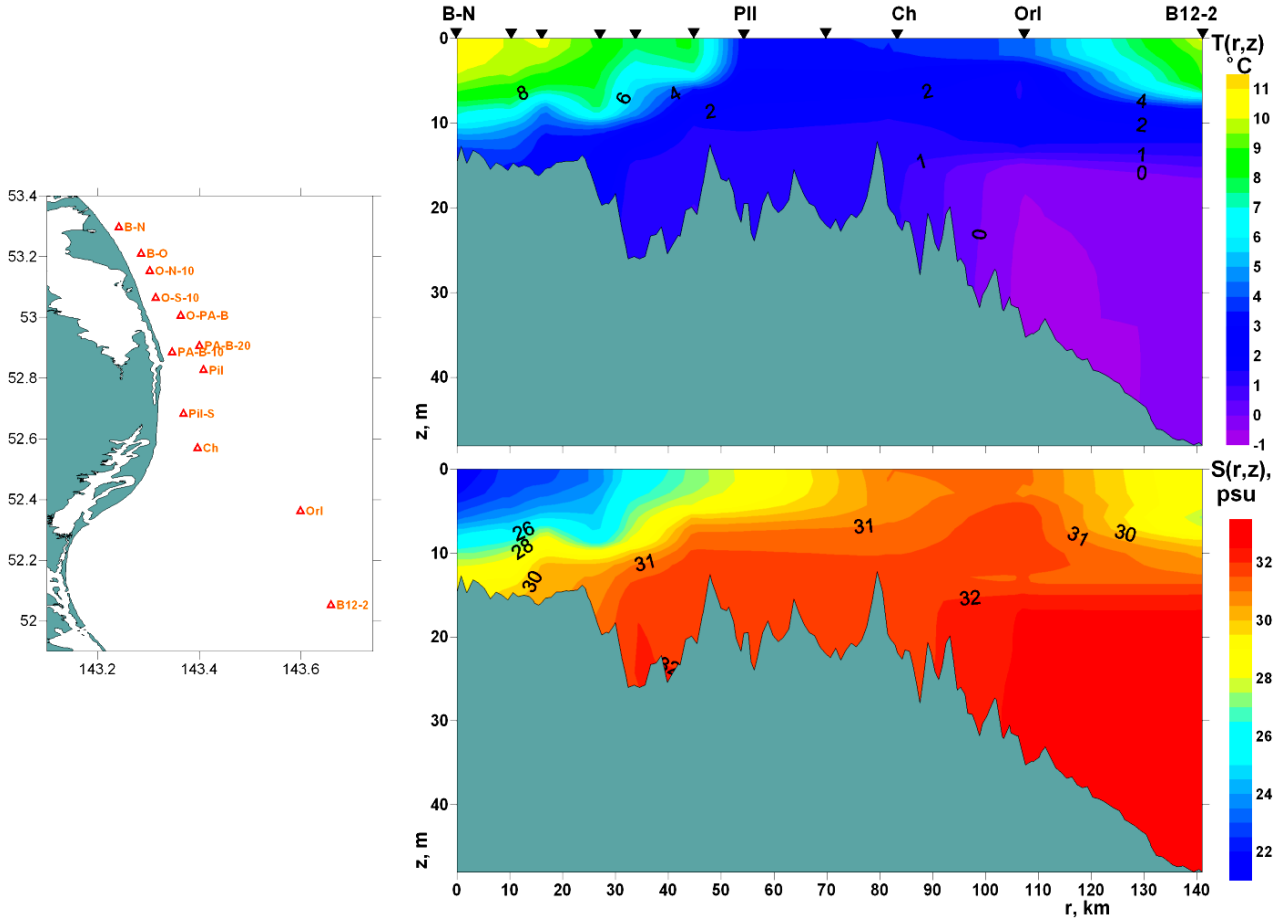

Figure 7.2 – Location of the sampling stations for a hydrological transect along the coast from the A10 (BEH-North) acoustic station to the Orlan monitor station and distribution of Temperature *T(r,z)* and salinity *S(r,z)* along the transect.

The low salinity in the northern part of this transect (to Piltun lighthouse) is also supported by the transfer of fresh water from Piltun Bay. A lens of Amur river water in which the surface water temperature reached 11 °C can easily be seen on this transect. The boundary of the plume of fresh water could be visually traced by the sharp change in water color from brownish to dark blue. A hydrological front, with significant salinity and water

temperature differentials, was also seen near Piltun Lighthouse (Figure 7.2). The front dividing the relatively fresh water (due to discharges from the Amur River) from the more saline shelf water is located northeast of Niyskiy Bay. South of Piltun lighthouse the water temperature decreased to 2.5-3.5°C, and the salinity increased to 31.2 psu. Only at the southernmost point of the transect did the water temperature at the surface rise as high as 10°C, but with higher salinity. Waters with temperatures below 1.5 °C and salinity above 32.5 psu were found at depths greater than 12 m in the channels off Piltun lighthouse and south of Chayvo. The transect clearly shows that high density cold (-1 to -1.5 °C at depths greater than 15 m) near-bottom shelf waters are present not far off shore, and come even closer to shore along deep seabed channels during high tides.

Studies conducted in July 2003 [Жабин et. al, 2003] showed that the elements required for biogenic growth are less concentrated in the lens of Amur River water than in the surface waters of the Okhotsk Sea shelf, due to photosynthesis. However, mineralization of organic matter does cause these elements to accumulate in the near-bottom layer under the lens.

As a result of the concentrated warming of surface waters and inflows of significant quantities of warm, fresh Amur River water from Sakhalin Bay, the hydrological front had shifted considerably southwards by mid-August. This can be seen in the southernmost part of the transect run south from Chayvo on August 11 (Figure 7.3), where the water temperature decreases from 15 °C to 12 °C along the transect. A cold-water layer with negative temperatures was present beyond the 35-meter isobath, rising to a depth of 12-15 m from the surface.

A transect run opposite the northern part of Piltun Bay, shown in Figure 7.4, clearly shows a lens of Amur waters more than 20 km wide. In the central part of the lens, freshening occurs to a depth of 12 m. The freshest waters (S < 25 psu) formed a uniform surface layer up to 10 m deep. The water temperature in the layer was more than 16 °C, which is significantly higher than the background surface temperature of the shelf waters of the Sea of Okhotsk. High-density shelf waters formed during winter convection, and caused by salinization as a result of ice growth, with temperatures less than 0 °C and salinities greater than 32 psu are present near the seabed at a distance of more than 10 km from shore (Figure 7.4). In comparison, the surface water temperature in the near-shore, relatively

mixed zone did not exceed 10-13 °C in August 2004, the salinity was above 28 psu, and the water temperature in the near-bottom shelf waters was above 0 °C.

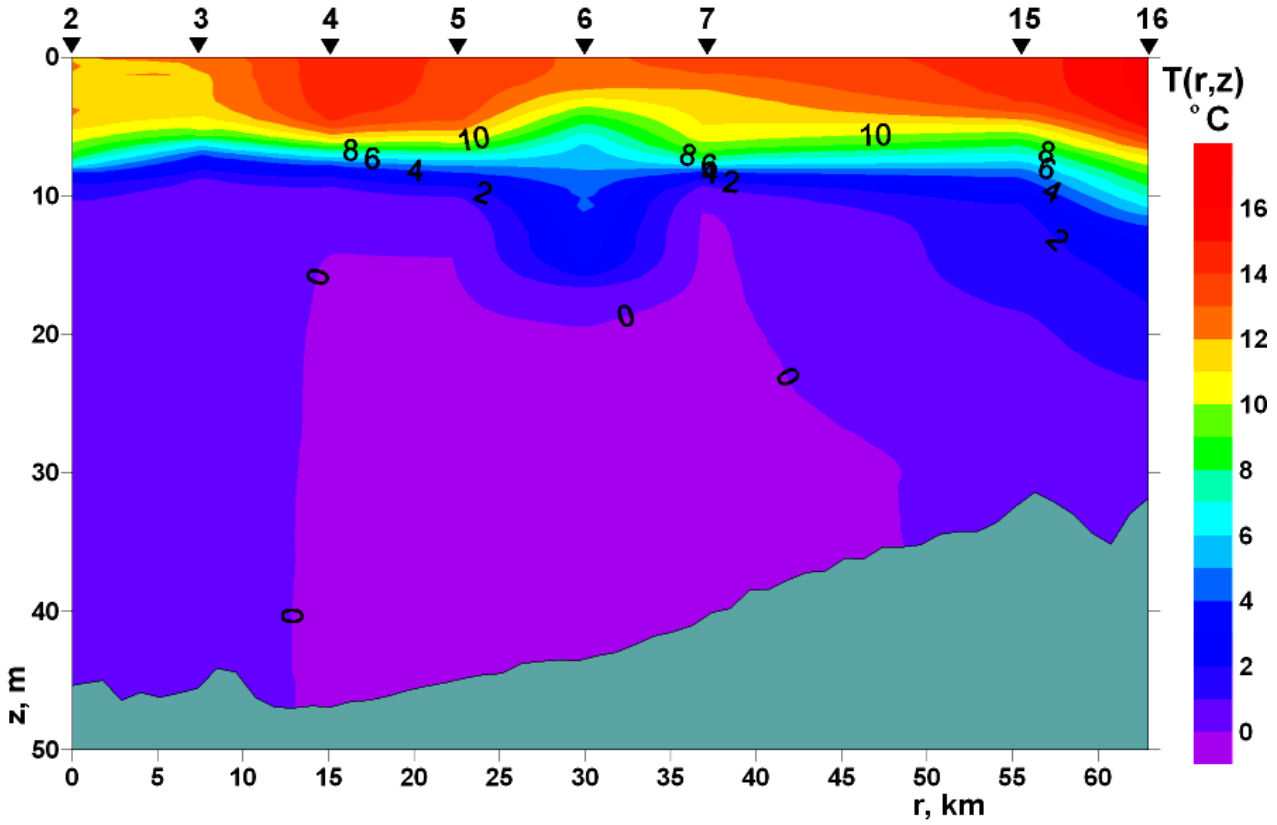

Figure 7.3 – Distribution of Temperature *T(r,z)* along a meridian transect on 143°35' acquired on 11 August 2005.

After intensive mixing as a result of the prolonged effect of gale force winds – initially southerly winds and then northerly winds – during the period of 12-16 August, there were substantial changes in the hydrological structure of near-shore shelf waters. A meridian transect run south of Chayvo on 19 August (Figure 7.5) clearly shows that as the depth of the uniform surface layer increased to 5-10 m, the water temperature in the layer dropped to 12-13.5 °C, and the thermocline grew much wider, with a decrease in the maximum vertical temperature gradient from 4 °C to 1 °C per m. Throughout the transect, waters with salinity below 28 psu were present to a depth of 15 m, and cold waters with maximum density receded beyond the 40-meter isobath.

Intensification of the southward flow along the shore occurs in the fall and is generally associated with changes in atmospheric circulation and the temperature and salinity fields.

The hydrological front disappears, and the temperature and salinity isolines are oriented parallel to the shore.

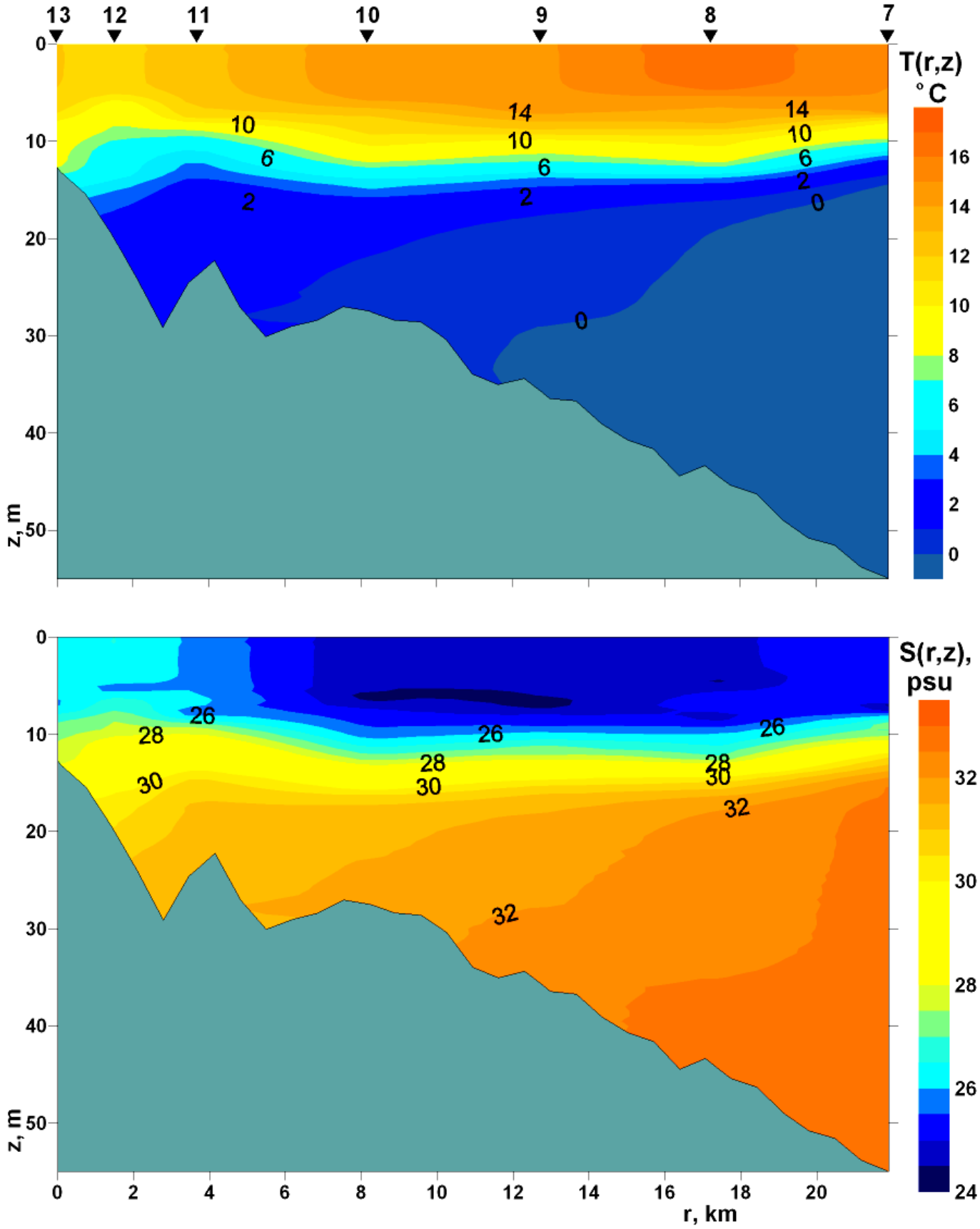

Figure 7.4 – Distribution of Temperature *T(r,z)* and salinity *S(r,z)* along the transect near the Odoptu-S stations acquired on 11 August 2005.

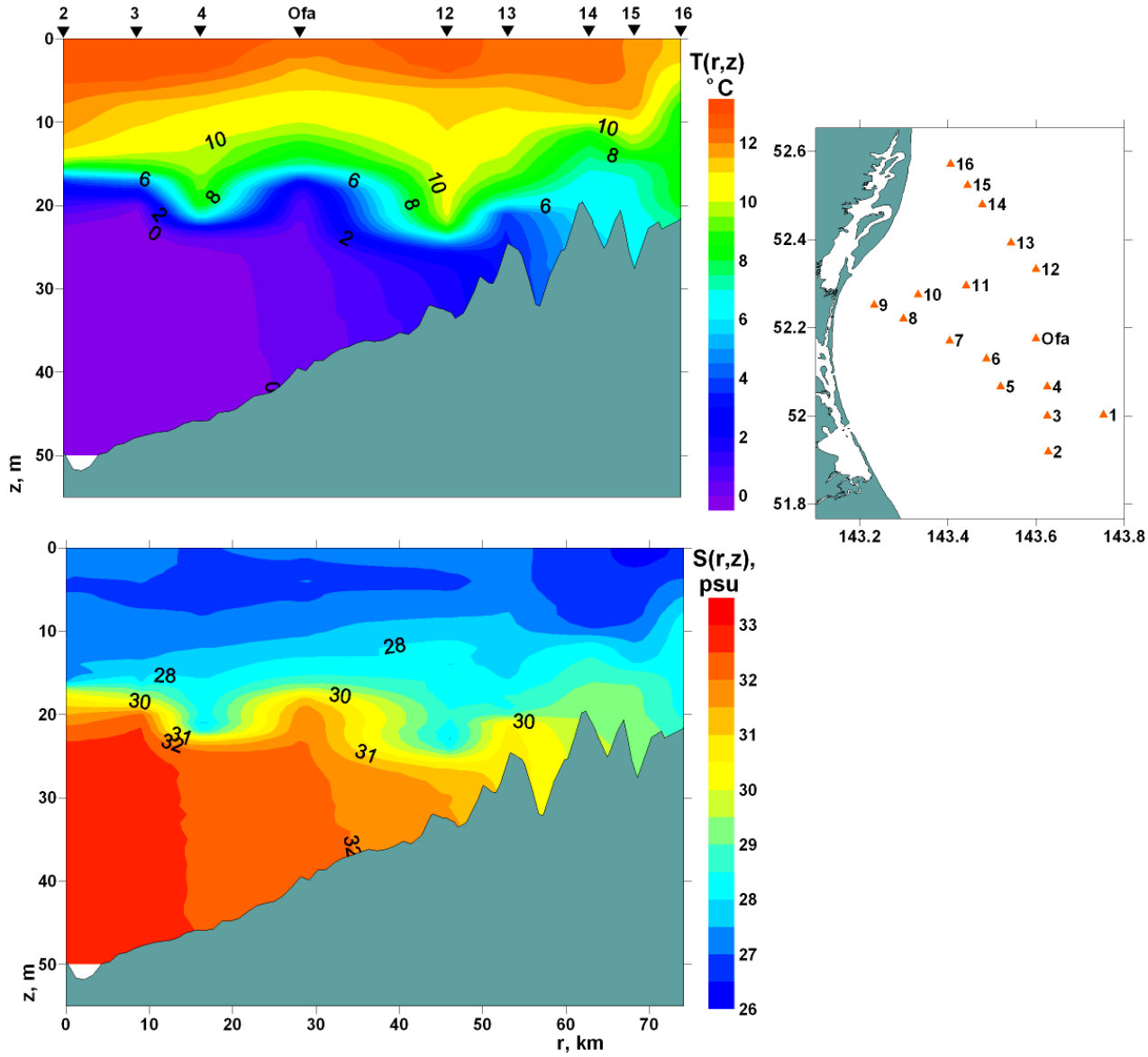

Figure 7.5 – Location of the sampling stations for a hydrological transect from the Lunskoye to the Orlan monitor stations and distribution of Temperature *T(r,z)* and salinity *S(r,z)* along the transect acquired on 19-20 August 2005.

In early September, after the passage of several cyclones and the prolonged effect of northerly winds, the uniform surface layer had grown even larger (to 20-25 m), and water with a uniform temperature (11-13 °C on 7 September, and 9-11 °C on 14 September), was present off Chayvo at a depth of less than 30 m. This was also supported by tidal mixing, and water with negative temperatures was not recorded, even at depths greater than 40 m (Figure 7.6). By comparison, the water temperature in the 20-30 m layer was 3-5 °C lower in September 2004.

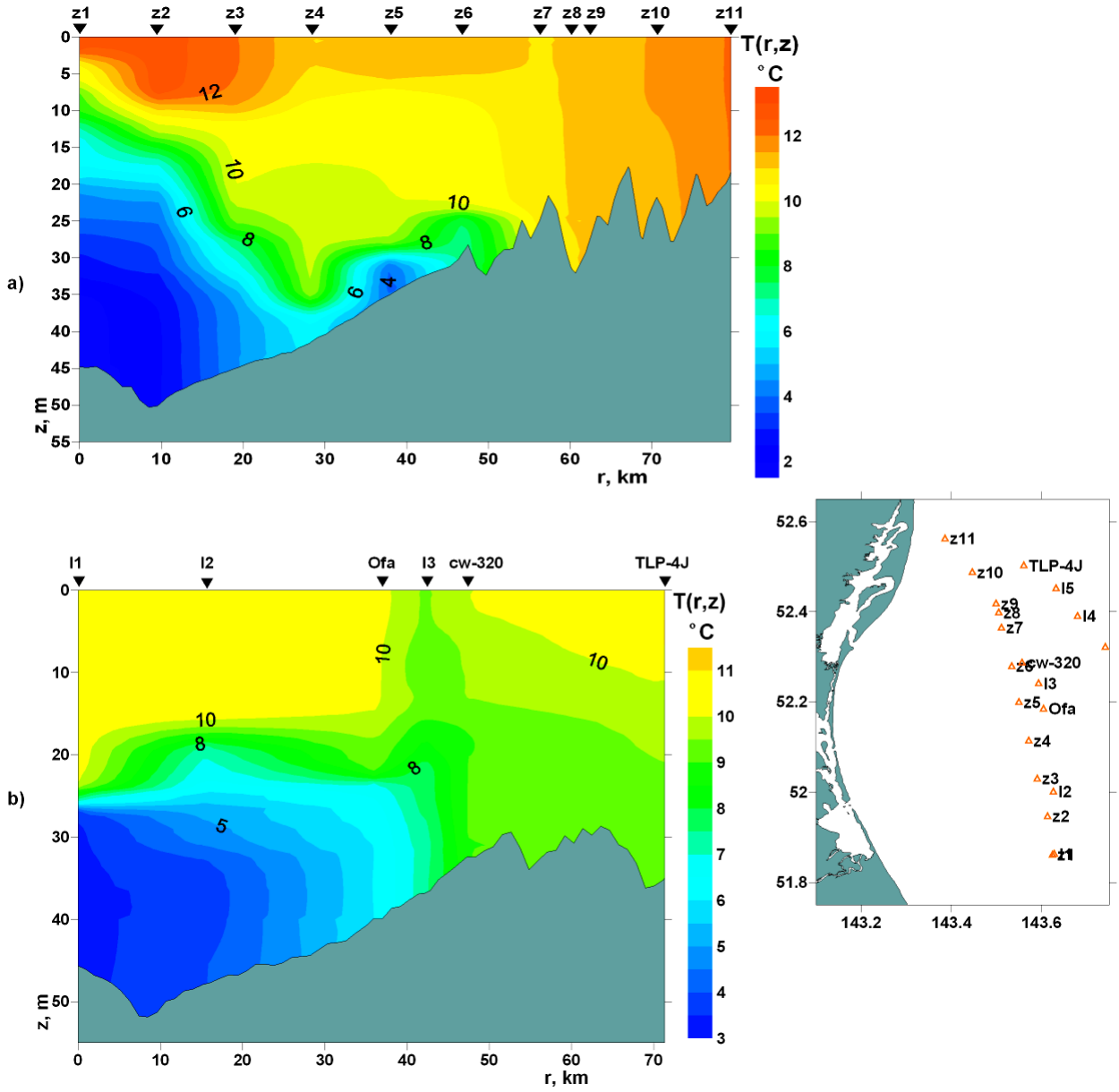

Figure 7.6 – Location of the sampling stations and distribution of Temperature *T(r,z)* for hydrological transects from the Lunskoye monitor station north acquired on 7 (mixed semidiurnal tide, amplitude 0.4 m); and 14 September (maximum diurnal tide amplitude 1.5 m).

Hence, considerable spatial and temporal variation occurs in the hydrological characteristics of the study area as a result of the periodic effects of tidal processes and the non-periodic impact of multi-directional winds. In July the surface water temperature along the coast varied from 2.5 to 11.5 °C, and the salinity varied from 21 to 31.3 psu, while the temperature near the seabed varied from 1 to 4 °C, and the salinity varied from 29 to 31.5 psu; beyond the 30-meter isobath, the water temperature was below 0 °C, and the salinity was higher than 32 psu.

The greatest variations in hydrological characteristics were observed in August. The water temperature in the near-shore zone varied from 4 °C to 17 °C, and the salinity varied from 24 to 30 psu. The maximum variations were observed on the shallow-water shelf within the 20-meter isobath; a local salinity minimum as low as 21 psu was recorded at the outlet from Piltun Bay and was associated with the outflow of water from Bay during the maximum amplitude tides.

Temperature and salinity fluctuations are not so large beyond the 30-meter isobath. The temperature varied from 8 °C to 16 °C, and the salinity from 24 psu to 31.5 psu. The lowest salinity and the highest water temperature were measured in a lens of mixed Amur River and Okhotsk Sea water flowing from the north.

In September, due to the passage of several cyclones and the prolonged effect of northerly winds, the uniform surface layer grew to 20-25 m, and water with a uniform temperature of 9 °C to 13 °C was present off the coast at depths less than 20 m. The minimum salinity increased to 29.2-29.4 psu. This was also supported by intensive tidal mixing, and water with negative temperatures was not recorded, even at depths greater than 40 m.

7.2 Upwelling

The prevailing southerly winds result in coastal upwelling during the summer season, this effect is frequently encountered in the world's oceans. In the Northern Hemisphere, upwelling is conditioned by longshore winds blowing with the coast on the left [Bowden; 1983], with characteristic opposing zonal flows in the surface and benthic layers. It is caused by steady winds driving surface waters out to sea, to be replaced by deeper waters rising to the surface.

Instrumental current data acquired on the NE Sakhalin shelf during the 1990's [Попудрибко et. al.; 1998] and satellite images provide support for the theory that the upwelling observed during the summer season is typical of the entire coastal strip from Nabil Bay to Cape Lowenstern. In the presence of high wind speeds (>12 m/s), typical wind (Ekman) drift is observed, with a characteristic current divergence of 90 degrees to the right of the wind direction. A pressure differential emerges as a result of the wind-driven ebb and flow of the water and is equalized by the Coriolis force and friction at the seabed and the shore.

The hydrological characteristics (seawater temperature and salinity, as well as measured sound speed) in July-September 2005 were characterized by large temporal and spatial variations. The variations were conditioned by the formation of non-periodic currents under the influence of southerly and northerly winds, as well as by tidal conditions (changes in the level, speed and direction of tidal flows). Wind currents have different directions in the surface and benthic layers. Southerly winds drive surface waves toward the sea, and the cold waters of the deeper layers rise toward the surface along the coast; the opposite effect is observed under the effect of prolonged northerly winds, with surface waters driven toward the coast, while cold benthic waters are forced farther from shore. Figure 7.7 presents wind speeds and directions (daily averages), as well as a wind rose plotted from data obtained from the Molikpaq Platform.

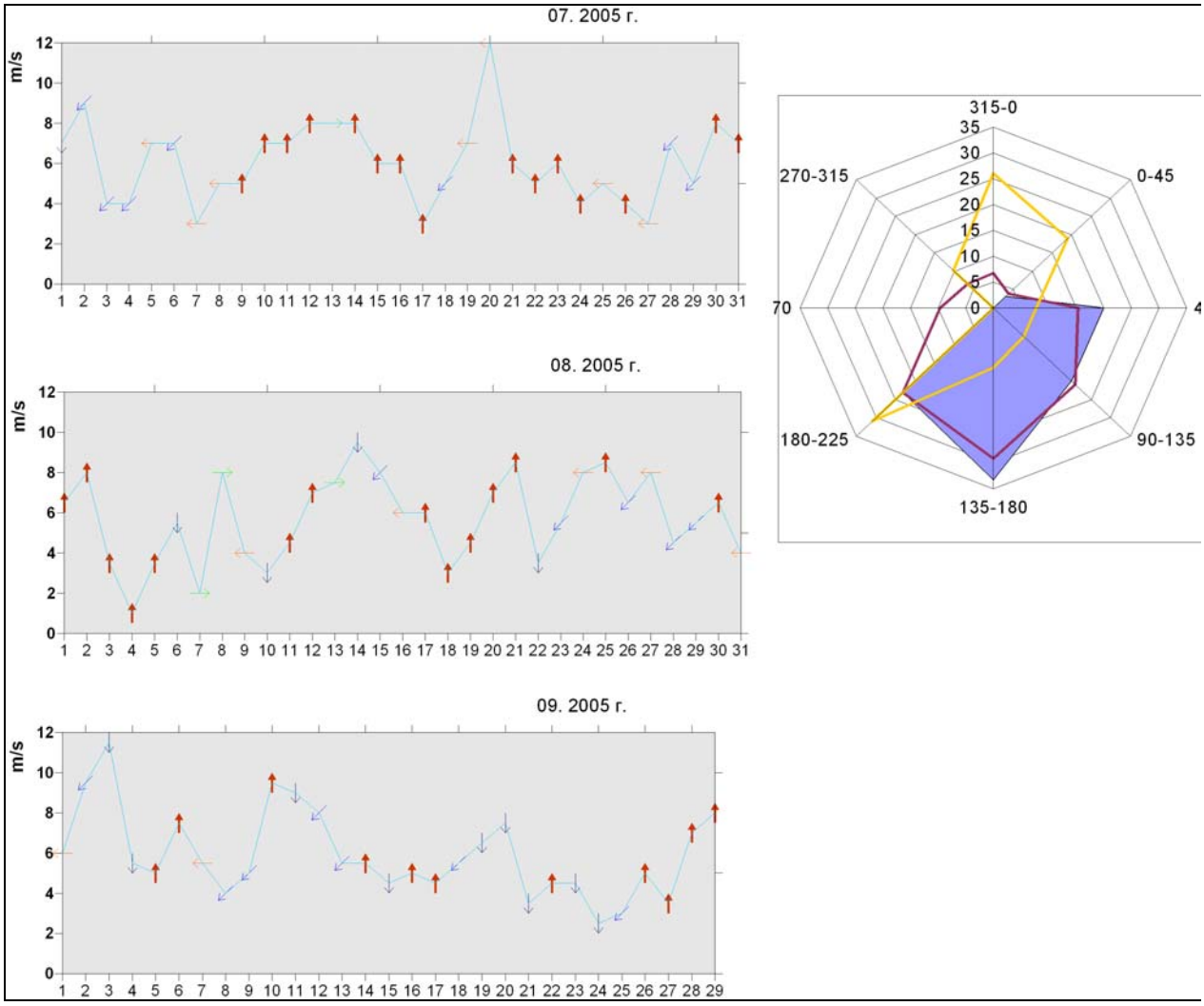

Figure 7.7 – Daily average wind speed and direction and a wind rose (in percent) for July-September 2005. Blue - July; brown - August; yellow - September.

Two hydrological transects, corresponding to the impact on the sea of a southerly wind for the first two days and then a northerly wind for two more days were run to assess the effect of wind on water circulation in the study area, and the related hydrological distribution. The upwelling phenomenon was clearly observed on 12-13 August, when the speed of the southerly wind averaged 8 m/s for the day and sometimes exceeded 15 m/s. In the presence of a strong gale force northerly wind on 14-15 August (averaging 12-14 m/s), the opposite situation was observed. In the former situation, an onshore current was observed in the surface layer, while an offshore current was observed in the near-bottom layer. Figure 7.8 shows the distribution of temperature and salinity fields for a transect completed on 11 August (before upwelling). Throughout the transect, there is a semi-uniform layer with a water temperature of 12 °C -16.5 °C and a salinity of less than 26 psu from the water surface to a depth of 8-10 m; only at the shore is the temperature somewhat lower and the salinity somewhat higher, indicating a tidal influence. Water with a negative temperature and a salinity above 32 psu is present at a distance of more than 10 km from shore, beyond the 30-meter isobath.

Figures 7.9 and 7.10 show the spatial distributions of the temperature and salinity fields obtained on the same transect on 13 August after upwelling and 16 August after the onshore surge. Due to the upwelling, warm, less saline water has moved 6-10 km away from the shore and cold (below 4 °C) and saline (up to 30 psu) near-bottom water from the Sea of Okhotsk has filled in the near-shore zone and moved toward the surface. A near-bottom water layer with a negative temperature has approached within 2 km of the shore.

The opposite situation was observed on 16 August, when warm (above 12 °C), fresh (less than 26 psu) water filled the coastal shallows to a depth of more than 20 m and a distance of more than 12 km from shore, and water with negative temperatures was not observed, even at the deepest station of the transect.

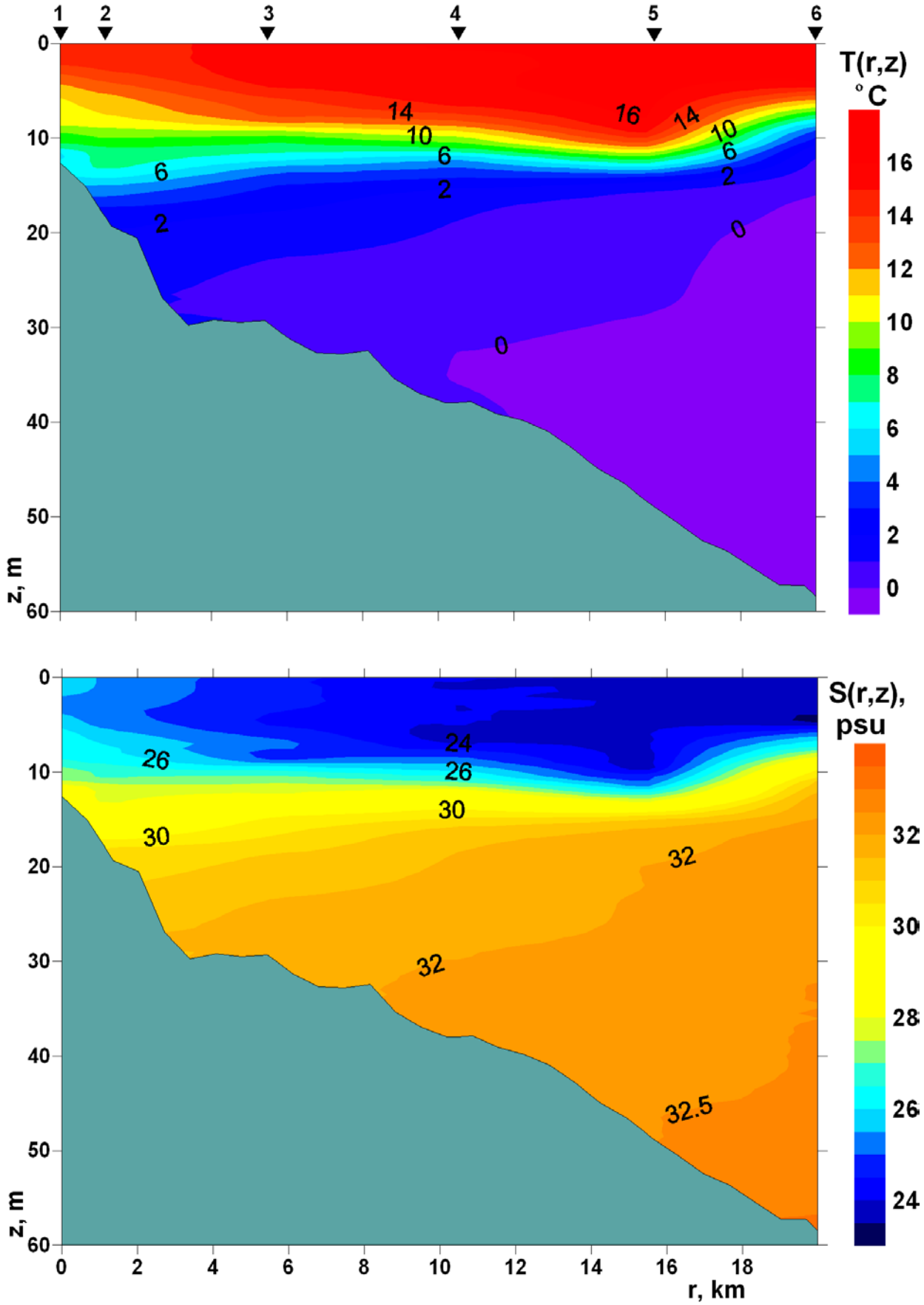

Figure 7.8 – Distribution of Temperature *T(r,z)* and salinity *S(r,z)* along a transect near the Odoptu-N stations acquired on 11 August 2005.

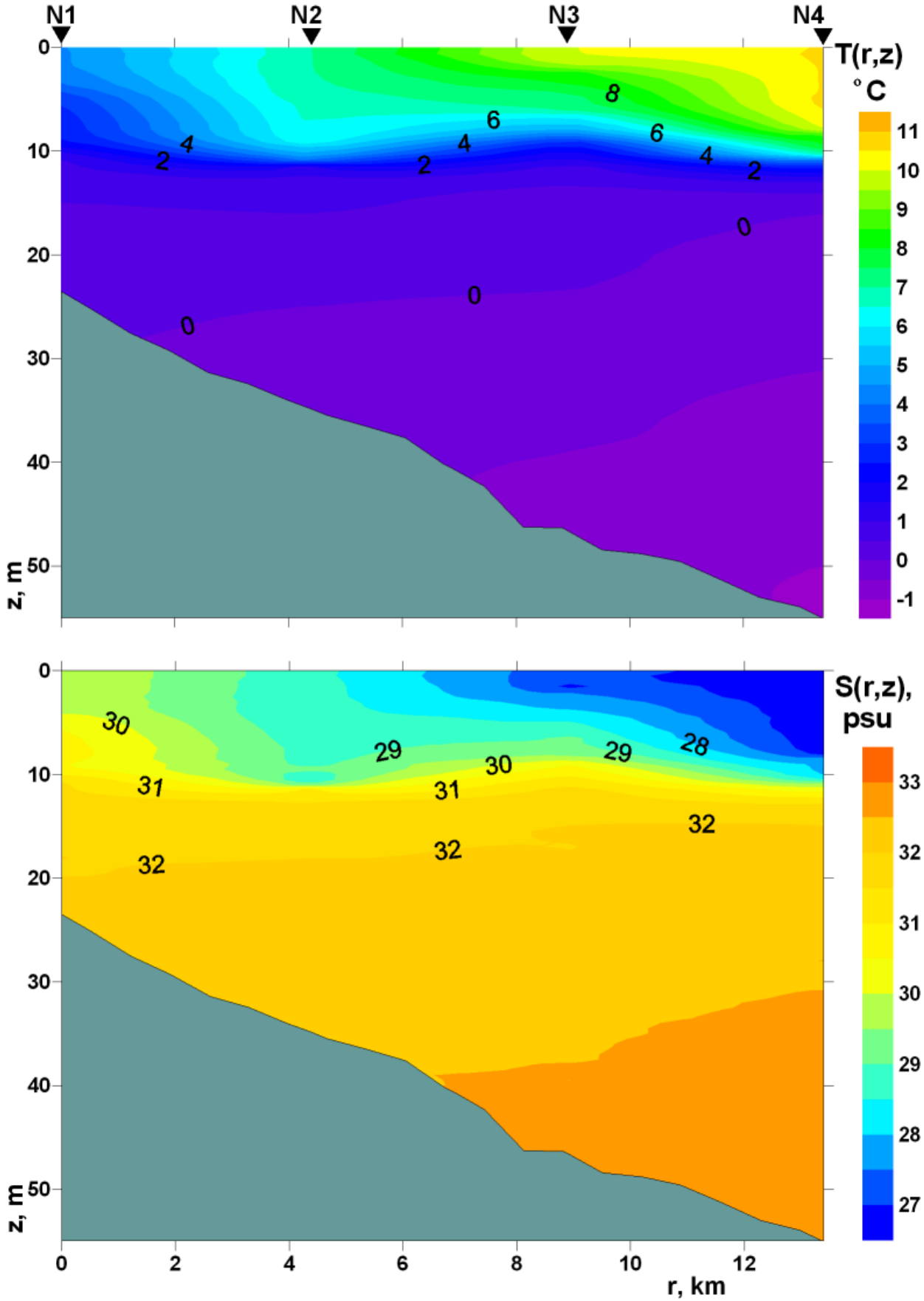

Figure 7.9 – Distribution of Temperature *T(r,z)* and salinity *S(r,z)* along a transect near the Odoptu-N stations acquired during upwelling on 13 August 2005.

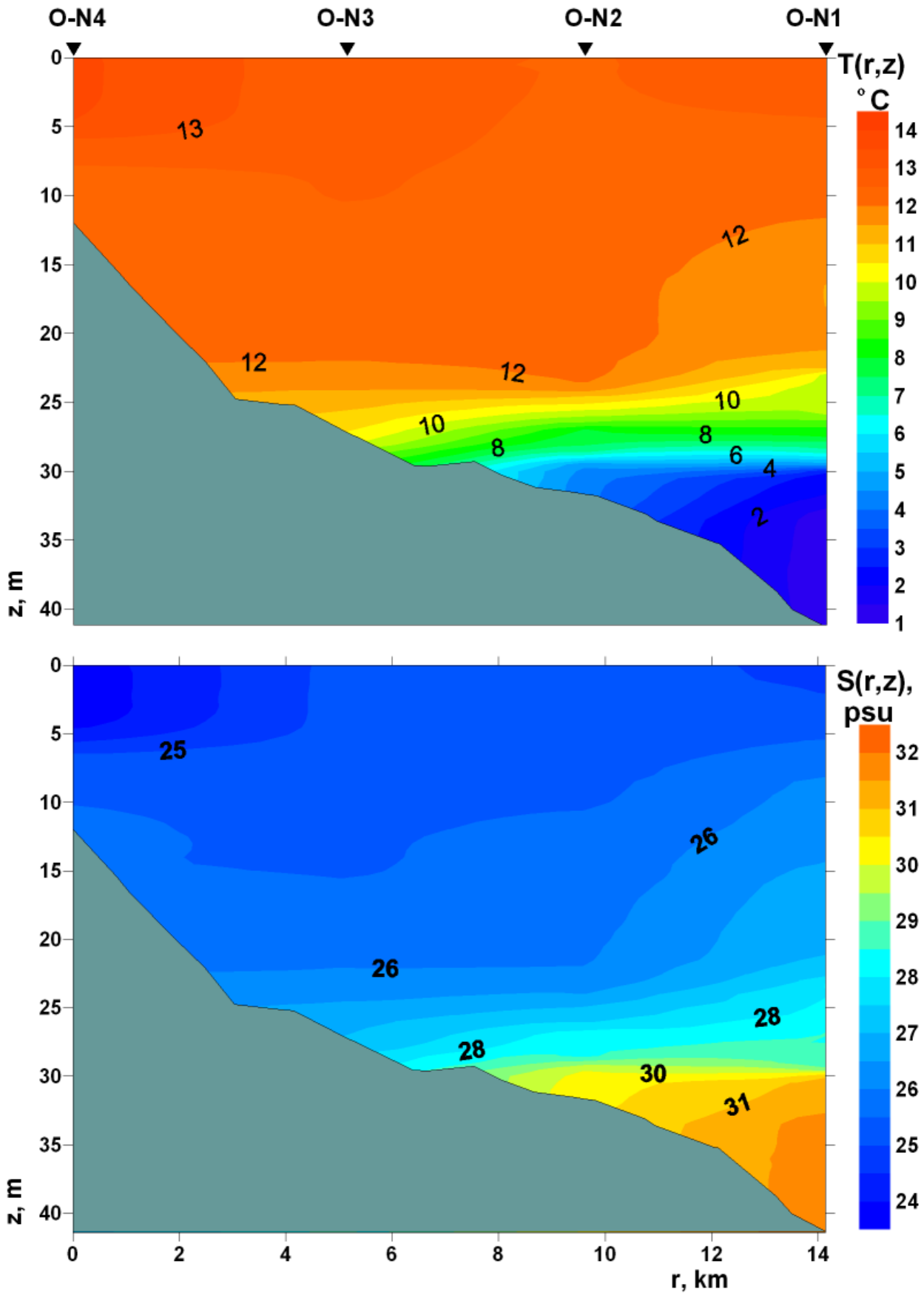

Figure 7.10 – Distribution of Temperature *T(r,z)* and salinity *S(r,z)* along a transect near the Odoptu-N stations acquired a wind surge on 16 August 2005.

7.3 Impact of tides and the sea bed bathymetry on the hydrological fields

Wind has a dominant effect on the formation of the hydrological fields on the shelf; tidal processes are also dominant factors. Transects completed on 20 August during the high tide phase (see Figure 7.11) show the tidal influence on variations in the temperature and salinity structure of the area. The figure clearly shows the two-layered current structure. The flow at the surface is toward shore, as indicated by the transfer of warmer, less saline waters from the seaward section. At depths below 20 m, the current flows out to sea, as reflected in the decrease in salinity and increase in temperature. The opposite situation is observed at low tide (Figure 7.12). The flow at the surface is away from shore, as indicated by the transfer of warmer and less saline water into the seaward section. At greater depths, the current flows toward shore, as reflected in the increase in salinity and the decrease in temperature near the coast.

One of the key tasks of the hydrological studies was to establish the relationship between the benthos distribution and the hydrology of the area. The effect of the sea floor bathymetric features on the shoreward movement of cold, benthic Okhotsk Sea water, which is rich in biogenic matter, therefore received special attention. These bathymetric features are dominated by the alternation of ridges and channels in the seabed bathymetry (Figure 7.1). Hydrological transects were run both over ridges and over deeper troughs. In addition, two transects were run along the 20-meter isobath (Figure 7.13), crossing deep channels that come close to shore.

This task was complicated by the fact that measured depths often fail to match the depths indicated on navigational charts. Figure 7.13 clearly shows that colder, more saline water is found in the deeper troughs and comes close to shore along those troughs.

7.4 Impact of tides and the sea bed bathymetry on the hydrological fields

The primary prey of the western gray whale is benthos which depends for its development on zooplankton and phytoplankton which in turn depend on biogens, the temperature, salinity and oxygen concentration of the seawater as well as other oceanographic parameters such as current development. One of the oceanographic characteristics that most significantly influences the development of the benthos communities on the Sakhalin shelf during summer is the near-bottom water temperature. This temperature can differ

significantly from year to year, depending on the weather and ice conditions during the prior cold season. Unfavorable temperatures, especially during spawning, could limit the abundance of the next generations of benthic communities. Figure 7.14 gives a map of the temperature field near the seabed, generated from data acquired from 12 to 16 August in 2004 and 2005.

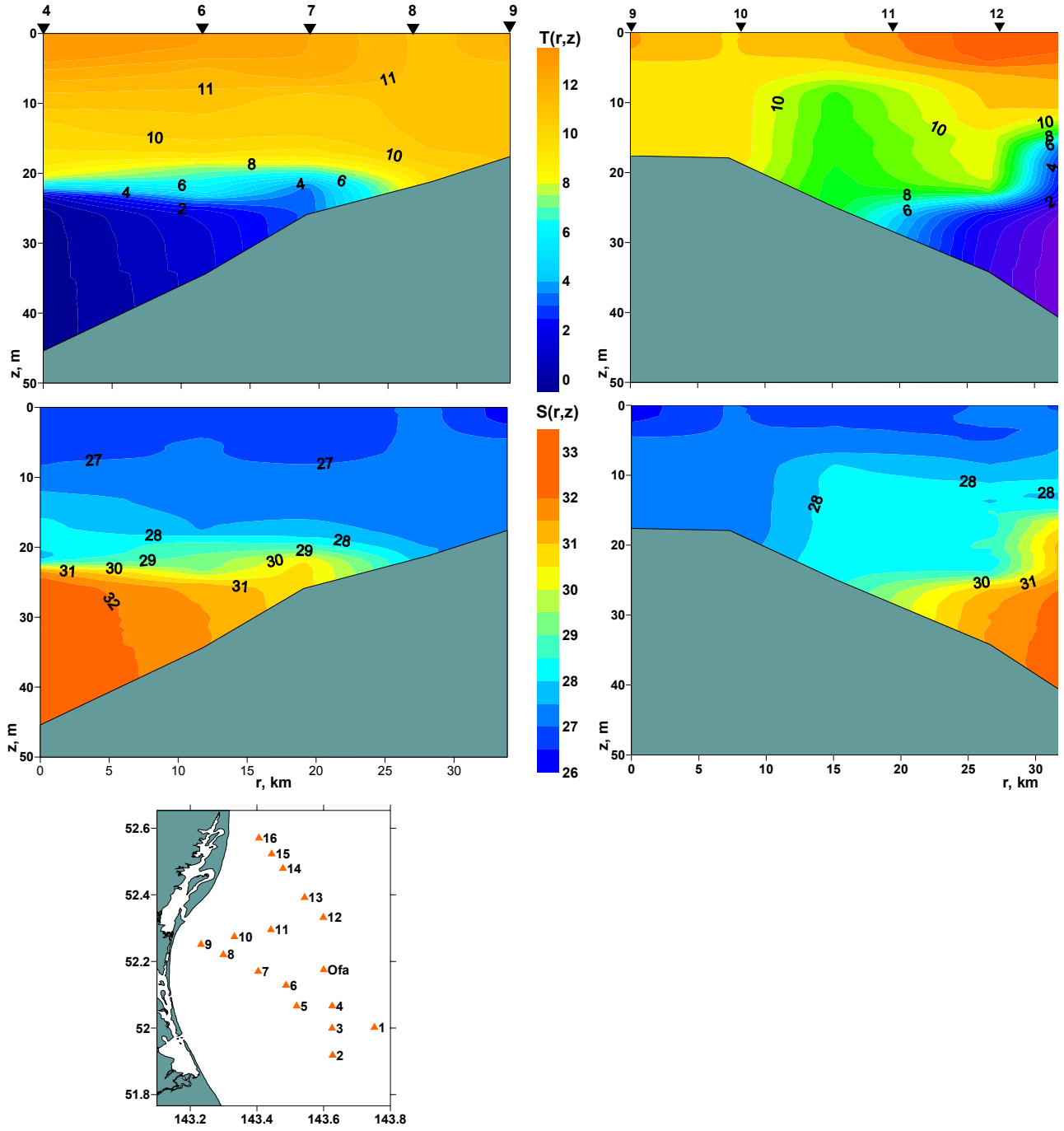

Figure 7.11 – Location of the sampling stations for a hydrological transect south of the Orlan platform and distribution of Temperature *T(r,z)* and salinity *S(r,z)* along the transect acquired at high tide on 20 August 2005.

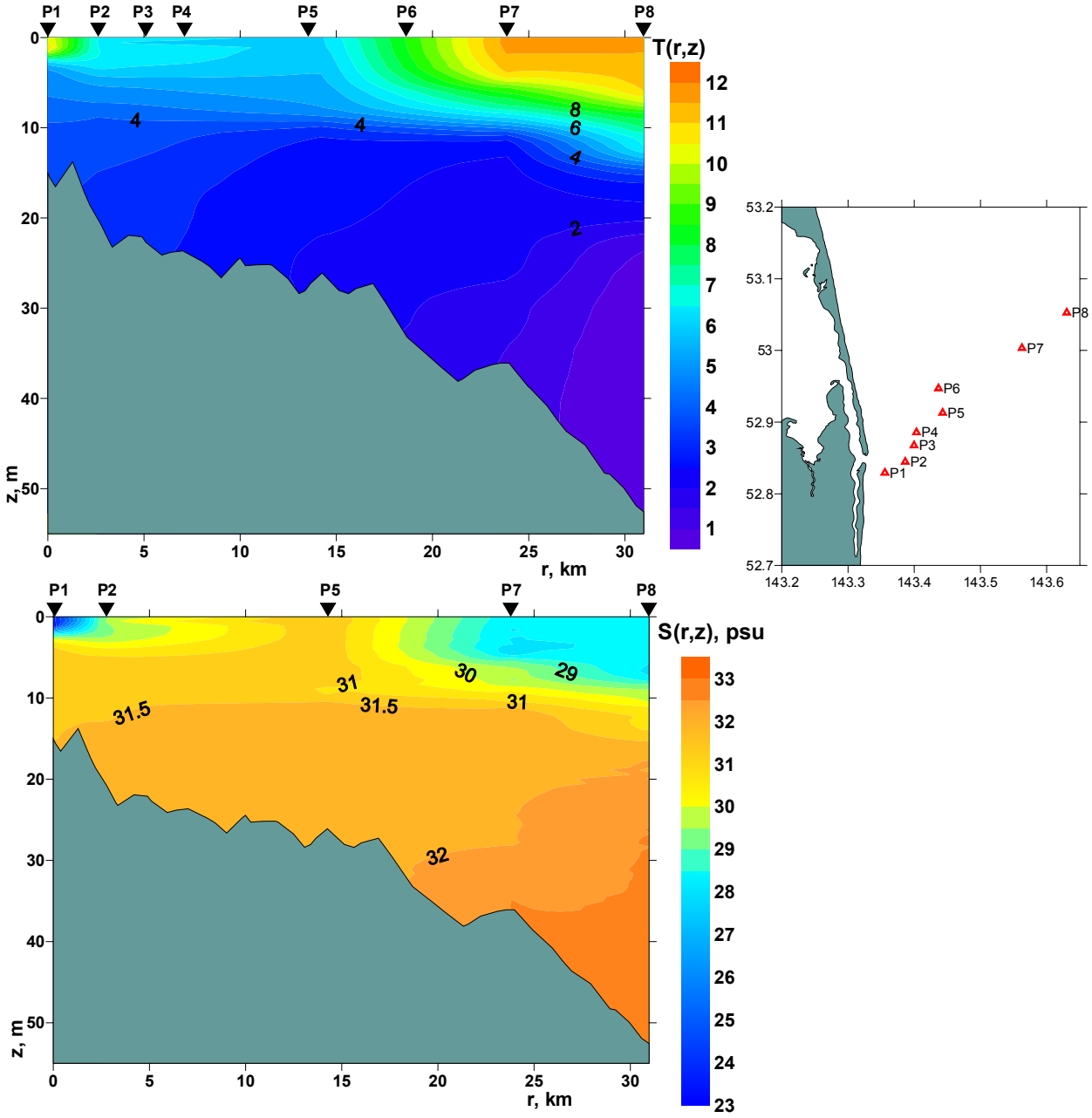

Figure 7.12 – Location of the sampling stations for a hydrological transect along the channel off Piltun lighthouse and distribution of Temperature *T(r,z)* and salinity *S(r,z)* along the transect acquired at low tide on 26 August, 2005.

It can be clearly seen from Figure 7.14 that in mid-August 2005 the temperature in the offshore feeding area was on average 2 °C degrees lower and in the Piltun feeding area 4 °C lower than in mid-August 2004. In mid-August 2004 negative temperatures were recorded only at a depth of more than 40 m opposite the mouth of Piltun lagoon. In 2005 temperatures below freezing were observed along the whole coastline at depths greater than 35 m.

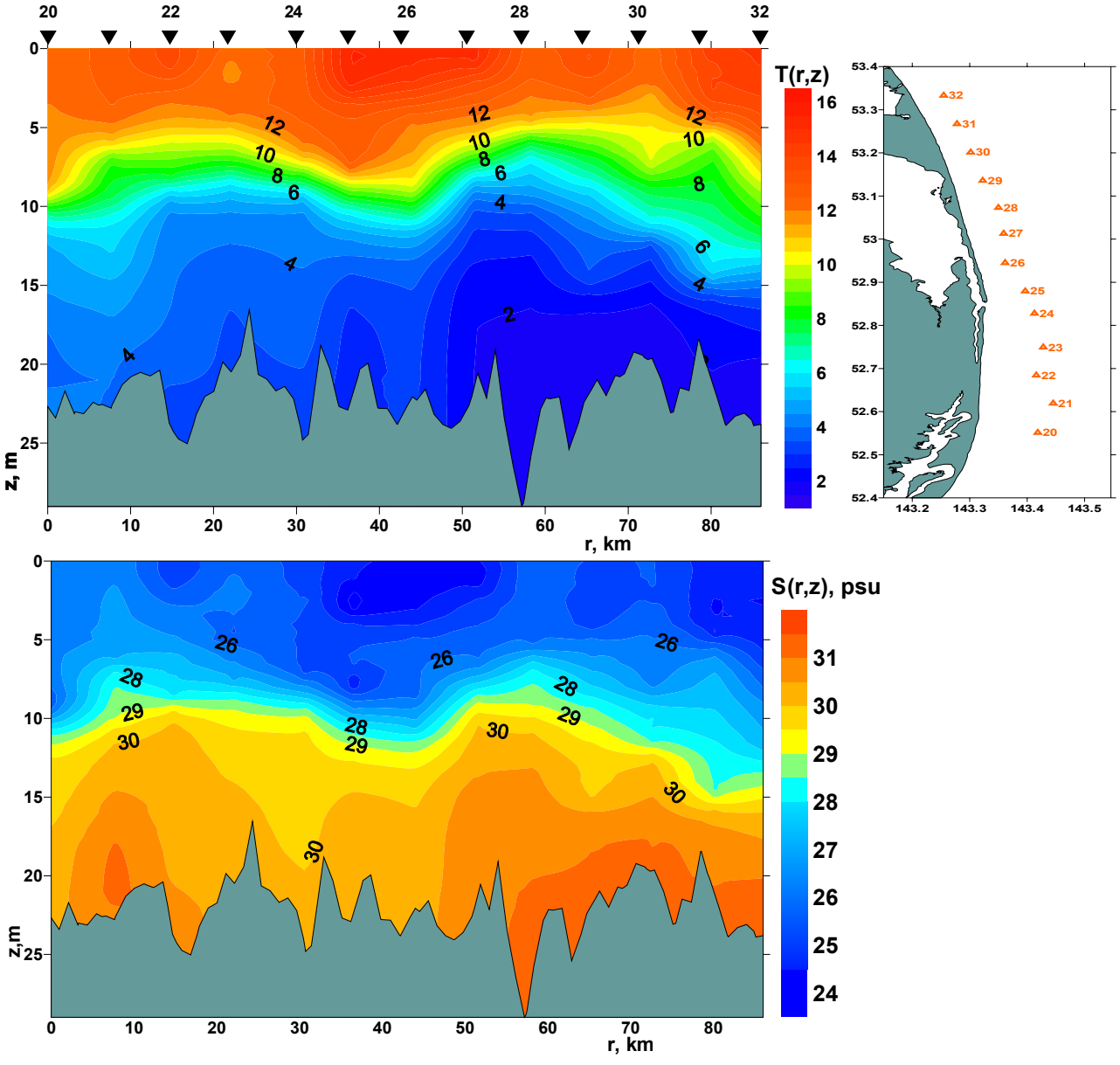

Figure 7.13 – Location of the sampling stations for a hydrological transect along the 20 m isobath north of Chayvo Bay and distribution of Temperature *T(r,z)* and salinity *S(r,z)* along the transect acquired on 11 August 2005.

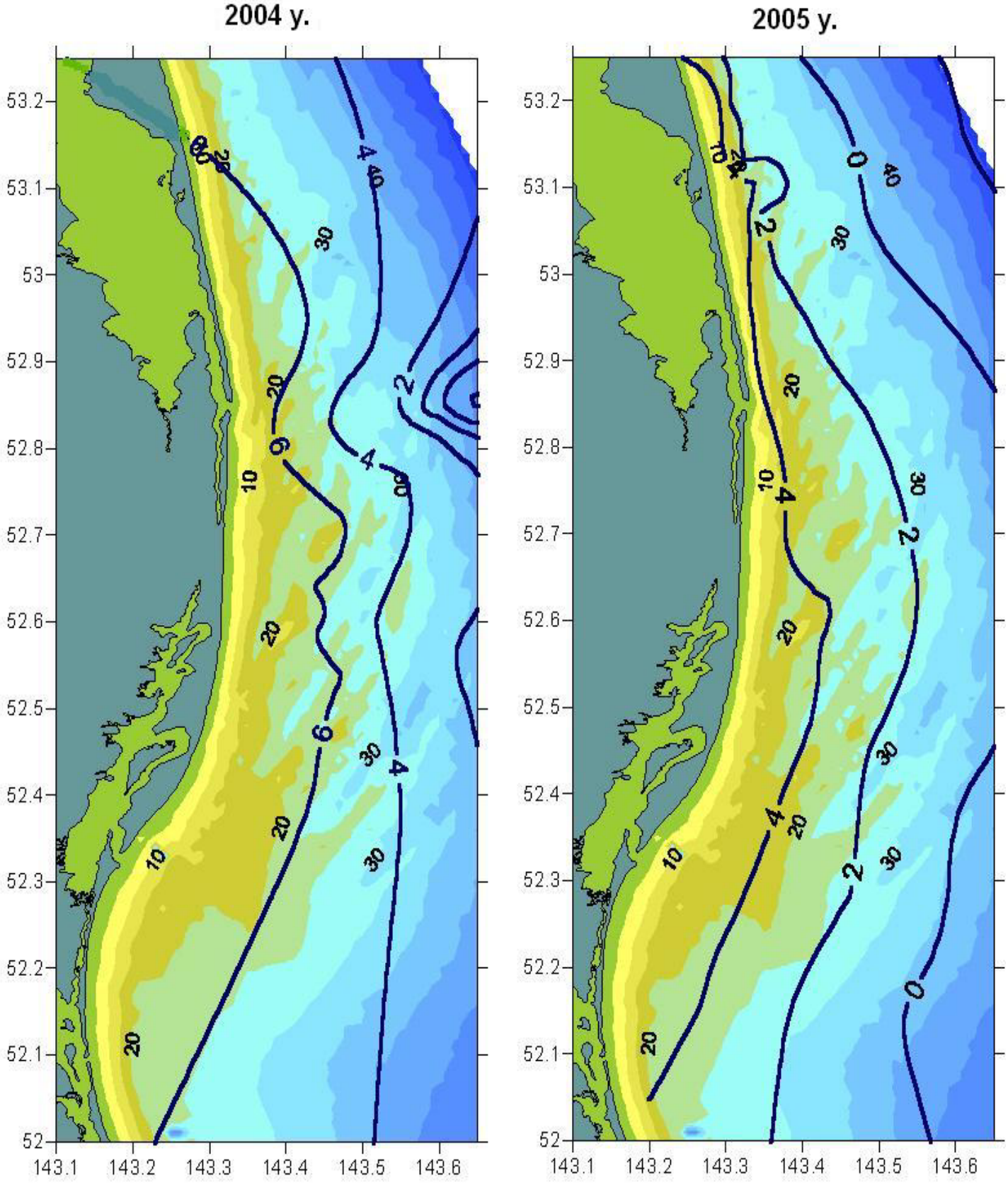

Figure 7.14 – Bottom water temperature on 12 - 16 August 2004 and 2005.

8 Main Results

1. One new AUAR was built by POI in 2005; bringing the total to 14 (one AUAR was lost in 2003). Radio transmitters were added to four of the AUARs giving them a real-time transmit capability for a bandwidth of 10 Hz to 5 kHz. Two mini-AUARs with a 3-day operational life were constructed for short term TL or source level measurements. All the AUARs (T-AUAR, AUAR and mini-AUAR) recorded high fidelity data for frequencies from of 1 Hz to 30 kHz (1 Hz to 15 kHz unaliased). In 2005 a new LF transducer was manufactured to supplement the old LF transducer.
2. Two digital and four analog sonobuoys were upgraded in 2005 to enhance their operational reliability and longevity.
3. The 10 AUARs and four AUARs were used to record ambient and anthropogenic acoustic levels on the NE Sakhalin shelf. The acoustic monitoring area extended for a distance of over 180 km from its northerly to southerly extent. They were also used to make synchronous measurements of broadband signals from proposed facilities locations to the edge of the gray whale feeding areas. These measurements allow an accurate estimation of the TL between the proposed facilities and the gray whale feeding areas.
4. The upgraded Autonomous Underwater Acoustic Recorders designed and developed at POI recorded 17,625 hours (over 734 days) of acoustic data. Acoustic monitoring was conducted almost continuously from 10 July to 27 September 2005. All the data acquired in 2005 is displayed, as daily sonograms (2 Hz to 15 kHz, 1 minute averaging) and plots of sound pressure level for five frequency bands (2 Hz - 15 kHz, 20 Hz - 15 kHz, 10 - 100 Hz, 100 - 2000 Hz, 2 - 15 kHz) are on a DVD in the first volume of this report [Rutenko, 2006].
5. Real-time acoustic monitoring was conducted from 10 July to 12 September using four T-AUARs, and (periodically) sonobuoys, deployed at the edge of the inshore feeding area. This report presents the results of the analysis of the data recorded by these four T-AUARs and two AUARs deployed near the offshore feeding area and between Chayvo and the Piltun feeding area.
6. Transmission loss studies were acquired on seven profiles[42] for frequencies from 15 Hz to 15 kHz (Figure 3.8). The TL studies included bathymetric profiling and sampling of

the hydrology at the transmitting and receiving locations and at locations in between if the distances were greater than 7 km. The TL was estimated for known sound velocity profiles - *C(r,z)*. Analysis of the variation of TL with frequency and range TL(*f,r*) has shown that for relatively long (8-20 km) shallow (20-30 m) profiles the TL is affected much more by the influence of the bottom and sea surface than by the spatial sound velocity C(*z,r*) distribution. The impact of sea-surface waves is greatest for acoustic energy at frequencies above 2 kHz, and is proportional to frequency and profile length.

7. Analysis of frequency dependent transmission loss TL(*f*) along profile TLP-4, a profile with 12 source locations, starting at the PA-B platform location and extending through the Orlan monitor station to the center of the offshore feeding area (OFA monitor station) shows that:
   - TL profile TLP-4 is 85 km long and has smooth bottom profile from the OFA to the Orlan acoustic stations where AUARs and mini-AUARs were deployed. The bathymetry from the Orlan acoustic station to the PA-B CGBS location is irregular with some fluctuations reaching 10 km in length and 15 m in height, and some less then 1 km in length and 6 m in height.
   - The hydrology measurements acquired on 30 August along TLP-4 (Figure 3.8) reveal that the profile crosses a hydrology front between source locations J and K. The southern section of the profile, up to source point J, is beyond 14 m isobath, the temperature is below 3 °C, the salinity is as much as 32 psu, and the sound velocity is less then 1460 m/s. The northern section of the profile has warmer and less salty water as it is closer to the mouth of the Amur River. This spatial differentiation is probably caused by the bathymetry. Figure 3.8 illustrates that the division is above a peak in the bathymetry.
   - TL measurements along profile TLP-4 show that frequencies below 14 Hz cannot propagate in waters shallower 35 m as has been shown by model studies of propagation in a shallow waveguide.
   - Figure 3.4 demonstrates that the intensity dropped by 20 dB when the transducer was moved from 100 m to 150 m from the receiver. Nevertheless, this frequency propagates in the bottom and ensonifies the near-bottom layer (Figure 3.5).

[42] Two comprehensive profiles (TLP-4 and TLP-15) and five point to point profiles (TLP-8, -9, -10, -11, -12, and TLP-13).

TL along the profile from source point J to the Orlan monitor station (16 km) is 80dB at 14 Hz and 95 db at 30 Hz. This is due to the acoustic energy below 14 Hz propagating in the bottom as seismic waves, these have less attenuation than 30 Hz acoustic energy which propagates in the water layer and is influenced by the bathymetry. This effect is also supported by measurements from source point E to the OFA monitor station, a profile of similar length (16 km), but with relatively smooth bathymetry. Here the TL at 30 Hz was 80 dB and acoustic energy at 14 Hz was not received as the attenuation was already 73 dB at 4 km (source point C to the OFA monitor station).

- TLP-4 was acquired as far as source point K (32 km from the Orlan acoustic station) as the transducer signal could not be received at greater distances. The TL from source point K to the Orlan monitor station was 105 dB for frequencies of 28-30 Hz and 80 dB for frequencies between 1.5-6 kHz.

8. Analysis of frequency dependent transmission loss TL(*f*) along profile TLP-15, a profile with 7 source locations, oriented east-west, the data being recorded on the Odoptu-N-10 and Odoptu-N-20 monitor stations shows that:
   - Profile TLP-15 crosses a lens of relatively warm, low salinity water formed by discharge of fresh water from the Amur River (Figure 3.23). Low ambient noise levels at the receiving locations Odoptu-N-10 and Odoptu-N-20 allowed TL measurements to be conducted at all the 7 source locations along the profile for the entire frequency range studied. The results are given on Figure 3.24. The profile from source point G to the Odoptu-N-10 monitor station (9.5 km) has a TL of ~82 dB for frequencies between 20-30 Hz; the profile from source point G to the Odoptu-N-20 monitor station has a TL of ~65 dB as the depth changes very sharply between Odoptu-N-20 and Odoptu-N-10 (Figure 3.22). Frequencies above 100 kHz have a more comparable TL as the distance between the stations is 1.5 km and acoustic energy at these frequencies is mostly carried by normal modes with lower attenuation (60 dB).
   - A dedicated study of the impact of tidal changes on the accuracy of TL measurements was conducted during the night of the 21st September in the frequency range from 1-15 kHz range. The HF transducer was deployed from the *Academik Oparin* while it was anchored at source point G (Figure 3.22a); a broadband FM signal was generated with a sweep rate of 10 kHz. Figure 3.25 shows

spectra *G(f),* sonograms *G(f,t)* and sound pressure level plots *D(Δf,t)* created from data synchronously recorded at acoustic stations Odoptu-N-20 and Odoptu-N-10. Figure 3.25 shows that tidal variations in hydrology and sea level along a 10 km profile oriented perpendicular to the shore can produce sound pressure level variations in the 1-4.5 kHz, 5-7 kHz, 7-10 kHz and 10-15 kHz bands of less than 3 dB (Figure 3.25b, *D(Δf,t)* 02:00-07:00, 22nd September, 2005).

9. Frequency dependent transmission loss TL(*f*) was estimated along a series of point-to-point TL profiles extending from the PA-B CGBS location to the Piltun feeding area:
   - TL profiles TLP-9 and TLP-13 (Figure 3.2) have similar bathymetry and hydrology as shown in Figures 3.12 and 3.19. These figures characterize the variations in hydrology along the profiles due to the continuous influence of the wind on the sea surface. Chapter 7 demonstrates that the southerly winds cause upwelling in this area, relatively warm surface water leaving the shallow area and near-bottom cold water moving in. The northerly wind triggers the opposite effect, relatively warm surface water fills the shallow area.
   - Figure 3.12 shows that the distance between monitor stations P-AB-2 (A8) and P-AB-1 (A7) on TL profile TLP-9 is 2.2 km; while it is ~4 km between acoustic stations PA-B-20 and PA-B-10 on TLP-13. The differences between the stations cause differences in the relative attenuation of low frequency noise. Figures 3.13, 3.20 and 3.21 illustrate that the TL from the PA-B CGBS location, for frequencies from 20-30 Hz, is 75 dB to the 20 m contour and 85 dB to 10 m contour. For frequencies from 40-70 Hz the TL is approximately 70 dB and 80 dB on TLP-9 and 68 dB and 90 dB on TLP-13. For frequencies from 100-300 Hz, acoustic attenuation was 64 dB to the 20 m contour and 72 dB to the 10 m contour, for 0.6-10 kHz it was 55 dB and 65 dB respectively.
   - TL measurements were acquired along profile TLP-13 on both the 21st and 30th August 2005, and it can be seen from Figures 3.12 and 3.19 that the hydrology differs significantly. However, TL values for the different hydrology (Figures 3.20 and 3.21) illustrate that the hydrology has a less significant impact than frequency; as different frequencies can have dramatically different TL over similar hydrology.
   - Multiyear TL studies on acoustic profile TLP-13 (from the PA-B CGBS location to the 10m contour inside the Piltun feeding area) were extended using numerical modeling

for frequencies of 14-150 Hz using a wide-angle parabolic equation model with an elastic bottom.

- TLP-11 is a profile from the PA-B CGBS location to the Odoptu-S-10 monitor station (20 km). The TL at 29 Hz was 103 dB (Figure 3.18), for frequencies between 700-3000 Hz it was 75 dB, and between 4-8 kHz it was ~85 dB.
- TLP-12 is a 27 km profile extending from the PA-B CGBS location to the Odoptu-N-20 monitor station (Figure 3.2). Figure 3.18 illustrates that on this profile the TL (76 dB) is at a minimum at 1 kHz. The TL increases as the frequency increases (90 dB between 1.5-3 kHz), and reaches 111 dB at 6 kHz. Scattering by surface waves (1.5-2 m) during the experiment, generated this sharp TL increase.
- Acoustic profile TLP-10 (Figure 3.2) is 12.5 km long and extends from the PA-B CGBS location to the Odoptu-PA-B monitor station. TLP-8 is the same length and stretches from the PA-B CGBS location to the Piltun monitor station. Figures 3.10 and 3.14 demonstrate that synchronous TL measurements were made on these profiles in similar bathymetric and hydrology conditions, so the TL above 200 Hz is approximately equal. The TL is approximately 76 dB for frequencies between 200-300 Hz, for frequencies between 600-3000 Hz it is approximately 65 dB, increasing to 70 dB for frequencies between 3-8 kHz. Higher frequencies have higher TL, probably caused by scattering by surface waves, at 14 kHz the TL was 116 dB. At frequencies between 27-30 Hz the TL is ~82 dB to the Odoptu-PA-B monitor station and 86 dB to the Piltun monitor station. For TLP-8 the TL is higher, for frequencies between 70-120 Hz it is 80-90 dB, it is 70-76 dB for these frequencies along TLP-10. This difference is probably related to the properties of the bottom sediments. The low TL for infrasonic frequencies should be noted for TLP-10 (Figure 3.15), the TL was 72 dB for frequencies below 20 Hz.

10. Data was recorded on stations at the 10 m bathymetric contour directly offshore from the South, 1st, 2nd, station 07 and Odoptu land based behavioral monitoring stations. These stations were synchronously occupied for seventeen days (26 stations) during the 2005 field season. Acoustic energy in 1 and 10 min intervals has been estimated for the frequency bands 20 Hz to 2 kHz and 20 Hz to 15 kHz for these days and the three previous days.

11. Measurements of the source signature of the research vessel *Academik Oparin* were taken as it sailed along TL profile TLP-15 and drifted while sampling the hydrology (Figure 6.1(a)). These showed that:
    - The vessel generated its maximum acoustic levels when slowing down and drifting with its engine running, the acoustic levels were significantly lower when the vessel was sailing at a constant speed.
    - Figure 6.2 illustrates that the sound pressure level $D(\Delta f,t)$ recorded in the frequency range from 2 Hz to 15 kHz at the Odoptu-N-10 monitor station, for a source 2.5 km away and sailing at a constant speed was more then 10 dB down.
    - Figure 6.4 shows the spectra of sound produced by the *Academik Oparin* and recorded at the Odoptu-N-10 and Odoptu-N-20 monitor stations (2.5 km and 0.9 km from the vessel respectively), while it was sailing at a speed of 6 knots. Figure 6.4 (09:15) shows that the spectra are similar.
        - The level of narrow band components in the frequency range from 20-70 Hz reached 104 dB re 1 μPa^2/Hz at point p1 and 115 dB re 1 μPa^2/Hz at point p2, these levels are approximately 10 dB higher than the broadband level.
        - There are clear quazi-tonal components in 500-1000 Hz range that are lower than 100 dB re 1 $mkPa^2$/Hz at the 10 m contour (point p1).
        - The broadband acoustic energy level dropped by 10 dB between the Odoptu-N-20 and Odoptu-N-10 monitor stations.
    - The acoustic levels at an average distance of 800 m from both the stations recorded as the vessel was moving at a speed of 4.5 knots were significantly (up to 11 dB at 34 Hz) higher behind the stern of the vessel at frequencies below 70 Hz and above 800 Hz (Figure 6.1).
12. Figure 6.5(b) shows spectral measurements of the acoustic output of the Photo-ID zodiac equipped with a 40 hp 4-stroke outboard motor as it maneuvered at speeds of 19 and 6 knots:
    - Figure 6.5(b) demonstrates that the Zodiac is much quieter when sailing at 19 knots than at 6 knots, confirming the 2004 results.
    - The Zodiac hull is probably a more effective acoustic transmitter than the outboard motor. The lower rotational speed of the motor (at 6 knots rather than 19 knots), excites a resonant vibration in the solid part of the zodiac hull that is effectively coupled into the water.

- The spectral *G(f)* plot for 6 knots on Figure 6.5 shows a clear peak at approximately 68 Hz. The power spectral density at this frequency reaches 130 dB re 1 μPa^2/Hz, this is more than 20 dB higher than that generated below 85 Hz by a Zodiac sailing at 19 knots.

13. The bathymetric and hydrologic parameters of the area were studied in detail using the sonar of the *Academik Oparin* and a hydrologic sonde. 7788 km of bathymetry data and 354 vertical hydrologic profiles were acquired in 2005. All the bathymetric data recorded in 2004 and 2005 was tide-corrected and was used to generate a bathymetric map. This data, together with hydrology data is available on DVD's in the first report [Rutenko, 2006].
    - Wind mixing, especially under the effects of southerly and northerly winds, which cause upwelling and wind driven tides, respectively.
    - The dynamics of the near-bottom layer of high-density water, which is formed during the winter season on the shelf due to convection and salinization (brine discharge) during ice growth. The maximum concentration of elements required for biogenic growth is observed in this water layer [Жабин et. al., 2005].

9 Conclusions

1. Spectral analysis of the acoustic energy generated by wind and surface waves again showed a good correlation between noise and sea state proposed by Knudsen and data from the NE Sakhalin shelf. The analysis also confirmed that the noise produced by wind and surface waves is much lower at shallow (10 m) than at deeper (20 m) water depths.
2. Transmission loss studies were acquired on seven profiles for frequencies from 15 Hz to 15 kHz (Figure 3.8). The TL studies included bathymetric profiling and sampling of the hydrology at the transmitting and receiving locations and at locations in between if the distances were greater than 7 km. The TL was estimated for known sound velocity profiles - *C(r,z)*. Analysis of the variation of TL with frequency and range TL(*f,r*) has shown that for relatively long (8-20 km) shallow (20-30 m) profiles the TL is affected much more by the influence of the bottom and sea surface than by the spatial sound velocity C(*z,r*) distribution. The impact of sea-surface waves is greatest for acoustic energy at frequencies above 2 kHz, and is proportional to frequency and profile length.
3. Analysis of frequency dependent transmission loss TL(*f*) along profile TLP-4, a profile with 12 source locations, starting at the PA-B platform location and extending through the Orlan monitor station to the center of the offshore feeding area (OFA monitor station) shows that:
   - TL profile TLP-4 is 85 km long and has smooth bottom profile from the OFA to the Orlan acoustic stations where AUARs and mini-AUARs were deployed. The bathymetry from the Orlan acoustic station to the PA-B CGBS location is irregular with some fluctuations reaching 10 km in length and 15 m in height, and some less than 1 km in length and 6 m in height.
   - TL measurements along profile TLP-4 show that frequencies below 14 Hz cannot propagate in waters shallower 35 m as has been shown by model studies of propagation in a shallow waveguide.
   - TLP-4 was acquired as far as source point K (32 km from the Orlan acoustic station) as the transducer signal could not be received at greater distances. The TL from source point K to the Orlan monitor station was 105 dB for frequencies of 28-30 Hz and 80 dB for frequencies between 1.5-6 kHz.

4. Analysis of frequency dependent transmission loss TL(*f*) along profile TLP-15, a profile with 7 source locations, oriented east-west, the data being recorded on the Odoptu-N-10 and Odoptu-N-20 monitor stations shows that:
   - Profile TLP-15 crosses a lens of relatively warm, low salinity water formed by discharge of fresh water from the Amur River (Figure 3.23). Low ambient noise levels at the receiving locations Odoptu-N-10 and Odoptu-N-20 allowed TL measurements to be conducted at all the 7 source locations along the profile for the entire frequency range studied. The profile from source point G to the Odoptu-N-10 monitor station (9.5 km) has a TL of ~82 dB for frequencies between 20-30 Hz; the profile from source point G to the Odoptu-N-20 monitor station has a TL of ~65 dB as the depth changes very sharply between Odoptu-N-20 and Odoptu-N-10 (Figure 3.22). Frequencies above 100 kHz have a more comparable TL as the distance between the stations is 1.5 km and acoustic energy at these frequencies is mostly carried by normal modes with lower attenuation (60 dB).
   - A dedicated study of the impact of tidal changes on the accuracy of TL measurements was conducted during the night of 21 September in the frequency range from 1-15 kHz range. Figure 3.25 shows that tidal variations in hydrology and sea level along a 10 km profile oriented perpendicular to the shore can produce sound pressure level variations in the 1-4.5 kHz, 5-7 kHz, 7-10 kHz and 10-15 kHz bands of less than 3 dB (Figure 3.25b, $D(\Delta f,t)$ 02:00-07:00, 22 September, 2005).
5. Data was recorded on stations at the 10 m bathymetric contour directly offshore from the South, 1st, 2nd, station 07 and Odoptu land based behavioral monitoring stations. These stations were synchronously occupied for seventeen days (26 stations) during the 2005 field season. Acoustic energy in 1 and 10 min intervals has been estimated for the frequency bands 20 Hz to 2 kHz and 20 Hz to 15 kHz for these days and the three previous days.
6. The following conclusions can be drawn from the analysis of the hydrological data acquired in 2004 and 2005:
   - Wind is one of the dominant factors affecting the formation of hydrological fields on the shelf. During the summer, due to the frequent shifting between southerly and northerly winds, there is frequent switching between the ebbs and flows of the wind driven tides in the coastal area. This stimulates the mixing of warm, fresh, Amur River waters with cold, saline, near-bottom Okhotsk Sea waters. These wind driven

currents can cause the water temperature in the coastal area to change by 8-10 °C, and the salinity by 5 psu within 2-3 days.

- Tidal processes are another dominant factor affecting the formation and variation in the characteristics of the hydrological fields on the shallow shelf. Variations in temperature and salinity in the coastal region are somewhat smaller; however, these variations continuously occur, reaching a maximum during syzygial tides.
- Cold Okhotsk Sea shelf water, rich in oxygen and biogenic matter, flows into the shallow coastal area during upwelling. The movement of this water is channeled by the seabed bathymetry, which is characterized by alternating ridges and channels.

7. The following factors have the greatest influence on the hydrological and acoustic properties of the waters of the shallow shelf off Piltun Bay and Chayvo Bay:
   - The dimensions and dynamics of the Amur River discharge lens, in which the water temperature is higher and the salinity lower than in the waters of the shelf of the Okhotsk Sea. In addition, water flowing from Piltun Bay and Chayvo Bay also contributes to the freshening of the water near the coast.
   - The intensity of vertical mixing on the shelf, which depends upon the tides (especially in the summer). A complete breakdown of stratification is possible during syzygial tides.
   - Wind mixing, especially under the effects of southerly and northerly winds, which cause upwelling and wind driven tides, respectively.
   - The dynamics of the near-bottom layer of high-density water, which is formed during the winter season on the shelf due to convection and salinization (brine discharge) during ice growth. The maximum concentration of elements required for biogenic growth is observed in this water layer [Жабин et. al., 2005].

10 Future plans

Seventeen digital AUARs were designed and manufactured by POI from 2003 to 2005. Three AUARs were lost (one in 2003 and two in 2005). For operational measurements including near field TL studies, POI developed in 2005 two digital mini-AUARs with a limited recording time (approx 72 hours). For real-time acoustic monitoring four AUARs were upgraded with radio transmitters that allow acoustic data in the frequency range from 10 Hz to 5 kHz to be transmitted to a radio station at the Piltun lighthouse Additionally, two digital and four analog sonobuoys were upgraded in 2005 to increase their operational reliability. All the AUAR variants are self-contained recorders, having 96 dB of dynamic range and a bandwidth of 1 Hz to 15 kHz, allowing accurate, synchronous acoustic measurements to be made across the NE Sakhalin shelf. Digital sonobuoys also have 96 dB of potential dynamic range over the frequency range from 1-2600 Hz.

Three new AUARs and one new T-AUAR will be constructed in 2006, bringing the total number of AUARs available to the program to 11 and the number of T-AUARs to 5. One extra mini-AUAR will also be fabricated, bringing the total to three. Some refinements will be made on the 12 AUARs fabricated between 2003 and 2005, building on the experience gained from the 2005 field expedition to improve the handling and operating time for the recorders. These include:

- After the initiation of the AUAR storage system the onboard computer will perform a software start and storage test with an audible confirmation signal.
- The T-AUAR radio-telemetry will be evaluated and synchronized using a calibration signal transmitted at the beginning and end of the transmission cycle. These calibration signals will allow the radio noise to be estimated and the mean sound pressure level measured by each T-AUAR to be more accurately estimated.
- The radio equipment for the radio station at the Piltun lighthouse will be upgraded to increase the reliability in the harsh environment at the lighthouse.
- The recording software used at Piltun lighthouse will be upgraded to enable it to be synchronized with the AUAR hard drive data.
- The new AUARs will a 100 GB hard drive, providing 20 days of continuous recording at a 30 kHz sampling rate.
- Mechanical upgrades to the sonobuoys, AUARs and T-AUARs will enhance their operational reliability.

- Standardized waterproof battery containers will be constructed for the sonobuoys and mini-AUARs. Using these battery packs will minimize failures due to leakage and allow a simplified battery change operation at sea.
- Two AUARs deployed at the 10 m contour were lost in 2005 and were presumed stolen. To prevent the loss of further equipment deployed in shallow water ten AUARs will be equipped with acoustic releases.

The comprehensive TL studies initiated in 2002 will be completed in 2006 with the main objective being the calibration of acoustic models along key profiles over the NE Sakhalin shelf. These TL and model studies will investigate sound propagation from the planned construction/development areas to the Piltun and offshore gray whale feeding areas. As in 2005 detailed hydrologic profiling using the sonde and vessel sonar will be conducted in the study area. The bathymetric and hydrologic data will be used in the construction of theoretical acoustical and hydrodynamic models and numerical experiments. These 2D acoustic models will be used to estimate the acoustic fields produced by multiple sources with known characteristics along the calibrated profiles. These models will extend the experimental TL data to other frequencies, sources and hydrology. This data will allow the impact of variations in the hydrologic field on sound propagation to be estimated (i.e. by internal waves, hydrologic fronts and tidal and eddy currents) and will improve the accuracy of the numerical modeling. The modeling will also allow the impact of spatial fluctuations in the hydrodynamics of the area on TL to be estimated. These models will compensate for weaknesses in the TL methodology and equipment, and allow the TL variations due to hydrology variations to be estimated.

During the multiyear western gray whale program POI has gathered a large quantity of hydrologic and bathymetric data; this data will be uploaded into a database allowing easy access and reliable storage and backup. Bathymetric and hydrologic data will be acquired from the vessels involved into the WGW program in 2006 (*Akademik Oparin* and *Professor Bogorov*). Again, all the data collected in 2006 will be uploaded into the database.

The integration between the acoustic and hydrologic research and other components of the western gray whale research program will be expanded in 2006. Two integrated programs will be conducted in 2006, these are:

- Recording of ambient and anthropogenic acoustic levels at the 10 m bathymetric contour offshore from the behavioral monitoring stations. Computation of the energy level in one minute windows over the frequency range from 20 Hz to 15 kHz for the monitoring period and three days beforehand.
- Investigation of the correlation between the spatial distribution and development of benthos and variations in bathymetry and hydrology in the study area. The study, conducted with the benthic team will:
  - Determine the size and dynamics of the discharge lens from the Amur River, where the temperature is higher and the salinity lower than the Sea of Okhotsk.
  - Determine the impact of water discharge from Piltun lagoon on the salinity of the water in the Piltun area.
  - Study the intensity of the tide driven (especially summer) and wind driven vertical mixing on the shallow part of the shelf.
  - Determine the location and dynamics of the high density, near-bottom, biogen rich layer formed by convection during the winter.

11 Acknowledgements

The authors would like to thank the V.I. Il`icev Pacific Oceanological Institute, FEB Academy of Sciences of Russia (POI), (Тихоокеанский океанологический институт им. В.И. Ильичева ДВО РАН), for assistance in performing this work. The first part of the expedition on the *Academik Lavrent'ev* was made possible by the efforts of Academic V.A. Akulichev (академик Акуличев В.А.).

The authors wish to thank the crew of the *Academik Lavrent'ev and Academik Oparin* for their hospitality and assistance while conducting acoustic measurements on the NE Sakhalin shelf. They would also like to thank the leader of the expedition Yuri Yakovlev (IBM) for the management of the safety program for the 2005 field season on the *Academik Oparin* and all the scientists participating in the expedition.

The authors would also like to acknowledge the following personnel from POI, who while they did not contribute to the report, contributed significantly to the success of the program in the field. Dr. A.A. Solov'ev (Соловьев А.А.), Sc. S.V. Borisov (Борисов С.В.), A.V. Gritsenko (Гриценко А.В.), Sc. R.A. Korotchenko (Коротченко Р.А.); engineers: V.V. Lihachev (Лихачев В.В.), D.G. Kovzel` (Ковзель Д. Г.), main laboratory assistant T.Y. Antipenkova (Т.Я. Антипенкова) and Sc. T.V. Soltanova (Т.В. Солтанова).

Finally the authors would like to express their gratitude to Associate of the Russian Academy of Sciences G.I. Dolgih (член-корр. РАН Долгих Г. И.)(POI), Dr. Sc. V.G. Petnikov (д.ф-м.н Петников В.Г.) (Institute of general physics, Moscow), Drs. Richard T. Houck, H.R. Melton, and M. Santala (ExxonMobil Upstream Research Co.), Dr. Lisanne M. Aerts (Sakhalin energy investment Company) as well as Dr. C.I. Malme (LGL) for reviewing this report.

Our special thanks go to the investment companies, their employees and consultants, without whom the present work could not have been conducted. These include:
LGL Ltd. - S.R. Johnson, S. Meier, S.B. Yazvenko and I. Zhmaev.
Exxon Neftegas Ltd. - M.R. Jenkerson, and H.R. Melton.
Sakhalin Energy Investment Company Ltd. - L.M. Aerts, V.E. Nechayuk.

12 Authors

The following members of staff from the V.I. Il`icev Pacific Oceanological Institute, Far East Branch, Academy of Sciences of Russia have contributed to the report:

Sc. M.V. Kruglov (Круглов М.В.)

Dr. Sc. A.N. Rutenko (Рутенко А.Н.)

Dr. F.F. Khrapchenkov (Храпченков Ф.Ф.)

13 Bibliography

1. Allen J.S. (1973). Upwelling and coastal jets in a continuously stratified ocean // J. Phys. Oceanography. Vol. 3, pp. 245 – 257.
2. Borisov S.V., Gritsenko A.V., Jenkerson M.R., Rutenko A.N., and Hodzevich A.V. (2002) Evaluating and Monitoring Acoustic Transmission from the Odoptu 3D seismic Survey 5 August - 9 September, 2001; Sakhalin, Russian Federation // Pacific Oceanological Institute (FEB RAS) report for Exxon Neftegas Ltd.

   Борисов С.В., Гриценко А.В., Дженкерсон М.Р., Рутенко А.Н., Ходзевич А.В. (2002). Оценка и наблюдение распространения акустических сигналов, при проведении трехмерной сейсморазведки в районе Одопту с 5 августа по 9 сентября 2001 г. на о.Сахалин, Россия // Отчет Тихоокеанского океанологического института ДВО РАН для компании Эксон Нефтегаз Лимитед.
3. Borisov S.V., Gritsenko A.V., Rutenko A.N., and Hodzevich A.V. (2003) Results of Acoustic Studies Within and Adjacent to the Piltun-Astokh License Area 1-6 August, 2001 and 17-24 September, 2001; Sakhalin, Russian Federation // Pacific Oceanological Institute (FEB RAS) report for Exxon Neftegas Ltd. and Sakhalin Energy Investment Co.

   Борисов С.В., Гриценко А.В., Рутенко А.Н., Ходзевич А.В. (2003). Результаты акустических исследований, проведенных с 1 по 16 августа 2001 г. и с 17 по 24 сентября 2001 г. в акватории Пильтунско-астохской лицензионной зоны, а также прилегающей к ней акватории на о.Сахалин, Россия / Отчет Тихоокеанского океанологического института ДВО РАН для компаний Эксон Нефтегаз Лимитед и Сахалин Энерджи Инвестмент Компани.
4. Borisov S.V., Gritsenko A.V., Kruglov M.V., Korotchenko R.A., and Rutenko A.N. (2003) Results of Acoustic Studies between Molikpaq and Piltun and Near Chayvo Bay, 12 September to 23 September, 2002; Sakhalin, Russian Federation // Pacific Oceanological Institute (FEB RAS) report for Exxon Neftegas Ltd. and Sakhalin Energy Investment Co.

   Борисов С.В., Гриценко А.В., Круглов М.В., Коротченко Р.А., Рутенко А.Н. (2003). Результаты акустических исследований, проведенных с 12 по 23 сентября 2002 г. на акваториях между платформой Моликпак и заливом Пильтун, и прилегающей к заливу Чайво, на о.Сахалин, Россия / Отчет Тихоокеанского океанологического института ДВО РАН, г. Владивосток, для компаний Эксон Нефтегаз Лимитед и Сахалин Энерджи Инвестмент Компании .

5. Borisov S.V., Gritsenko A.V., and Rutenko A.N. (2004) Acoustic Studies on the North East Sakhalin Shelf, Volume 1: Equipment, Methodology and Data; 15 August to 20 September, 2003; Sakhalin, Russian Federation // Pacific Oceanological Institute (FEB RAS) report for Exxon Neftegas Ltd. and Sakhalin Energy Investment Co.

   Борисов С.В., Гриценко А.В., Рутенко А.Н. (2004). Результаты акустических исследований, проведенных с 15 августа по 20 сентября 2003 г. на северо-восточном шельфе о. Сахалин, Россия. Том 1: «Оборудование, методика и данные» / Отчет Тихоокеанского океанологического института ДВО РАН, г. Владивосток, для компаний Эксон Нефтегаз Лимитед и Сахалин Энерджи Инвестмент Компании.

6. Borisov S.V., Gritsenko A.V., Dmitrieva A.V., Karnauhov A.A., Kruglov M.V. and Rutenko A.N. (2005) Acoustic Studies on the North East Sakhalin Shelf, Volume 1: Equipment, Methodology and Data; 30 July to 7 October, 2004; Sakhalin, Russian Federation // Pacific Oceanological Institute (FEB RAS) report for Exxon Neftegas Ltd. and Sakhalin Energy Investment Co.

   Борисов С.В., Гриценко А.В., Дмитриева А.В., Карнаухов А.А., Круглов М.В., Рутенко А.Н. (2005). Результаты гидро-акустических исследований, проведенных с 30 июля по 07 октября 2004 г. на северо-восточном шельфе о. Сахалин, Россия. Том 1: «Оборудование, методика и данные» / Отчет Тихоокеанского океанологического института ДВО РАН, г. Владивосток, для компаний Эксон Нефтегаз Лимитед и Сахалин Энерджи Инвестмент Компании.

7. Borisov S.V., Gritsenko A.V., Korotchenko R.A., Kovzel D.G., Kruglov M.V., Rutenko A.N. and Solovyev A.A. (2006) Acoustic Studies on the North East Sakhalin Shelf, Volume 2: Equipment, Calibration and Methodology; 7 July to 7 October, 2005; Sakhalin, Russian Federation // Pacific Oceanological Institute (FEB RAS) report for Exxon Neftegas Ltd. and Sakhalin Energy Investment Co.

   Борисов С.В., Гриценко А.В., Коротченко Р.А., Ковзель Д.Г., Круглов М.В., Рутенко А.Н., Соловьев А.А. (2006). Гидроакустические есследования, проведенные с 07 июля по 07 октября 2005 г. на северо-восточно шельфе о,Сахалин, Россия. Том 2: «Обороудование, калибровка и методика» / Отчет Тихоокеанского океанологического института ДВО РАН для компаний Эксон Нефтегаз Лимитед и Сахалин Энерджи Инвестмент Компани.

8. Bowden K. F. (1983). Physical oceanography of coastal waters. Ellis Horwood Ltd. Chichester. 324 p.

   Боудэн К. (1988) Физическая океанография прибрежных вод. М.: Мир. С. 324.

9. Defant A. (1961) Physical oceanography. Vol. I and II. Pergamon Press, Oxford.

10. Fadeev V.I. (2005). Benthos and food supply studies in feeding areas of the Okhotsk-Korean gray whale population. // Institute of Marine Biology (FEB RAS), Vladivostok, Russia. Final report for Exxon Neftegas Ltd. and Sakhalin Energy Investment Co. 150 p.

    Фадеев В.И. (2005) Исследования бентоса и кормовой базы в районах питания охотско-корейской популяции серого кита. // Заключительный отчет Института биологии моря ДВО РАН для компаний Сахалин Энерджи и Эксон Нефтегаз. Владивосток. 150 с.

11. Karnauhov A.A., Kruglov M.V. and Rutenko A.N. (2005) Acoustic Studies on the North East Sakhalin Shelf, Volume 2: Analysis, Conclusions and Recommendations; 30 July to 7 October, 2004; Sakhalin, Russian Federation // Pacific Oceanological Institute (FEB RAS) report for Exxon Neftegas Ltd. and Sakhalin Energy Investment Co.

    Карнаухов А.А., Круглов М.В., Рутенко А.Н. (2005). Результаты гидроакустических исследований, проведенных с 30 по 07 октября 2004 г. на северо-восточном шельфе о. Сахалин,Россия. Том 2: «Оборудование методика и данные» / Отчет Тихоокеанского океанологического института ДВО РАН, г. Владивосток, для компаний Эксон Нефтегаз Лимитед и Сахалин Энерджи Инвестмент Компании.

12. Knudsen V.O., Alford R.S. and Emling J.W. (1948) Underwater ambient noise // J. Mar. Res. Vol. 7. № 3, pp. 410-429.

13. Kruglov M.V., and Rutenko A.N. (2003) Transmission Loss Studies on the North east Sakhalin Shelf 2001 and 2002; Sakhalin, Russian Federation // Pacific Oceanological Institute (FEB RAS) report for Exxon Neftegas Ltd. and Sakhalin Energy Investment Co.

    Круглов М.В., Рутенко А.Н. (2003). Исследования потерь акустических шумов, проведенные в 2001, 2002 гг. На северо-восточном шельфе о.Сахалин, Россия / Отчет Тихоокеанского океанологического института ДВО РАН для компаний Эксон Нефтегаз Лимитед и Сахалин Энерджи Инвестмент Компани.

14. Kruglov M.V., and Rutenko A.N. (2004) Acoustic Studies on the North East Sakhalin Shelf, Volume 2: Analysis, Conclusions and Recommendations; 15 August to 20 September, 2003; Sakhalin, Russian Federation // Pacific Oceanological Institute (FEB RAS) report for Exxon Neftegas Ltd. and Sakhalin Energy Investment Co.

Круглов М.В., Рутенко А.Н. (2004) Результаты акустических исследований, проведенных с 15 по 20 сентября 2003 г. на северо-восточном шельфе о.Сахалин, Россия. Том 2: «Анализ, выводы и рекомендации» / Отчет Тихоокеанского океанологического института ДВО РАН для компаний Эксон Нефтегаз Лимитед и Сахалин Энерджи Инвестмент Компани.

15. Kruglov M.V., Rutenko A.N. and Khrapchenkov F.F. (2006) Acoustic Studies on the North East Sakhalin Shelf, Volume 3: Analysis, Conclusions and Recommendations; 7 July to 7 October, 2005; Sakhalin, Russian Federation // Pacific Oceanological Institute (FEB RAS) report for Exxon Neftegas Ltd. and Sakhalin Energy Investment Co.

    Круглов М.В., Рутенко А.Н., Храпченков Ф.Ф. (2006). Гидроакустические исследования, проведенные с 07 июля по 07 октября 2005 г. на северо-восточном шельфе о.Сахалин. Том 3: «Анализ, выводы, рекомендации». / Отчет Тихоокеанского океанологического института ДВО РАН для компаний Эксон Нефтегаз Лимитед и Сахалин Энерджи Инвестмент Компани.
16. Miller J.F. and Wolf S.N. (1980) Modal acoustic transmission loss (MOATL): A transmission loss computer program using a normal mode model of acoustic field in the ocean // Naval research laboratory, Washington.
17. Richardson W.J., Greene C.R., Malme C.I. and Thomson D.H. (1995). Marine mammals and noise. Academic Press Limited. 576 p.
18. Rutenko A.N. (2006) Acoustic Studies on the North East Sakhalin Shelf, Volume 1: Objectives and Data; 7 July to 7 October, 2005; Sakhalin, Russian Federation // Pacific Oceanological Institute (FEB RAS) report for Exxon Neftegas Ltd. and Sakhalin Energy Investment Co.

    Рутенко А.Н. (2006) Гидроакустические исследования, проведенные с 07 июля по 07 октября 2005 г. на северо-восточном шельфе о.Сахалин, Россия. Том 1: «Цели и полученные данные». / Отчет Тихоокеанского океанологического института ДВО РАН для компаний Эксон Нефтегаз Лимитед и Сахалин Энерджи Инвестмент Компани.
19. Бровко П.Ф., Микишин Ю.А. (1999) Современные тенденции развития берегов северо-восточного Сахалина // Гидрометеорологические и экологические условия дальневосточных морей: оценка воздействия на морскую среду. Владивосток, с. 193-203. (Тематический выпуск № 2).

Brovko P.F., Mikishin Y.A. (1999) Modern tendencies in the development of the North East Sakhalin coasts // FERHRI Special Issue # 2, Vladivostok, Dalnauka, pp. 193-203.

20. Блохин С.А., Язвенко С.Б., Владимиров В.Л., Лагерев С.И. (2002). Численность, распределение и характер поведения серого кита (*Eschrichtius robustus)* на основании авиационных наблюдений на северо-восточном шельфе острова Сахалин летом и осенью 2001 г. // Доклад на конференции Морские млекопитающие в удаленных районах Арктики, 11-13 сентября 2002 г., озеро Байкал, Россия.
21. Жабин И.А., Пропп Л.Н., Волкова Т.И., Тищенко П.Я. (2005). Изменчивость гидрохимических и гидрологических параметров вблизи устья реки Амур.// Океанология, том 45, № 5, с. 703-709.
22. Красавцев В. Б., Пузанков К. Л., Шевченко Г. В. (2000) Формирование апвеллинга на северо-восточном шельфе острова Сахалин под воздействием ветра. // Тематический вып. ДВНИИГМИ № 3. Владивосток: Дальнаука, С. 106-120.
23. Курьянов Б.Ф. (1998) Развитие представлений о низкочастотных шумах океана за 50 лет // Акустика океана. М.: ГЕОС, с. 116-124.
24. Kuryanov B.F. (1998) Ocean low-frequency noise conception development for 50 years // Ocean acoustics. M.: GEOS, pp. 116-124.
25. Леонтьев И. О. (2001) Прибрежная динамика: волны, течения, потоки наносов. – М.,: ГЕОС.- 272 с.
26. Перлов А.С., Маминов М.К. (2002) Численность, распределение и характер поведения серого кита (*Eschrichtius robustus)* в прибрежных водах северо-восточного Сахалина в 2002 г. (судовые наблюдения) / Отчет Тихоокеанского научно-исследовательского рыбохозяйственного центра, г. Владивосток, для компаний Эксон Нефтегаз Лимитед и Сахалин Энерджи Инвестмент Компании ЛТД.
27. Попудрибко К.К., Путов В.Ф., Шевченко Г.В. (1998). Оценка характеристик морских течений на Пильтун-Астохской нефтегазоносной площади (северо-восточный шельф о. Сахалин)// Метеорология и гидрология. С. 82-95.
28. Яковлев Ю.М. (2003). Фотоидентификация корейско-охотской популяции серого кита *(Eschrichtius Robustus)* в 2002 г. / Отчет для Эксон Нефтегаз и Сахалин Энерджи Инвестмент Компании.

29. Гидрометеорология и гидрохимия морей. (1998) Том IX. Охотское море. Выпуск 1. Гидрометеорологические условия. Санкт-Петербург: Гидрометеоиздат, 342 С.
30. Динамика океана (1980). Под ред. Ю. П. Доронина. Л.: Гидрометеоиздат, 303 С.

Station		Date		Time		Time	AUAR	Location		Depth	Gain	Sens.
Name	#	Start	End	Start	End	(hr)	#	Latitude	Longitude	(m)		(mV/Pa)
Lunskoye	1	15-Sep	30-Sep	16:15	12:30	356.3	№ 11	52°51'47"	143°37'.29'	48	40	56.5
OFA	2	3-Aug	19-Aug	10:15	16:30	390.3	№ 9	52°10'20"	143°36'02"	42	40	48.0
OFA	2	19-Aug		17:00		FAIL	№ 11	52°10'19"	143°36'03"	40	40	56.5
OFA	2	6-Sep	23-Sep	13:30	09:00	403.5	№ 10	52°10'18"	143°36.05"	42	40	49.5
Orlan	3	9-Jul	22-Jul	14:35	17:30	314.9	№ 8	52°21'35"	143°35'01"	33	40	50.0
Orlan	3	22-Jul	6-Aug	18:00	10:00	352.0	№ 5	52°21'35"	143°34'59"	33	40	51.5
Orlan	3	9-Aug	24-Aug	20:10	20:15	360.1	№ 5	52°21'41"	143°34'58"	33	40	49.0
Orlan	3	24-Aug	11-Sep	20:40	09:00	420.3	№ 8	52°21'37"	143°34'59"	33	40	50.0
Orlan	3	10-Sep	26-Sep	15:00	16:30	385.5	№ 9	52°22'21"	143°34.58"	31	40	48.0
Arkutun-Dagi	4	3-Aug	19-Aug	09:00	10:00	385.0	№ 10	52°19'12"	143°44'01"	47	40	49.5
Arkutun-Dagi	4	19-Aug	5-Sep	10:00	17:30	415.5	№ 6	52°19'15"	143°43'54"	45	40	50.0
Arkutun-Dagi	4	14-Sep	30-Sep	14:04	09:00	378.9	№ 8	52°19'15"	143°44'06"	46	40	50.0
Piltun-S	5	11-Jul	22-Jul	18:00	13:00	259.0	№ 4	52°40'54"	143°22'36"	16	10	49.0
Piltun-S	5	23-Jul	6-Aug	22:00	14:30	328.5	№ 4	52°40'43"	143°22'32"	17	10	49.0
Piltun-S	5	7-Aug	22-Aug	23:20	13:00	349.7	№ 4	52°41'13"	143°22'32"	17	10	49.0
Piltun-S	5	23-Aug	7-Sep	11:00	10:30	359.5	№ 4	52°41'17"	143°22'42"	19	10	49.0
Piltun-S	5	10-Sep	26-Sep	12:15	13:30	385.3	№ 4	52°40'26"	143°22'17"	15	10	49.0
Piltun	6	13-Jul	22-Jul	11:00	10:00	215.0	№ 3	52°49'18"	143°25'13"	20	10	50.0
Piltun	6	23-Jul	6-Aug	21:00	16:00	331.0	№ 3	52°49'14"	143°25'13"	21	10	50.0
Piltun	6	7-Aug	22-Aug	22:20	16:30	354.2	№ 3	52°49'15"	143°25'01"	22	10	50.0
Piltun	6	23-Aug	7-Sep	13:10	12:00	358.8	№ 3	52°49'12"	143°24'57"	22	10	50.0
Piltun	6	10-Sep	26-Sep	10:55	11:30	384.6	№ 3	52°49'19"	143°25'13"	21	10	50.0

Station		Date		Time		Time	AUAR	Location		Depth	Gain	Sens.
Name	#	Start	End	Start	End	(hr)	#	Latitude	Longitude	(m)		(mV/Pa)
PA-B-10	7	13-Jul	27-Jul	13:40	09:30	331.8	№ 6	52°53'03"	143°20'10"	11	40	50.0
PA-B-10	7	27-Jul	14-Aug	9:20	13:00	435.7	№ 7	53°03'54"	143°18'17"	12	40	50.0
PA-B-10	7	16-Aug	1-Sep	12:15	17:00	388.8	№ 7	52°53'06"	143°20'13"	9	40	50.0
PA-B-20	8	13-Jul		13:00		FAIL	№ 2	52°54'08"	143°23'28"	20	10	49.0
PA-B-20	8	24-Jul	8-Aug	19:20	15:40	356.3	№ 2	52°53'54"	143°23'21"	18	2	49.0
PA-B-20	8	9-Aug	23-Aug	16:00	15:00	335.0	№ 2	52°54'00"	143°23'17"	20	10	49.0
PA-B-20	8	24-Aug	5-Sep	11:30	12:40	289.2	№ 2	52°54'03"	143°23'20"	20	10	50.8
PA-B-20	8	10-Sep	26-Sep	10:15	10:00	383.8	№ 2	52°54'05"	143°23'21"	20	10	49.0
Odoptu-PA-B	9	10-Jul	23-Jul	16:30	11:00	306.5	№ 16	53°00'00"	143°21'17"	22	10	50.0
Odoptu-PA-B	9	24-Jul	7-Aug	18:30	16:30	334.0	№ 16	53°00'02"	143°21'19"	21	10	50.0
Odoptu-PA-B	9	8-Aug	23-Aug	10:00	14:00	364.0	№ 16	53°00'02"	143°21'14"	21	10	50.0
Odoptu-PA-B	9	24-Aug	7-Sep	10:00	15:00	341.0	№ 16	53°00'01"	143°21'13"	21	10	50.0
Odoptu-PA-B	9	10-Sep	26-Sep	09:00	08:30	383.5	№ 16	53°00'03"	143°21'10"	22	10	50.0
Odoptu-S-10	10	10-Jul	27-Jul	17:00	12:00	403.0	№ 11	53°03'53"	143°18'25"	11	40	49.0
Odoptu-S-10	10	27-Jul		11:40		LOST	№ 1	53°03'54"	143°18'17"	12	40	49.0
Odoptu-S-20	11	30-Jul	17-Aug	09:30	11:00	433.5	№ 8	53°03'43"	143°19'55"	21	40	50.0
Odoptu-S-20	11	23-Aug	7-Sep	16:22	16:30	360.1	№ 9	53°03'42"	143°19'33"	18	40	48.0
Odoptu-S-20	11	9-Sep		21:35		FAIL	№ 13	53°03'40"	143°20'03	23	40	50.8
Odoptu-N-10	12	10-Jul	27-Jul	17:30	13:00	403.5	№ 9	53°08'57"	143°17'24"	10	40	48.0
Odoptu-N-10	12	28-Jul	13-Aug	21:35	15:30	377.9	№ 11	53°09'06"	143°17'25"	12	10	56.5

Station		Date		Time		Time	AUAR	Location		Depth	Gain	Sens.
Name	#	Start	End	Start	End	(hr)	#	Latitude	Longitude	(m)		(mV/Pa)
Odoptu-N-20	13	20-Aug	5-Sep	18:30	09:00	374.5	№ 10	53°08'58"	143°18'33"	18	40	49.5
Odoptu-N-20	13	5-Sep	22-Sep	09:50	12:00	410.2	№ 7	53°09'12"	143°18'53"	22	40	50.0
Control	14	25-Aug	20-Sep	20:50	14:00	617.2	№ 5	53°25'58"	143°11'00"	20.5	40	49.0
BEH-Odoptu	A.9	11-Jul		13:30		LOST	№ 12	53°12'32"	143°16'12"	11	40	49.0
BEH-north	A.10	11-Jul	27-Jul	15:00	17:20	386.3	№ 10	53°18'00"	143°13'48"	10	40	52.8
BEH-north	A.10	28-Jul	13-Aug	20:30	12:30	352.0	№ 6	53°17'57"	143°13'47"	11	40	52.4
Chayvo-4	A.11	9-Jul	22-Jul	16:00	14:20	310.3	№ 7	52°33'56"	143°23'09"	16	40	50.31
Chayvo-4	A.11	22-Jul	6-Aug	15:30	12:10	332.7	№ 13	52°34'02"	143°23'00"	16	40	52.8
Chayvo-4	A.11	9-Aug	22-Aug	18:15	17:00	310.8	№ 13	52°34'06"	143°23'00"	18	40	52.3
Chayvo-4	A.11	23-Aug	7-Sep	10:05	08:30	334.4	№ 13	52°34'11"	143°22'56"	15	40	50.31
Chayvo-4	A.11	7-Sep	24-Sep	09:40	10:50	409.2	№ 6	52°34'09"	143°22'56"	17.5	40	52.1